LUDWIG-MAXIMILIANS-UNIVERSITÄT MÜNCHEN

# Fibroblast growth factor 1 in multiple sclerosis:

## Localization in brain lesions and effects on cultured human astrocytes

**Dissertation**

der Fakultät für Biologie
der Ludwig-Maximilians-Universität München

**Anita Ines Friese**

München 2014

1. Gutachter: Prof. Dr. Elisabeth Weiß
Ludwig-Maximilians-Universität, München
Fachbereich Biologie

2. Gutachter: Prof. Dr. Michael Schleicher
Ludwig-Maximilians-Universität, München
Institut für Zellbiologie

Sondergutachter: Prof. Dr. Edgar Meinl
Klinikum der Universität München, München
Institut für klinische Neuroimmunologie

Doktorarbeit eingereicht am: 18.02.2014
Tag der mündlichen Prüfung: 27.05.2014

# TABLE OF CONTENTS

# SUMMARY

Multiple Sclerosis (MS) is an inflammatory demyelinating disease of the central nervous system (CNS) in which remyelination of lesions is often limited or absent. Evidence for the involvement of fibroblast growth factor 1 (FGF1) in MS lesion development arose from previous work in our laboratory, analyzing the gene expression in different types of MS lesions. FGF1 peaked out as an abundant factor upregulated in remyelinated areas. The present study aimed at: (1) the establishment of an *in vitro* myelinating culture which could be used to identify FGF1-mediated effects on myelination, (2) the detection of FGF1-mediated functions in cultured human astrocytes and (3) the identification of FGF1-positive cells in MS lesions.

An *in vitro* myelinating culture mimicking developmental myelination was introduced in our laboratory. The validity of a microscopy-based method for the quantification of myelination and axonal density was proven by antibody-mediated complement dependent demyelination. FGF1 was found to promote myelination in this culture system (independent study). This effect might be directly mediated by oligodendrocytes or indirectly by astrocytes, both known to express FGF receptors (FGFRs).

To decipher FGF1-mediated effects on primary human astrocytes in cell culture, modulations in RNA and protein levels were analyzed by a transcriptome microarray analysis and a secretome analysis, respectively. The transcriptome approach revealed a FGF1-dependent induction of RNAs involved in modulation of remyelination and the regulation of inflammation. Results obtained from the secretome approach pointed to a FGF1-mediated disintegration of extracellular matrix (ECM). Results of the screenings were validated by reverse transcription quantitative PCR (RT-qPCR) and enzyme-linked immunosorbent assay (ELISA). Comparison of the results obtained from the transcriptome and the secretome approach revealed a correlation of RNA and protein levels for the majority of proteins detected in both approaches.

Using immunohistochemistry (IHC), FGF1-positive subsets of neurons in gray matter and oligodendrocytes in white matter of control brain and in normal appearing white matter (NAWM) of MS lesions were detected. FGF1-positive astrocytes were identified in remyelinated and demyelinated lesions. In active MS lesions, microglia, macrophages and lymphocytes were found to be FGF1-positive.

In the present study, FGF1 was localized to different cells in MS lesions and an extensive characterization of FGF1-mediated effects revealed, to our knowledge, so far unknown functions in human astrocytes. This strongly suggests FGF1 to be an important mediator in MS lesion development. A detailed understanding of FGF1 functions could provide a therapeutic basis for promoting repair mechanisms in MS.

# ZUSAMMENFASSUNG

Multiple Sklerose (MS) ist eine demyelinisierende Erkrankung des zentralen Nervensystems, in der die Remyelinisierung oft stark limitiert ist. Hinweise auf eine Beteiligung des Fibroblasten-Wachstumsfaktors 1 (FGF1) in Multipler Sklerose gingen aus einer Studie unseres Labors hervor, in der die Genexpression verschiedener MS Läsionen untersucht wurde und in der FGF1 in remyelinisierten Läsionen erhöht war. Die Ziele der hier beschriebenen Studie waren: (1) Die Etablierung einer Myelinisierungskultur zur Untersuchung von FGF1-vermittelten Effekten auf die Myelinisierung. (2) Die Detektion von FGF1-vermittelten Effekten auf humane Astrozyten in Zellkultur. (3) Die Identifikation von FGF1-positiven Zellen in MS Läsionen.

Es wurde eine Myelinisierungskultur etabliert, mit der entwicklungsabhängige Myelinisierung nachvollzogen werden kann. Zudem wurde eine, auf Fluoreszenzmikroskopie basierende Quantifizierungsmethode entwickelt, um die Myelinisierung und die Dichte der Axone zu bestimmen. Diese wurde durch Antikörper-vermittelte, komplementabhängige Zytolyse validiert. In diesem Zellkultursystem wurde ein myelinisierungsfördernder Effekt von FGF1 nachgewiesen (unabhängige Studie). Dieser könnte direkt von Oligodendrozyten aber auch indirekt von Astrozyten vermittelt werden, welche beide FGF Rezeptoren exprimieren.

Die Effekte von FGF1 auf humane Astrozyten in Zellkultur wurden mithilfe einer Transkriptom- und einer Sekretomanalyse untersucht. In der Transkriptomanalyse wurden sowohl Faktoren mit Einfluss auf die Remyelinisierung, als auch solche mit entzündungsmodulatorischer Wirkung identifiziert. Aus der Sekretomanalyse gingen Effekte von FGF1 auf den Abbau von extrazellulärer Matrix hervor. Die Ergebnisse beider Analysen wurden mittels RT-qPCR und ELISA validiert. Der Vergleich von Proteinen, detektiert in der Sekretomanalyse, mit den Transkriptomergebnissen zeigte eine Korrelation zwischen detektierter RNA- und den zugehörigen Proteinen.

Mittels Immunhistologie wurden zudem FGF1-positive Zellen in verschiedenen Läsionsarealen identifiziert. Es wurden FGF1-positive Neurone, sowie FGF1-positive Oligodendrozyten in der weißen Substanz von Kontrollhirn und in normal erscheinender weißer Substanz (NAWM) von MS Gewebe detektiert. In re- und demyelinisierten Regionen wurden Astrozyten detektiert, in aktiven Läsionen hingegen Mikroglia, Makrophagen und Lymphozyten.

In der vorliegenden Arbeit wurden FGF1-positive Zellen in MS Läsionen detektiert und es wurden, nach unserem Wissen, bislang unbekannte FGF1-vermittelte Effekte in Astrozyten charakterisiert. Dies stützt die Vermutung, dass FGF1 ein wichtiger Modulator in der Pathogenese von MS ist. Ein genaueres Verständnis der von FGF1 vermittelten Funktionen könnte eine therapeutische Grundlage dafür schaffen, Reparaturmechanismen in MS zu unterstützen.

# 1 INTRODUCTION

## 1.1 MULTIPLE SCLEROSIS

Multiple Sclerosis (MS) is considered an autoimmune inflammatory demyelinating disease of the central nervous system (CNS). MS is typically affecting people between their second and third decade of life and it is one of the most common causes of disability in young adults. Around 122 000 patients in Germany and 2.5 million worldwide[69] suffer from this disease with women being more often affected than men. Traditionally, MS was considered to be mediated by T cells attacking CNS structures, especially myelin. However, also a vast range of other immune cells do participate in the inflammatory process, with T cells, macrophages and microglia being the dominating cell types. This leads to demyelinated areas in the white and gray matter of the brain, which is the pathological hallmark of MS, to axonal damage and finally to neuronal death. Besides demyelination, also inflammation itself is critical for neuronal and axonal loss[228]. Commonly affected sites are the subpial cerebral cortex, the periventricular white matter, the optic nerve, the brainstem and the spinal cord.

The appearance of MS is heterogeneous with a vast spectrum of differences in clinical symptoms, lesion number and location as well as in efficacy of available therapies[111]. The symptoms can include impaired physiological and cognitive functions, fatigue, disturbance of vision as well as loss of coordination and sometimes paralysis. Oligoclonal bands, resulting from immunoglobulin G in the cerebrospinal fluid (CSF), as well as transient gadolinium enhanced lesions in magnetic resonance scans, indicating an inflammation and the breakdown of the blood-brain barrier (BBB), are often found in patients and are used as diagnostic criteria.

### 1.1.1 Clinical disease course

Depending on the clinical course, MS is classified as relapsing remitting (RR), primary progressive (PP) or secondary progressive (SP) (figure 1). In the vast majority of patients (approximately 85 %), the disease starts with a RR course which is characterized by alternating periods of acute disease and recovery. Relapses, caused by inflammation and formation of white matter lesions, usually do not last more than several months and patients can fully, or at least partially, recover. The clinical recovery results from the resolution of focal inflammation and edema, the recovery of demyelinated neurons and partial remyelination. Depending on the affected brain area, not all inflammation will result in a relapse as it is known from brain imaging studies. Therefore, depending on the area affected, lesions can be silent[20].

In approximately two-thirds of the patients, the RR form converts into the SP form with accumulating neurological disabilities in the absence of attacks and newly forming inflammatory lesions. As no therapeutics is available to antagonize the progressing physical and cognitive damages, this transition has to be considered very problematic and current MS therapies mainly aim at the reduction of the number of relapses.

About 15 % of all MS patients suffer from the rather aggressive PP form of MS which is characterized by a later clinical onset and a steadily accumulating disability without or with rare relapses. As for the SP form, new inflammatory demyelinating lesions are infrequent. However, changes and atrophy of the so called normal appearing white matter (NAWM) and the gray matter appear[102, 176, 203]. It seems that with increasing chronicity of the disease the inflammation in the CNS persists behind an intact BBB and is, therefore, not controlled by the peripheral immune system[102].

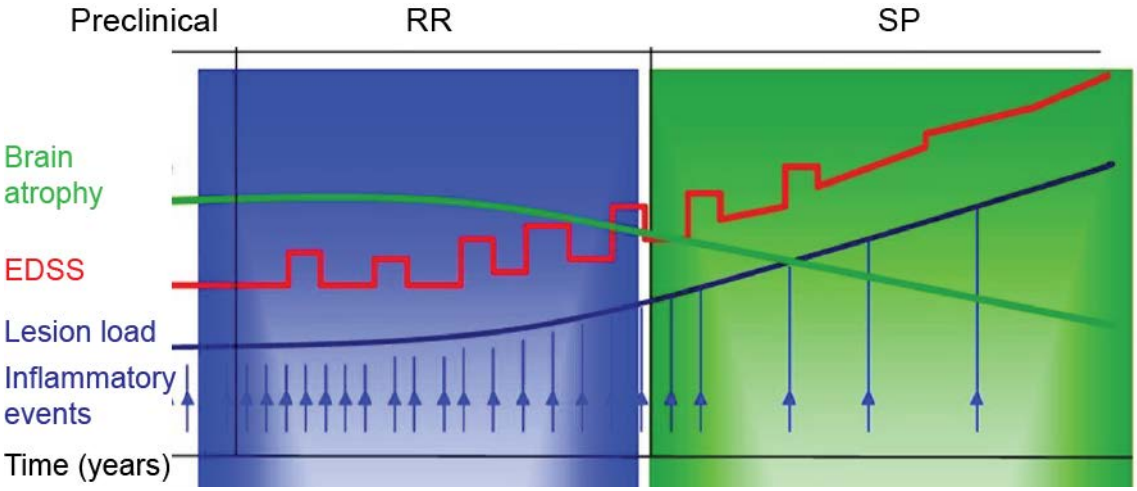


Figure 1: Clinical courses of RR and SP MS

RR: relapsing remitting; SP: secondary progressive; EDSS: expanded disability status scale
Clinical evolution of MS (EDSS, red line), brain atrophy (green line), overall tissue damage (blue line) and the frequency of inflammatory events (blue arrows) during the progression of RR and SP MS are shown (modified from[176]).

### 1.1.2 Lesion pathology

A complex pathogenic cascade is involved in initiating inflammation in the CNS with many different immune cells participating. To induce inflammation, potentially autoreactive CD4-positive T cells must be activated in the periphery, enter the brain and become reactivated by antigen-presenting cells in the CNS parenchyma[73, 176].

Usually, cellular migration into the CNS is prohibited by the BBB which is formed by tight junctions of endothelial cells[79]. To overcome this barrier, lymphocytes have to adhere to endothelial cells. This process is mediated by adhesion molecules such as very late antigen-4 (VLA-4) and lymphocyte function-associated antigen-1 (LFA-1), chemokine receptors and integrins. Natalizumab, a therapeutic antibody approved for

the treatment of MS, binds to VLA-4 and blocks the transmigration of lymphocytes into the CNS thereby inhibiting inflammation[142].

Subsequently to extravasation, CD4-positive T cells become reactivated by MHC class II-positive antigen-presenting cells which induces cell proliferation. Antigen-presenting cells include perivascular macrophages, microglia and peripheral dendritic cells. Reactivation also leads to the release of a vast range of cytokines and chemokines and to the activation of astrocytes, microglia and endothelial cells[79]. This in turn allows the recruitment of other immune cells from the blood into the brain parenchyma including CD8-positive T cells, monocytes, B cells and mast cells. Damage of the myelin sheath, of oligodendrocytes and axons can already occur during this early inflammatory phase.

The formation of the initial inflammatory lesion is mostly dependent on potentially autoreactive T cells, whereas, in subsequent events myelin degradation, oligodendrocyte and axonal damage is caused by a wide range of processes. These include: direct or antibody-mediated complement binding, direct lysis of axons by CD8-positive T cells, phagocytosis of myelin as well as an increased release of radicals, proteases and glutamate[139]. The acute inflammation can last up to 14 days[176]. The lesion resolution involves the clearing of debris by macrophages, the activation of oligodendrocyte precursor cells (OPCs) and, in a minority of the lesions, the remyelination of demyelinated axons. However, the original myelin thickness cannot be restored and myelin produced by remyelination differs from the composition of mature myelin. Therefore, conduction velocity in these damaged areas is slower. In the long term, the cellular composition in the plaque areas can change heavily regarding cell types, formation of glial scars and cell number. An overview of the pathological processes involved in MS lesion formation is given in figure 2.

According to the stage and cellular composition, white matter lesion can be classified as (1) demyelinated lesions, including active lesions and chronic active lesions, and (2) remyelinated lesions (figure 3).

Active lesions are mostly found in patients with acute and RR MS and become rare at later stages or during the progressive phase of the disease[101]. Active lesions are completely demyelinated. In contrast-enhanced magnetic resonance imaging they are characterized by the uptake of gadolinium, indicating an opening of the BBB[46]. Furthermore, active lesions are characterized by infiltrating immune cells. Macrophages or microglia are dispersed throughout the lesion and commonly incorporate phagocytosed myelin, particularly in early active lesions[204].

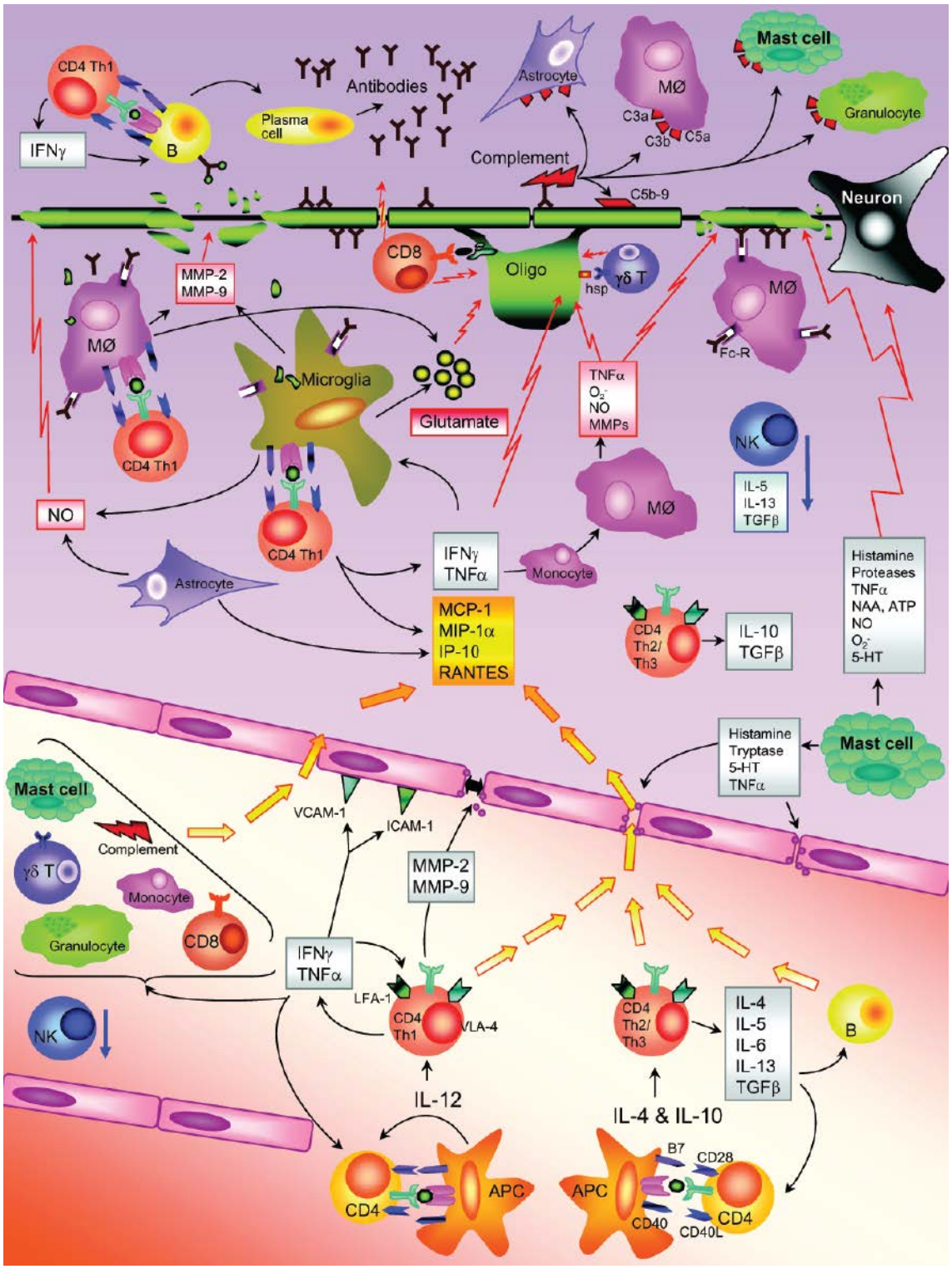


Figure 2: Model of pathological processes in MS lesions

Processes during acute inflammation in MS. Contributing inflammatory and CNS resident cells as well as involved cytokines and chemokines are depicted (see text for details. Modified from[176]).

Chronic active lesions are also completely demyelinated and are predominantly seen in patients with progressive MS. In contrast to active lesions, macrophages and microglia are located only at the edge of the lesion and myelin-laden macrophages or microglia are rare[144].

During early stages of the disease, lesions become frequently remyelinated[143]. This process is believed to be mediated by OPCs which are recruited to the lesion site and ensheath demyelinated axons[145]. Remyelination can occur within the whole lesion area, resulting in so called “shadow plaques”. Shadow plaques are sharply demarcated areas exhibiting thin myelin with a reduced density. In a luxol fast blue (LFB) staining these areas appear as light blue spots (figure 3). More frequently, however, lesions do not become completely remyelinated but only at the peripheral margins of the plaque. At later stages and during the progressive phase of the disease remyelination becomes less frequent or is completely absent. Only little is known about the reasons for remyelination to fail. However, there are individual differences in patients. Not surprisingly, longer disease durations and older age at death were associated with a higher number of remyelinated lesions[137].

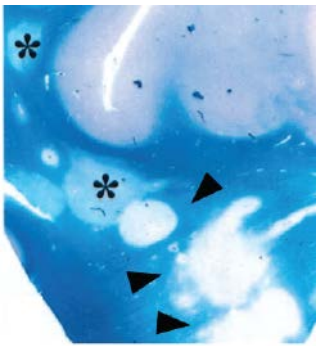

Figure 3: De- and remyelination in MS

Luxol fast blue staining (LFB) of a post-mortem tissue of a patient with RR MS (autopsy, female, aged 34 years, 156 months’ disease duration). Remyelinated shadow plaques (asterisks) and demyelinated lesion plaques (arrowheads) are visible (modified from[111]).

## 1.2 ROLE OF ASTROCYTES IN MS

Astrocytes are the most abundant cell type in the CNS and constitute nearly half of the brain cells in humans[119]. They have important functions in the trophic support of neurons and the maintenance of extracellular ion balance. Furthermore, astrocyte foot processes extend to capillaries in the CNS and biochemically support endothelial cells which form the BBB. Endothelial cells, astrocytes, the basal lamina and pericytes constitute the neurovascular unit which limits the molecular transport and cellular migration into the CNS[79]. Additionally, astrocytes play an important role in repair processes following any kind of brain injury.

In response to injury, astrocytes leave their quiescent state. They become hypertrophic, start to proliferate and upregulate glial fibrillary acidic protein (GFAP), nestin and vimentin[37]. Moreover, they can migrate to the site of injury and, by continuously proliferating, form a glial scar (reactive astrogliosis). In MS, astrogliosis is a characteristic feature and astrocytes constitute the majority of cells in demyelinated

lesions. The activation of astrocytes leads to a shift in the gene expression of adhesion molecules, antigen-presenting molecules, cytokines, growth factors and growth factor receptors as well as enzymes and enzyme inhibitors which influences the inflammatory response and cellular repair mechanisms[37, 216]. By interacting with neurons and other glial cells, astrocytes can additionally convey multifaceted functions during CNS injury and repair. It is difficult to separate the vast spectrum of astrocytic contributions in beneficial and detrimental as the outcome largely depends on the cellular composition of the lesion, the presence of other cytokines and the lesion stage. Established aspects of the astrocytic impact in lesion formation are briefly summarized in the following section. More comprehensive reviews on the role of astrocytes in lesion formation can be found elsewhere[36, 37, 173, 216].

### 1.2.1 Acute inflammation

During acute inflammation, astrocytes can impact the integrity of the BBB, the migration and direction of immune cells into the CNS parenchyma, promote survival of immune cells and directly damage neuronal structures[216] (figure 4, A). Astrocytes can mediate the migration of T cells by expression of vascular cell adhesion protein 1 (VCAM1) which binds to VLA-4 expressed on lymphocytes[71]. Furthermore, astrocytes are known to express matrix metalloproteinases (MMPs) in response to CNS injury which might break open tight junctions and impact the integrity of the BBB[53, 219]. Besides increasing the expression of MMPs, astrocytes can also upregulate MMP modulators, such as tissue inhibitor of metalloproteinases 1 (TIMP1). These inhibitors can counteract MMP-mediated impacts and convey protective effects[9]. Having entered the brain parenchyma immune cells can be directed by astrocytes through expression of various chemokines and guidance molecules. Monocyte chemoattractant protein 1 (MCP1)[147], chemokine (C-X3-C motif) ligand 1 (CX3CL1)[23] and chemokine (C-X-C motif) ligand 12 (CXCL12)[75] were found to be upregulated in astrocytes in MS lesions[40, 121] or experimental autoimmune encephalomyelitis (EAE)[186], an animal model recapitulating important aspects of MS. Indirect recruitment can be accomplished by upregulation of chemokines and cytokines in response to autocrine stimulation of astrocytes with tumor necrosis factor α (TNFα) and lymphotoxin α (LTα). The survival and expansion of B cells as well as the production of IgG in MS lesion is stimulated by the B cell-activating factor BAFF, which was found to be strongly induced in astrocytes present in active and chronic active MS lesions[98]. However, astrocytes do not only pave the way for immune cell-mediated cell damage but can also directly cause damage in acute inflammation. An increase in nitric oxide and superoxide radicals, by an upregulation of inducible nitric oxide synthase (iNOS) expression in astrocytes

present in MS plaques[51], is thought to directly harm oligodendrocytes and the myelin sheath. Axonal disruption that occurs in NAWM is attributed to reactive astrogliosis in the affected regions[28, 52]. In contrast to neuromyelitis optica (NMO), a loss or damage of astrocytes is not a feature of acute MS lesions.

### 1.2.2 Lesion resolution

Apart from the guidance of immune cells into brain parenchyma, astrocytes can also be involved in the recruitment of OPCs to the lesion plaque, in OPC differentiation and maturation and, therefore, participate in remyelination and lesion repair[216] (figure 4, B). The induction of interleukin 8 (IL8), CXCL1 and CXCL10 was observed in reactive astrocytes surrounding lesions[136]. The corresponding receptors (CXCR1, 2 and 3) were found increasingly expressed on oligodendrocytes in MS[136]. Moreover, semaphorins 3A and 3F (SEMA3A, SEMA3F) were shown to affect OPC migration and expression was increased in astrocytes surrounding active lesions[215]. SEMA3A acts as a repulsive and SEMA3F as an attractive signal[215].

Following migration, both oligodendrocyte proliferation as well as differentiation can be supported by astrocytes. Ciliary neurotrophic factor (CNTF), e.g., promotes OPC survival[6] and maturation into a myelinating phenotype[181]. Furthermore, it is an upstream regulator of fibroblast growth factor 2 (FGF2)[6] which is known to be a mitogen for OPCs[19]. Further molecules which were attributed to be involved in oligodendrocyte differentiation are: Adenosine triphosphate (ATP)[81], its degradation product adenosine[182], insulin-like growth factor 1 (IGF1)[65, 77], interleukin 1β (IL1β)[116], interleukin 11 (IL11)[225] and leukemia inhibitory factor (LIF)[81] which were shown to directly (adenosine, IGF1, IL11, LIF) or indirectly (ATP, IL1β) stimulate OPC differentiation and maturation. Additionally, transforming growth factor β (TGFβ), in the presence of platelet-derived growth factor (PDGF), also reduces proliferation and enhances differentiation *in vitro*[120]. On the other hand, TGFβ promotes Jagged1 production in astrocytes which can bind to Notch1 on oligodendrocytes and retains them in a premature state[86] (figure 4, A). Even the role of the glial scar in remyelination is ambivalent. Mostly, OPCs are found at the rim of demyelinated lesions and remyelination can be supported by above-mentioned mechanisms. However, as astrogliosis might impair migration of OPCs, they are barely found in the lesion center[17, 37].

The outcome of MS pathology and the degree of neuronal damage is widely influenced by the astrocyte response and their interaction with other cell types. Therefore, understanding astrocyte-mediated functions and the impact of astrogliosis at

different lesion stages is crucial to regulate tissue damage and repair in MS and makes astrogliosis a potential therapeutic target.

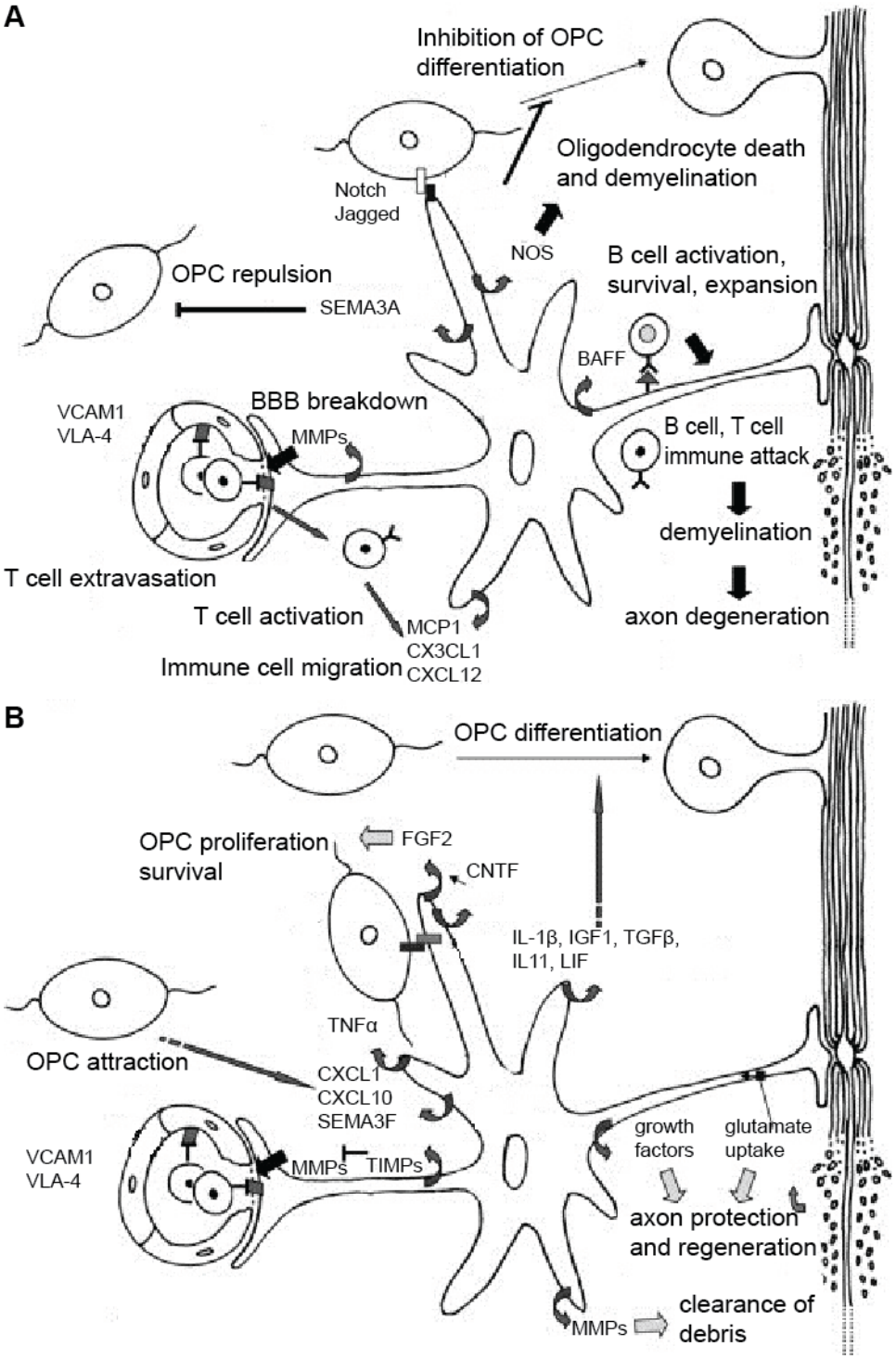


Figure 4: Putative effects of astrocytes in MS

**(A)** Acute inflammation. Astrocytes are involved in T cell extravasation, activation and in the recruitment of immune cells into the CNS parenchyma. Thereby, they support the immune attack, demyelination and degeneration of axons. Furthermore, astrocytes can indirectly damage myelin and oligodendrocytes and inhibit OPC differentiation. **(B)** Lesion resolution. Astrocytes can attract OPCs to the lesion site, support their proliferation, survival and differentiation. Moreover, protective effects are conveyed by secretion of growth factors and glutamate uptake. Expression of TIMPs might restore integrity of the BBB (see text for details. Modified from[216]).

## 1.3 GENE EXPRESSION PROFILING IN MS

Gene expression profiling and microarray based analysis enables the detection of thousands of regulated genes in a single RNA sample. This offers a wide range of possibilities to unravel pathways, molecular mechanisms and biological functions involved in the pathology of MS. Gene expression profiling in MS was performed in a broad range of studies mainly using peripheral blood mononuclear cells or brain tissue isolated from MS patients (reviewed in[55]). The application of gene expression profiling in peripheral blood mononuclear cells has revealed to be particularly useful to study the impact of different therapies in MS patients, as changes in peripheral leukocytes might precede changes in the CNS[55]. Studies using MS brain tissue, often have to struggle with poor RNA quality and a small number of samples. Furthermore, as most samples are derived from post-mortem tissue, analysis mainly represents the late progressive phase of the disease. Also, a proper characterization of lesions and lesion stage is mandatory for the interpretability of the results. Nonetheless, using gene expression profiling, important and interesting insights in MS lesion environment, involved molecular mechanisms and pathways could be gained.

In a previous study performed in our laboratory (Mohan et al., unpublished data), different MS lesions were macro-dissected, including remyelinated lesions, demyelinated lesions as well as active lesions. Gene expression was analyzed using a low density array and compared to the gene expression of control brain white matter and NAWM surrounding the plaque areas. In this analysis, FGF1, an abundant factor in human brain (figure 5, A) appeared to be upregulated in remyelinated areas (figure 5, B and C). This suggests a role of FGF1 in the regulation of MS pathology. These findings provided the basis for subsequent experiments aiming at the identification of FGF1-mediated mechanisms in MS pathology. FGF1 was found to promote myelination in an *in vitro* myelinating culture system as well as remyelination in a slice culture model (collaboration with T. Kuhlmann; Mohan et al., in preparation).

## 1.4 FIBROBLAST GROWTH FACTORS

FGFs convey a multitude of functions. During development, they are key players in tissue patterning and organogenesis, whereas, during adulthood they are involved in angiogenesis and repair in a plurality of mammalian tissues. The family of FGFs comprises 22 members. FGF1-FGF10 and FGF16-FGF23 can be further grouped into six subfamilies (FGF subfamilies 1; 4; 7; 8; 9 and 19) depending on their phylogeny and differences in sequence (figure 6)[84]. FGF11-FGF14 are factors highly homologue to FGFs but cannot activate the fibroblast growth factor receptors (FGFRs). They

constitute the FGF subfamily 11 (figure 6). FGF15 is the mouse homologue to human FGF19.

All FGFs, except of those belonging to the FGF1 and FGF9 subfamilies, do have signal peptides for secretion. Members of the FGF9 subfamily, although lacking a signal sequence, are secreted by the endoplasmic reticulum-Golgi pathway[153]. FGF1 and FGF2, in contrast, are secreted independently of the endoplasmic reticulum. Although the exact mechanism is not yet fully elucidated, they are probably released upon cell damage[66, 126]. All FGFs have a homologous core region, composed of 12 antiparallel β-strands (β1-β12) and variant N- and C-termini. The high affinity for proteoglycans, heparan sulfate and heparin is characteristic for FGFs. It can stabilize the interaction with the receptors[72, 220], increase the stimulation efficiency[168] and induce oligomerization[178]. Therefore, the interaction with heparan sulfate proteoglycan can be essential for the activation of FGFRs (figure 7). The heparan sulfate proteoglycan binding site is composed of the β1-β2 loop and regions of β10 and β12[26].

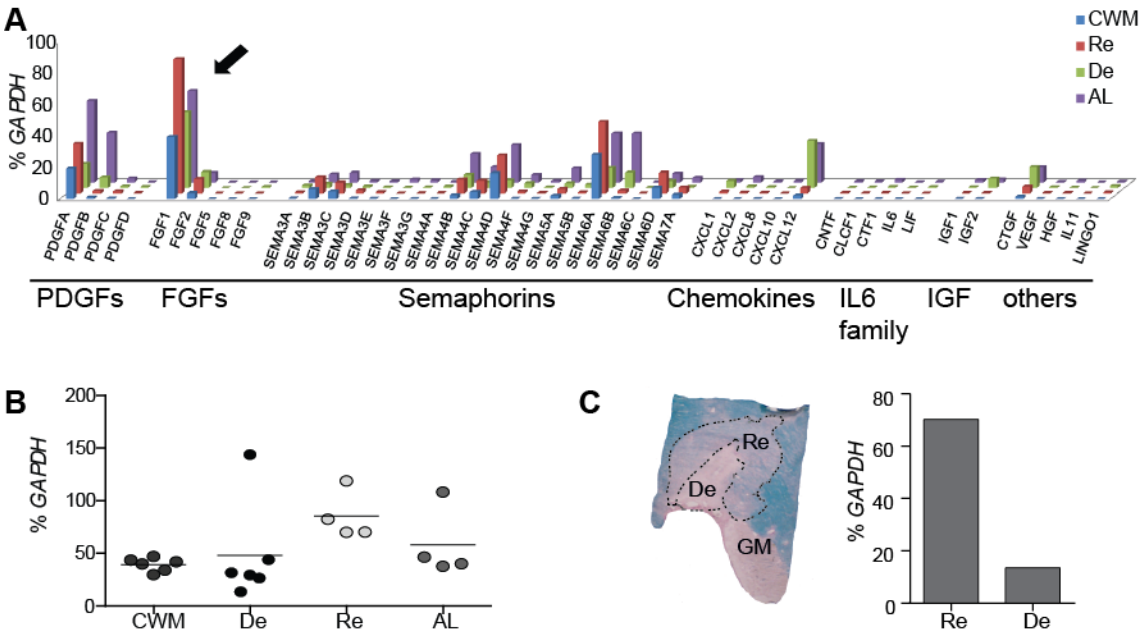


Figure 5: Enhanced expression of FGF1 in remyelinated plaques

CWM: control white matter; De: demyelinated; Re: remyelinated; AL: active lesion; GM: gray matter
**(A)** Relative RNA levels of factors potentially involved in oligodendrocyte regulation (% *GAPDH*, housekeeping gene). These include PDGFs, FGFs, semaphorins, chemokines, members of the IL6 family, IGFs and other factors with implications in the regulation of oligodendrocytes (*CTGF*, *VEGF*, *HGF*, *IL11*, *LINGO1*). *FGF1* is an abundant factor in human brain (arrow). **(B)** The relative *FGF1* level (% *GAPDH*, housekeeping gene) was elevated in remyelinated lesions compared to CWM, demyelinated and active lesions. **(C)** LFB/HE staining of a representative MS lesion. Marked areas were macro-dissected (left) and the corresponding relative *FGF1* level in re- and demyelinated areas (right) was determined by RT-qPCR (modified from Mohan at el., in preparation).

### 1.4.1 Fibroblast growth factor receptors

FGFs act by binding to FGFRs which belong to the tyrosine kinase receptor family. FGFRs have three extracellular immunoglobulin-like domains (domain I–domain III), a single pass transmembrane domain and an intracellular tyrosine kinase domain. It has been shown that domains II and III are necessary and sufficient for FGF binding. Four FGFRs have been identified (FGFR1-FGFR4) exhibiting a differential FGF-dependent binding affinity. The functional diversity of the FGF signaling can be further increased by alternative splicing of the domain III in FGFR1, FGFR2, and FGFR3 which impacts the FGF-FGFR binding specificity[214]. FGF1 is a universal ligand which can equally bind and activate all FGFRs and splicing variants and is, therefore, an exception of this rule. Furthermore, in some pathological conditions, such as cancer, FGF binding specificities can be abrogated[74].

Upon FGF binding, dimerization of FGFRs is initiated and followed by activation through intracellular autophosphorylation at a number of tyrosine residues (figure 7). Main intracellular substrates of activated FGFRs are phospholipase C (PLC) and FGFR substrate 2 (FRS2)[26] which are recruited to the activated receptors, become phosphorylated and initiate associated downstream pathways. Beside the activation of the PLC pathways, the phosphorylation of FRS2 results in activation of the Ras/mitogen activated protein kinase (MAPK) pathway as well as the phosphoinositide-3-kinase (PI3K)-Akt signaling pathway[50].

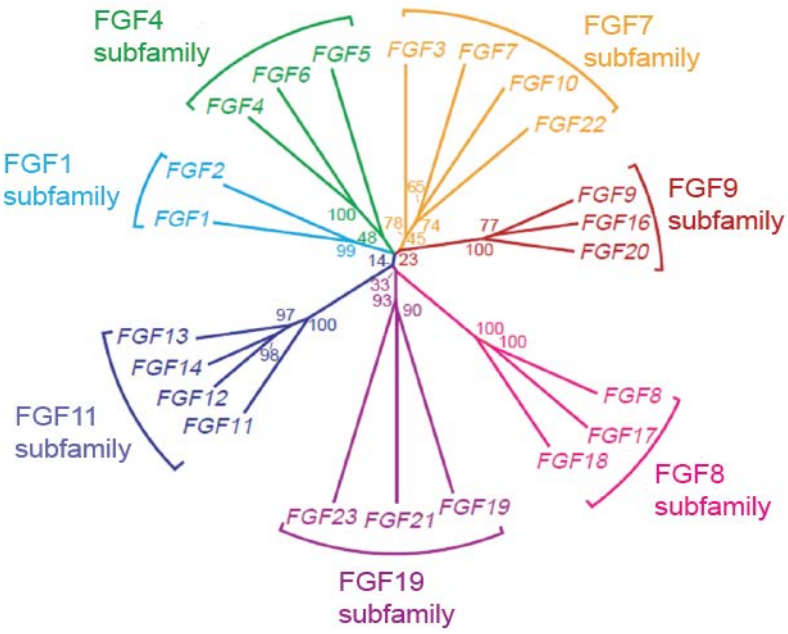


Figure 6: FGF subfamilies

Evolutionary relationship of the human FGF family. Branch length is proportional to the evolutionary distance between each gene (modified from[84]).

### 1.4.2 FGFRs in the CNS

The growth of several brain structures during development is controlled by differential FGF expression. In adults, FGFs regulate neurogenesis and axonal growth, they are implicated in the maintenance and repair of neural tissue and convey neuroprotective functions. Furthermore, the effects of FGFs were associated with learning and memory[153].

FGFR1, FGFR2 and FGFR3 are expressed by different cell types and in different areas of the adult CNS. FGFR4 is largely expressed during development and almost absent in the adult brain[153]. Regional differences in FGFR1-FGFR3 expression were observed. High levels of FGFR1-FGFR3 expression can be found in diencephalon and telencephalon, whereas, these receptors exhibit moderate expression levels in the metencephalon. Low expression is found in the myelencephalon[27]. Also, differential expression can be observed in different CNS cell types. Expression of FGFR1 is mostly localized to neurons[221] but can also be detected in astrocytes[189]. Furthermore, glia cells do express FGFR2 and FGFR3[13, 221].

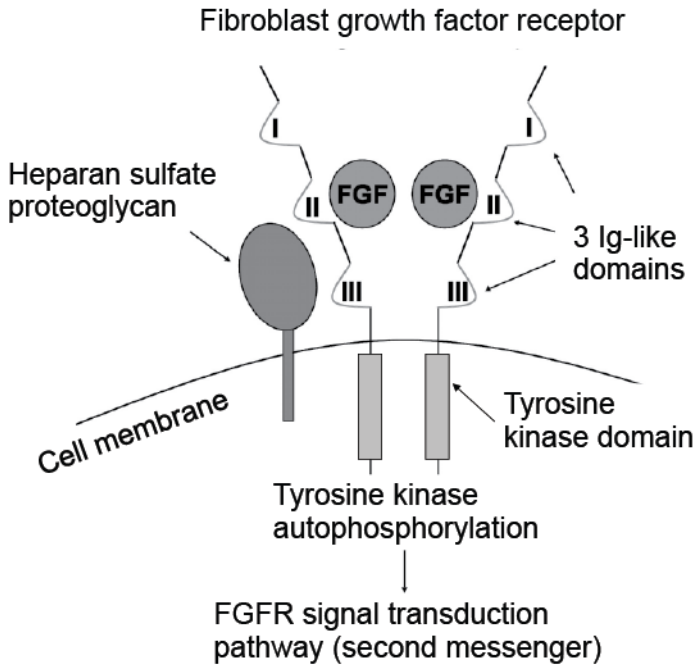


Figure 7: FGF receptor complex

Upon FGF binding, a complex of two FGFs, two FGFRs and heparan sulfate proteoglycan is formed. Autophosphorylation of tyrosine residues results in the activation of different downstream signaling pathways (modified from[193]).

### 1.4.3 FGF1

FGF1 (alternatively named acidic FGF) is a paracrine FGF ligand. Due to its high affinity for heparan sulfate proteoglycan, FGF1 acts in a localized manner close to the expressing cells[26]. Together with FGF2, FGF1 was the first FGF isolated from bovine brain and was named for its proliferative activity on fibroblasts[194]. As FGF1-/- mice are fully viable and fertile, its physiological role remains unclear. However, it was demonstrated to be involved in the maintenance of blood pressure[48] and seems to play a role in the regulation of adipogenesis[80]. Furthermore, it is thought to modulate organogenesis as it acts as a mitogen for mesoderm and neuroectoderm-derived cells and functions in angiogenesis.

In the CNS, FGF1 is widely expressed during the development and still present in adults with varying expression levels in different areas of the nervous system[56]. It is predominantly expressed by neurons[24, 57, 183] but can also be found in glial cells[83, 114]. In normal brain it seems to be implicated in learning processes and memory, as it was shown to impact long-term potentiation[161]. Furthermore, FGF1 acts as a potent mitogen for glial cells[59, 159, 163]. A role for FGF1 in CNS pathology has also been described. FGF1 was found to convey neuroprotective effects as it prevents neuronal death in seizure-associated brain damage[49] and ischemia[47, 162].

# 2 OBJECTIVES AND STRATEGY

MS is an inflammatory demyelinating disease of the CNS in which remyelination is often limited or absent. A better understanding of the complex interactions in the MS lesion environment and a more detailed knowledge of features conveyed by involved factors could provide the basis for therapy improvements. In a previous work, FGF1 was identified as an abundant factor in MS brains which was particularly induced in remyelinated lesions (Mohan et al., in preparation).

The objective of the present study was to provide further insight into potential roles of FGF1 in MS lesion development. Therefore, the following strategy was used:

First, a published[58] *in vitro* myelinating culture system was established in our laboratory and a rapid and easy to use method for the quantification of changes in myelination and axonal density was developed. This *in vitro* myelinating culture was subsequently used to investigate effects of FGF1 on myelination (independent study).

Secondly, the effects of FGF1 on *FGFR*-expressing primary human astrocytes in cell culture were analyzed. Changes in FGF1-mediated gene expression were measured using an Affymetrix GeneChip® Human Gene 1.0 ST array and alterations in the secretion of glycosylated proteins were determined by application of a recently developed secretome approach[99].

Thirdly, FGF1 expression was localized to different cell types in control brain as well as MS lesions by IHC.

# 3 MATERIALS AND METHODS

## 3.1 MATERIALS

### 3.1.1 Antibodies

Table 1: Primary and secondary antibodies

3.1.1.a Antibody-mediated complement dependent effects in rat *in vitro* myelinating cultures

| Specificity | Conjugate | Clone | Species and isotype | c [mg/ml] | Dilution | Source |
|---|---|---|---|---|---|---|
| Isotype control | - | - | Mouse IgG1 | 1 | 1:100 | Invitrogen, Carlsbad, USA |
| Isotype control | - | - | Mouse IgG2a | 1 | 1:100 | Invitrogen |
| MOG | - | Z2 | Mouse IgG2a | 0.65 | 1:65 | In-house hybridoma[138] |
| MOG | - | 8-18C5 | Mouse IgG1 | 2.33 | 1:233 | In-house hybridoma[108] |
| Pan-neurofascin | - | A12/18.1 | Mouse IgG2a | 1.4 | 1:140 | In-house hybridoma[117] |

3.1.1.b Immunocytochemistry

| | | | | | | |
|---|---|---|---|---|---|---|
| MOG | - | Z2 | Mouse IgG2a | 0.65 | 1:65 | In-house hybridoma[138] |
| Mouse IgG1 | Alexa 568 | - | Goat IgG | 2 | 1:2000 | Invitrogen |
| Mouse IgG2a | Alexa 488 | - | Goat IgG | 2 | 1:2000 | Invitrogen |
| Neurofilament | - | SMI-310 | Mouse IgG1 | Ascites | 1:1000 | abcam, Cambridge, UK |

3.1.1.c Immunohistochemistry (IHC): primary anti-human antibodies

| | | | | | | |
|---|---|---|---|---|---|---|
| CD20 | - | EP459Y | Rabbit | Supernatant | 1:50 | Epitomics, Burlingame, USA |
| CD3 | - | CD3-12 | Rat IgG1 | 1 | 1:100 | AbD Serotec, Kidlington, UK |
| CD68 | - | PG-M1 | Mouse IgG3 | - | 1:1 | DAKO, Glostrup, Denmark |
| FGF1 | - | 2E12 | Mouse IgG1 | 1 | 1:50 | abcam |
| GFAP | - | - | Rabbit IgG | 2.9 | 1:500 | DAKO |
| Iba-1 | - | - | Rabbit IgG | 0.5 | 1:333 | Wako, Neuss, Germany |
| Isotype control | - | 107.3 | Mouse IgG1 | 0.5 | 1:100 | BD, Heidelberg, Germany |
| Isotype control | - | - | Rat IgG1 | 1 | 1:100 | abcam |
| Isotype control | - | - | Rabbit IgG | 15 | 1:5000 | DAKO |
| KiM1P | - | - | Mouse IgG | - | 1:1000 | Radzun et al.[146] |

#### 3.1.1.d IHC: secondary antibodies

| | | | | | | |
|---|---|---|---|---|---|---|
| Mouse IgG1 | Biotin | A85-1 | Rat IgG1 | 0.5 | 1:250 | BD |
| Mouse IgG2a | Alexa 488 | - | Goat | 2 | 1:1000 | Invitrogen |
| Mouse IgG3 | Alexa 488 | - | Goat | 2 | 1:1000 | Invitrogen |
| Rabbit IgG | Alexa 488 | - | Goat | 2 | 1:1000 | Invitrogen |
| Rat IgG | Alexa 488 | - | Goat | 2 | 1:1000 | Invitrogen |

#### 3.1.1.e IHC: streptavidin constructs

| | | | | | | |
|---|---|---|---|---|---|---|
| Streptavidin | Alexa 568 | - | - | 2 | 1:1000 | Invitrogen |
| Streptavidin | Peroxidase | - | - | 1 | 1:1000 | Jackson IR, Pennsylvania, USA |

#### 3.1.1.f Flow cytometry: anti-human antibodies

| | | | | | | |
|---|---|---|---|---|---|---|
| CD3 | RPE | UCHT1 | Mouse IgG1 | - | 1:10 | DAKO |
| CD20 | PerCP | L27 | Mouse IgG1 | - | 1:5 | BD |

### 3.1.2 Quantitative PCR assays

Table 2: Quantitative PCR (qPCR) assays

| Gene name | qPCR assay | Detection | Company |
|---|---|---|---|
| *COL1A1* | Hs00164004_m1 | FAM-TAMRA | Applied Biosystems, Foster City, USA |
| *COL1A2* | Hs.PT.56a.26714610 | FAM-Iowa Black® FQ | IDT, Coralville, USA |
| *COL4A2* | Hs00300500_m1 | FAM-TAMRA | Applied Biosystems |
| *COL5A2* | Hs.PT.56a.24969881 | FAM-Iowa Black® FQ | IDT |
| *EGR1* | Hs00152928_m1 | FAM-TAMRA | Applied Biosystems |
| *FGFR1* | Hs.PT.51.20650860 | FAM-Iowa Black® FQ | IDT |
| *FGFR2* | Hs00240792_m1 | FAM-TAMRA | Applied Biosystems |
| *FGFR3* | Hs00179829_m1 | FAM-TAMRA | Applied Biosystems |
| *FGFR4* | Hs.PT.51.19306610 | FAM-Iowa Black® FQ | IDT |
| *HMOX1* | Hs01110250_m1 | FAM-TAMRA | Applied Biosystems |
| *IL8* | Hs00174103_m1 | FAM-TAMRA | Applied Biosystems |
| *KCNN4* | Hs00158470_m1 | FAM-TAMRA | Applied Biosystems |
| *LIF* | Hs00171455_m1 | FAM-TAMRA | Applied Biosystems |
| *MMP1* | Hs.PT.56a.38692586 | FAM-Iowa Black® FQ | IDT |
| *MMP9* | Hs00234579_m1 | FAM-TAMRA | Applied Biosystems |
| *NT5E* | Hs.PT.56a.21216674 | FAM-Iowa Black® FQ | IDT |
| *PPIA* | 4326316E | VIC-MGB | Applied Biosystems |
| *PTX3* | Hs00173615_m1 | FAM-TAMRA | Applied Biosystems |
| *SPHK1* | Hs00184211_m1 | FAM-TAMRA | Applied Biosystems |
| *TIMP1* | Hs.PT.56a.27632928 | FAM-Iowa Black® FQ | IDT |

### 3.1.3 Enzyme-linked immunosorbent assay

Table 3: Kits

| Target protein | Target species | Product number | Company |
|---|---|---|---|
| IL11 | Human | DY218 | R&D Systems |
| LIF | Human | BMS242MST | Bender MedSystems, Vienna, Austria |
| MMP9 | Human | DY911 | R&D Systems |
| MMP9 activity assay | Human | QZBmmp9H | QuickZyme, Leiden, Netherland |

### 3.1.4 *In vitro* myelinating culture

#### 3.1.4.a Neurosphere-derived astrocytes

Table 4: Growth factors and medium supplements

| | | |
|---|---|---|
| Glucose | 30 % glucose (w/v) in $H_2O$, filtered (0.22 µm) | Sigma-Aldrich, Taufkirchen, Germany |
| $NaHCO_3$ | 7.5 % $NaHCO_3$ (w/v) in $H_2O$, filtered (0.22 µm) | Sigma-Aldrich |
| Putrescine | 966 µg/ml putrescine in $H_2O$, filtered (0.22 µm) | Sigma-Aldrich |
| Sodium selenite | 520 µg/ml sodium selenite in $H_2O$, filtered (0.22 µm) | Sigma-Aldrich |
| Progesterone | 630 µg/ml progesterone in 95 % ethanol | Sigma-Aldrich |
| Epidermal growth factor (EGF), murine | 0.5 mg/ml EGF in 0.1% BSA/PBS | PeproTech, Rocky Hill, USA |

Table 5: 10x Hormone supplement for neurosphere medium

| | | |
|---|---|---|
| DMEM | 42.5 % | Invitrogen |
| F12 | 42.5 % | Invitrogen |
| 30 % Glucose | 0.6 % | Sigma-Aldrich |
| 7.5 % $NaHCO_3$ | 0.1125 % | Sigma-Aldrich |
| HEPES | 5 mM | Invitrogen |
| Transferrin | 1 mg/ml | Sigma-Aldrich |
| Insulin solution, human, # I9278 | 240 µg/ml | Sigma-Aldrich |
| Putrescine (966 µg/ml) | 96.6 µg/ml | Sigma-Aldrich |
| Sodium selenite (520 µg/ml) | 52 ng/ml | Sigma-Aldrich |
| Progesterone (630 µg/ml) | 6.3 ng/ml | Sigma-Aldrich |

Table 6: Neurosphere medium

| | | |
|---|---|---|
| DMEM | 42 % | Invitrogen |
| F12 | 42 % | Invitrogen |
| 10x Hormone supplement | 10 % | table 5 |
| 30 % Glucose | 0.6 % | Sigma-Aldrich |
| 7.5 % $NaHCO_3$ | 0.1125 % | Sigma-Aldrich |
| 1 M HEPES | 5 mM | Invitrogen |
| 200 mM L-Glutamine | 2 mM | PAN Biotech, Aidenbach, Germany |

Table 7: Rat astrocyte medium

| | | |
|---|---|---|
| DMEM | 89 % | Invitrogen |
| Fetal calf serum (FCS) | 10 % | Biochrom, Berlin, Germany |
| Penicillin-streptomycin | 1 % | Invitrogen |

### 3.1.4.b Spinal cord culture

Table 8: Medium supplements

| | | |
|---|---|---|
| Biotin, stock solution | 1 mg/ml biotin in 1M NaOH | Sigma-Aldrich |
| Biotin, working solution | Biotin stock solution diluted to 10 µg/ml with $H_2O$, filtered (0.22 µm) | Sigma-Aldrich |
| Hydrocortisone | 100 µM hydrocortisone in $H_2O$, filtered (0.22 µm) | Sigma-Aldrich |
| Insulin, bovine pancreas, # I1882 | 0.5 mg/ml insulin in 10 mM HCl, filtered (0.22 µm) | Sigma-Aldrich |

Table 9: Digestive enzymes

| | | |
|---|---|---|
| Collagenase | 1 % (w/v) collagenase in Leibovitz L-15, filtered (0.22 µm) | Both Invitrogen |
| Trypsin | 2.5 % (w/v) trypsin in HBSS without $Ca^{2+}$ and $Mg^{2+}$, filtered (0.22 µm) | Trypsin: Sigma-Aldrich<br>HBSS: Invitrogen |

Table 10: Soybean trypsin inhibitor solution

| | | |
|---|---|---|
| BSA, fraction V | 3 mg/ml | Sigma-Aldrich |
| Deoxyribonuclease I, bovine pancreas | 40 µg/ml | Sigma-Aldrich |
| Trypsin inhibitor, soybean | 520 µg/ml | Sigma-Aldrich |

All components dissolved in Leibovitz L-15 medium, filtered (0.22 µm)

Table 11: Plating medium (PM)

| | | |
|---|---|---|
| DMEM (4,5 g/l glucose) | 49 % | Invitrogen |
| Horse serum | 25 % | Sigma-Aldrich |
| HBSS | 25 % | Invitrogen |
| 200 mM L-Glutamine | 2 mM | PAN Biotech |

Table 12: Differentiation medium (DM)

| | | |
|---|---|---|
| DMEM (4.5 g/l glucose) | 99.4 % | Invitrogen |
| Biotin, working solution | 10 ng/ml | table 8 |
| Hydrocortisone, 100 µM | 18.1 ng/ml | table 8 |
| N1 medium supplement | 5 µl/ml | Sigma-Aldrich |

Table 13: Differentiation medium with insulin (DM/I)

| | | |
|---|---|---|
| DMEM (4.5 g/l glucose) | 97.4 % | Invitrogen |
| Biotin, working solution | 10 ng/ml | table 8 |
| Hydrocortisone, 100 µM | 18.1 ng/ml | table 8 |
| Insulin, 0.5 mg/ml | 10 µg/ml | table 8 |
| N1 medium supplement | 5 µl/ml | Sigma-Aldrich |

### 3.1.5 Tissue specimen

Table 14: Formalin fixed, paraffin embedded (FFPE) tissue specimen

#### 3.1.5.a Post-mortem brain tissue of MS patients

| Lesion type | Age | Gender | Sample ID | Source |
|---|---|---|---|---|
| Active | 53 | f | Nbb 03-130 #9.10 | Netherlands Brain Bank (Amsterdam, Netherland) |
| Active (chronic) | 66 | m | Nbb 06-054 # 2 | Netherlands Brain Bank |
| Remyelinated | 54 | f | A136/09 34 | Dr. A. Junker (UMG, Göttingen, Germany) |
| Remyelinated | 52 | f | A212/07 | Dr. A. Junker |
| Remyelinated | 59 | m | Nbb 03-074 # 1 | Netherlands Brain Bank |
| Remyelinated | 59 | m | Nbb 03-074 # 2 | Netherlands Brain Bank |
| Remyelinated/active | 59 | m | Nbb 03-074 # 3 | Netherlands Brain Bank |
| Remyelinated | 66 | m | Nbb 06-054 # 6 | Netherlands Brain Bank |
| Remyelinated | 70 | f | Nbb 06-077 #3 | Netherlands Brain Bank |
| Remyelinated | 62 | m | T8/00-17 | Dr. A. Junker |

#### 3.1.5.b Post-mortem control tissue of accident victims

| | | | | |
|---|---|---|---|---|
| Control (cortex) | 18 | m | 14668-07-17 | Klinikum Großhadern (LMU, Munich, Germany) |
| Control (cortex) | 16 | m | 14670-07-26c | Klinikum Großhadern |
| Control (brainstem) | 66 | f | 151460-07-18 | Klinikum Großhadern |

### 3.1.6 Buffers and solutions

Table 15: Tris-EDTA buffer

| | | |
|---|---|---|
| Trizma® Base | 10 mM | Sigma-Aldrich |
| Titriplex® | 1 mM | Merck, Darmstadt, Germany |
| Tween-20 | 0.05 % (v/v) | Bio-Rad, Hercules, USA |
| pH was adjusted to 9.0 | | |

Table 16: Luxol fast blue (LFB) solution

| | | |
|---|---|---|
| Solvent Blue 38 | 10 mg/ml | Sigma-Aldrich |
| Acetic acid, glacial | 5 µl/ml | Sigma-Aldrich |
| Ethanol | 95 % (v/v) in $H_2O$ | Sigma-Aldrich |
| Filtered (0.22 µm) | | |

Table 17: Flow cytometry buffer

| | | |
|---|---|---|
| BSA | 1 % | Sigma-Aldrich |
| Sodium azide | 0.1 % | Sigma-Aldrich |
| In PBS, filtered (0.22 µm) | | |

## 3.2 METHODS

### 3.2.1 *In vitro* myelinating culture

All incubation steps were performed in a humidified incubator (Heraeus, Langenselbold, Germany) at 37°C, 5 % and 7 % $CO_2$, respectively.

#### 3.2.1.a Animals

*Wistar rats.* All animals used in this study were obtained from the animal facility at the Max Planck Institutes of Biochemistry and Neurobiology.

#### 3.2.1.b Neurosphere-derived astrocytes

*Neurosphere preparation*. The method is based on work published by Reynolds and Weiss[154, 155] and was performed as described[174, 195] with some modifications. Every step with exception of the dissection was performed under sterile conditions. Briefly, the corpus striatum from P1 Wistar rat brains was dissected and a maximum of 4 striata per bijoux was collected in 1-2 ml Leibovitz L-15 medium (Sigma-Aldrich). A single cell suspension was obtained using a Pasteur pipette, cells were pelleted by centrifugation (140 g, 5 min) and subsequently resuspended in 20 ml neurosphere medium (table 6). Cells were transferred to a T75 $cm^3$ cell culture flask (BD) and the medium was supplemented with 20 ng/ml EGF. Cells were incubated at 37°C, 5 % $CO_2$ and supplemented with 5 ml medium and 20 ng/ml EGF every three days. After seven days neurospheres were large enough to be plated to form astrocytes.

*Poly-L lysine coating.* Cover glasses (13 mm diameter; ThermoFisher, Waltham, USA) were coated with 13.2 µg/ml poly-L-lysine in $H_2O$ (Sigma-Aldrich) for 2 h at 37°C, washed three times with $H_2O$ and placed in a 24-well plate (Corning Incorporated, Corning, USA).

*Astrocyte monolayer generation.* Neurospheres were differentiated into astrocytes as described in detail before with minor alterations[174, 195]. Briefly, neurospheres were pelleted by centrifugation (140 g, 5 min, 9°C), supernatant was removed, cells were triturated with a Pasteur pipette in 1 ml rat astrocyte medium (table 7) and subsequently filtered using a 44 µm cell strainer (BD). Single cells obtained from one T75 $cm^3$ cell culture flask were filled up to a total volume of 12 ml with rat astrocyte medium, were distributed equally on a 24-well plate endowed with poly-L lysine coated coverslips (500 µl/well) and subsequently filled up to 1 ml/well with rat astrocyte medium. Cells were incubated at 37°C, 5 % $CO_2$ changing 50 % of the media every three days. After 7 to 10 days, astrocytes formed a confluent monolayer on which spinal cord cultures were plated to form *in vitro* myelinating cultures.

### 3.2.1.c Spinal cord culture

Spinal cord cultures from embryonic Wistar rats were prepared as previously described[174] with some modifications.

*Spinal cord dissection.* Wistar rats were kill time-mated with the day of plugging denoted as E0.5. Embryos were used at day E15.5. After killing with an overdose of $CO_2$, the gravid uterus was removed from the mother and placed into ice cold HBSS (Invitrogen). Embryos were removed from embryonic sacs and decapitated without removal of the cervical flexure. For dissection of the spinal cord, the skin was removed and after exposure, the spinal cord was carefully taken out. Meninges were stripped, a maximum of 7 spinal cords was placed in 1 ml fresh, ice cold HBSS and gently triturated using a Pasteur glass pipette.

*Spinal cord single cell suspension.* Trypsin and collagenase (table 9) were added to the minced spinal cords at a final concentration of 0.25 % and 0.1 %, respectively and were incubated at 37°C for 15 min. Enzymatic digestion was stopped by the addition of two volumes soybean trypsin inhibitor solution (table 10) and digested tissue was pelleted by centrifugation (160 g, 5 min, 4°C). The supernatant was discarded, the cell pellet was resuspended in PM (table 11) and the cell number was determined using a Neubauer hemocytometer (Paul Marienfeld, Lauda-Königshofen, Germany). The cell suspension was diluted to a density of $3x10^6$ cells/ml with PM (table 11).

*Plating on astrocytes.* Astrocytes, homogeneously grown on cover glasses, were transferred from 24-well plates to 35 mm cell culture-treated culture dishes (Corning Incorporated) with a maximum of three cover glasses per 35 mm culture dish. Spinal cord single cell suspension was added on top of the astrocyte monolayer with a density of $1.5x10^5$ cells/cover glass and incubated at 37°C, 7 % $CO_2$ for 20 min. After spinal cord single cells attached to the astrocytes, medium was topped up with 350 µl/dish PM and 500 µl/dish DM/I (table 11, table 13) to a total volume of 1 ml.

*In vitro myelinating culture.* The spinal cord cultures were incubated at 37°C, 7 % $CO_2$ 50 % of the medium was replaced by fresh DM/I (table 13) every three days until day 12 *in vitro*. From day 12 to day 26, insulin was omitted from the culture medium to stimulate myelination. Therefore, DM (table 12) was used to replace 50 % of the medium every three days.

#### 3.2.1.d Antibody/complement treatment

Antibody-mediated complement dependent demyelination and the induction of axonal loss in *in vitro* myelinating cultures were described in detail before [58] and the method was applied with modifications. Briefly, at day 26 *in vitro* the medium was completely removed and 500 µl/dish DM supplemented with 2.5 % baby rabbit complement (Cederlane, Burlington, Canada) as well as 10 µg/ml of the respective antibody (table 1) was added to the *in vitro* myelinating cultures and incubated for 90 min (37°C, 7 % $CO_2$). Subsequently, medium was completely removed and cells were washed twice with PBS (Invitrogen). They were fixed by addition of 4 % PFA (Merck) in PBS (15 min, room temperature) and washed three times with PBS. Additionally, control cultures were treated with either (1) complement alone, (2) antibody with heat-inactivated complement (56°C, 30 min) or (3) the corresponding isotype controls (table 1) in combination with complement. Three independent cover glasses were analyzed for each condition.

### 3.2.2 Immunocytochemistry

All images were acquired on an inverted AxioVert200M fluorescent microscope (Carl Zeiss, Oberkochen, Germany) and processed using MetaMorph software version 7.7 (Molecular Devices, Sunnyvale, USA) and ImageJ software (NIH, Bethesda, USA).

*Fluorescence immunocytochemistry.* For fluorescence staining of the PFA fixed *in vitro* myelinating cultures, the cover glasses were carefully transferred to a 24-well plate. For the staining of intracellular targets, the cells were permeabilized with 0.5 % TritonX-100 in 1 % BSA/PBS (Carl Roth, Karlsruhe, Germany; Sigma-Aldrich) for 10 min and washed once with PBS. Unspecific antibody binding was blocked by incubation with 10 % FCS (Biochrom) in 1 % BSA/PBS for 30 min. Primary antibodies in 1 % BSA/PBS were either incubated over night at 4°C or 2 h at room temperature. Cells were washed three times and appropriate fluorochrome-conjugated secondary antibodies (in 1 % BSA/PBS) were applied for 20 min in the dark, at room temperature. For visualization of the nuclei, 1 µg/ml DAPI (Carl Roth) was added and incubated for additional 10 min in the dark. After three final washes, cover glasses were mounted

with Fluoromount G (SouthernBiotech, Birmingham, USA) upside down on microscope slides (ThermoFisher).

*Image acquisition.* For quantification, images were acquired at 10x magnification. *In vitro* myelinating cultures were characterized by determination of the axonal density, the degree of myelination and the loss of axons and myelin upon treatment with antibodies and complement. These basic characteristics were determined from at least 10 images acquired from three independent cover glasses.

*Quantification.* MetaMorph Software Version 7.7 was used for quantification of the axonal density as well as for the determination of myelination and demyelination. Briefly, 16-bit grayscale images were acquired, brightness and threshold were adjusted consistently and the images were equally transformed into binary pictures. Binary pictures were corrected using "shape factor" (defined as $4\pi A/P^2$) and area analysis as criteria. All modifications were automatically and equally applied to all images using the MetaMorph "journal loop" tool. The axonal density was calculated by dividing the pixel values of the corrected binary picture by the pixel values of the total image area. Likewise, the myelin density was calculated by dividing the pixel values determined for the myelin (corrected binary) by the pixel values determined for axons (corrected binary).

### 3.2.3 Primary human astrocytes

All incubations steps were performed in a humidified incubator (Heraeus) at 37°C and 10 % $CO_2$.

*Routine cell culture.* Human astrocytes of embryonic origin were obtained from the laboratory of Francesca Aloisi[7] (ISS, Rome, Italy) and stored in liquid nitrogen until needed. Human astrocytes derived from two different embryos were used for independent experiments. For routine cell culture DMEM (Invitrogen) was supplemented with 10 % FCS (Biochrom) and 1 % penicillin-streptomycin (Invitrogen). For splitting, cells were rinsed with PBS (Invitrogen) and detached by incubation with Trypsin-EDTA (PAA Laboratories, Pasching, Austria) for 10 to 15 min at 37°C. Cells were pelleted by centrifugation at 160 g for 10 min at 4°C, resuspended in DMEM and plated as needed. Human astrocytes were used at passages 2-6.

*FGF1 stimulation.* For stimulation of primary human astrocytes with FGF1, cells were grown to confluence in 24-well plates (Corning Incorporated) with the following exceptions: For the transcriptome microarray analysis, cells were grown in 6-well plates (Corning Incorporated). For the secretome analysis primary human astrocytes were grown in T175 $cm^3$ cell culture flasks (BD). Medium was changed to serum-free Panserin 401 (PAN Biotech) supplemented with 1 % penicillin-streptomycin 24 h prior

to stimulation. Unless stated otherwise 10 ng/ml recombinant human FGF1 (R&D Systems) and 5 U/ml Heparin-Natrium-25000-ratiopharm® (ratiopharm, Ulm, Germany) in Panserin 401 were used for stimulation of primary human astrocytes for the indicated time periods. Control samples were incubated with 5 U/ml Heparin-Natrium-25000-ratiopharm® in Panserin 401.

### 3.2.4 RNA techniques

*RNA extraction.* Total RNA from primary human astrocytes or purified lymphocytes (3.2.8) was extracted using the RNeasy Mini Kit (Qiagen, Venlo, Netherland) following the instructions provided by the manufacturer. Briefly, cells were lysed in an appropriate amount of RLT buffer supplemented with 10 µl/ml 2-mercaptoethanol (Sigma-Aldrich). One volume of 70 % ethanol (Sigma-Aldrich) was added and the total RNA was purified using the silica-membrane-equipped spin columns included in the kit. Purified RNA was eluted with 20 to 30 µl ribonuclease free water (Invitrogen).

*Reverse transcription (RT).* RNA concentration and purity was estimated using NanoDrop ND-1000 (PeqLab, Erlangen, Germany) and 200 to 500 ng of RNA were diluted with ribonuclease free water to a total volume of 10 µl/reaction. cDNA was generated using the High Capacity cDNA Reverse Transcription Kit (Applied Biosystems) according to the manufacturer instructions with a final volume of 20 µl/reaction.

*Quantitative PCR (qPCR).* 10 to 25 ng cDNA per reaction were applied (determined by means of the total RNA concentration). Either TaqMan® assays (Applied Biosystems) or PrimeTime® qPCR assays (IDT), listed in table 2, were used in combination with the TaqMan® PCR Core Reagent kit (Applied Biosystems) according to manufacturer instructions. Samples were run in MicroAmp™ Optical 96-well reaction plates (Applied Biosystems) in a 7900HT Fast Real-Time PCR System (Applied Biosystems). Data were analyzed using SDSv2.3 software (Applied Biosystems).

### 3.2.5 Transcriptome microarray analysis

*FGF1 stimulation of primary human astrocytes.* Primary human astrocytes were incubated with either 5 U/ml heparin or 10 ng/ml FGF1 and 5 U/ml heparin for 8 h and 24 h, respectively. The experiment was performed in triplicates for each condition and time point, resulting in a total of 12 independent samples which were used for the transcriptome microarray analysis. RNA was purified as described (3.2.4) and samples were further processed by IMGM laboratories (Martinsried, Germany) as briefly summarized in the following paragraph.

*Affymetrix GeneChip® Human Gene 1.0 ST array.* Determination of RNA concentration, purity (NanoDrop ND-1000; PeqLab) and integrity (RNA 6000 Nano LabChip kits and 2100 Bioanalyzer; both Agilent Technologies, Santa Clara, USA) as well as the genome-wide expression profiling was provided by the genomic services of IMGM laboratories. As an index for RNA quality, the RNA integrity number (RIN) was used which is derived from the electrophoretic profile. The RIN scale ranges from 1 to 10. A RIN of 10 denotes an excellent RNA quality, while a RIN value of 1 indicates massive degradation. For RIN calculation, the algorithm does not rely on the 28S/18S-rRNA ratio alone, but takes the entire electrophoretic profile into account. GeneChip® Human Gene 1.0 ST arrays (Affymetrix, Santa Clara, USA) were used in combination with a random-priming and one-color based hybridization protocol. Briefly, 200 ng of total RNA was spiked with polyadenylated transcripts using the Gene Chip® Poly-A Control kit (Affymetrix). Subsequently, RNA was reverse transcribed into cDNA and then converted into cRNA by *in vitro* transcription. The generated cRNA was transcribed into anti-strand and strand cDNA during a second cycle transcription. The strand cDNA was purified using the Ambion WT Expression kit (Life Technologies, Carlsbad, USA). The WT Terminal Labeling and Control kit (Affymetrix) were used to fragment the single stranded cDNA and label it with biotin. The labeled and fragmented sense-strand cDNA was spiked with cDNA hybridization controls (GeneChip Hybridization Control kit; Affymetrix), hybridized at 45°C for 17 h on separate GeneChip® Human Gene 1.0 ST arrays and stained in two binding cycles using anti-biotin antibodies and streptavidin, R-phycoerythrin conjugates. For washing and preserving, the GeneChip® 3000 Fluidics Station in combination with the GeneChip® Command Console and the Fluidics Control software v3.2.0.1515 (all Affymetrix) were used. Fluorescent signal intensities were detected with the GeneChip® 3000 scanner and AGCC Scan Control software v3.2.3.1515 (both Affymetrix). An automatic grid was arranged and raw data (*.DAT files) were processed to generate image and intensity files (*.CEL, *.JPG) by the AGCC software.

*Transcriptome microarray analysis.* Analysis of raw data, obtained from IMGM laboratories, was performed in collaboration with the laboratory of Cinthia Farina (San Raffaele Scientific Institute, Milan, Italy). The Affymetrix GeneChip® Human Gene 1.0 ST array comprised 33297 probes. Data were normalized and 26839 probes passed filtering criteria (p-value ≤ 0.05 in 25 % of the samples). No outliers were present based on principal component analysis and unsupervised hierarchical clustering. Differential gene expression was performed using the oneChannelGUI package[160] implemented in the R-Bioconductor platform (FHCRC, Seattle, USA). The LIMMA[172] algorithm, which implements the empirical Bayes method, as well as the

Benjamini&Hochberg method were used to adjust the p-value. Genes, fulfilling the following criteria, were considered to be regulated: $p \leq 0.05$, fold-change $\geq |1.4|$ and expression level ≥ 100 in one group.

### 3.2.6 Secretome analysis

The secretome analysis was performed in collaboration with the laboratory of Stefan Lichtenthaler (DZNE, Munich). Protein enrichment using the recently developed SPECS method[99] and mass spectrometry measurements were performed by Peer-Hendrik Kuhn (DZNE, Munich), as briefly summarized in the following paragraphs.

*Astrocyte stimulation and azido sugar labeling.* Primary human astrocytes were grown and stimulated with FGF1 as described (3.2.3) with the following alterations: 30 ml Panserin 401 medium per T175 $cm^3$ cell culture flask was supplemented with 10 ng/ml FGF1 and 5 U/ml heparin as well as 1 mmol/l of tetraacetyl-N-azidoacetyl-mannosamine (ManNAz) obtained as a 50 µmol/l stock solution in ethanol (DZNE, Munich). Cells were grown in the presence of FGF1, heparin and ManNAz for 48 h at 37°C, 10 % $CO_2$. The conditioned supernatant was filtered (0.22 µm; Millipore, Billerica, USA) and further processed by Peer-Hendrik Kuhn.

*Secretome protein enrichment with click sugars (SPECS).* The development and procedure of the SPECS method was described in detail before[99]. Briefly, free ManNAz present in the cell culture supernatant, was removed by centrifugal concentration (30 kDa cutoff, 4600 rpm, 4°C) using Vivaspin20® columns (Satorius, Goettingen, Germany) and $H_2O$ as concentrate diluent. The azide-labeled glycoproteins were biotinylated by addition of 100 nmol/l DBCO-PEG12-biotin (Click Chemistry Tools, Scottsdale, USA) in $H_2O$ and were incubated over night at 4°C. Free DBCO-PEG12-Biotin was removed by centrifugal concentration as described for ManNAz. For denaturation, PBS with 2 mmol/l TCEP (Carl Roth) and 2 % SDS (v/v) (Bio-Rad) were added and the samples were loaded on a 10 ml Poly-Prep® chromatography column (Bio-Rad) equipped with streptavidin beads. Beads were washed with 1 % SDS (v/v) in PBS and boiled with 3 mmol/l biotin in urea sample buffer. Biotinylated glycoproteins were separated on a 10 % SDS gel. Bands, except of the BSA band (66.5 kDa), were cut and trypsin-digested[169].

*Mass spectrometry and data analysis.* Mass spectrometry analysis was performed on an Easy-nLC nanoflow HPLC system 1000 connected to an LTQ-Velos Orbitrap (both ThermoFisher). Peptides were separated by reverse phase chromatography (75-min gradient, 5 % to 40 % acetonitrile, 250 nl/min flow rate). The measurement method consisted of an initial FTMS scan recorded in profile mode with 30 000 m/z resolution, a mass range from 300 to 2000 m/z and a target value of 1 000 000. Subsequently,

collision-induced dissociation fragmentation was performed for the 20 most intense ions with an isolation width of 2 Da in the ion trap. A target value of 10 000, enabled charge state screening, a monoisotopic precursor selection, 35 % normalized collision energy, an activation time of 10 ms, wide band activation and a dynamic exclusion list with 30 s exclusion time were applied. Three biological replicates were analyzed using the MaxQuant suite software version 1 (MPI of Biochemistry, Martinsried, Germany) with a UniProt database for *Homo sapiens*.

Proteins displaying a significant change in expression in all experiments were categorized using a gene ontology enrichment tool[31] (The Gene Ontology Consortium, http://amigo.geneontology.org/cgi-bin/amigo/term_enrichment, accessed in October, 2013)

### 3.2.7 Immunohistochemistry

*Tissue sectioning.* Formalin fixed, paraffin embedded (FFPE) 4 µm sections of human control- and MS-brain as well as human adenoids (table 14) were cut at the laboratory of Tanja Kuhlmann (WWU Münster, Germany) within the scope of the SFB-TR128.

All images were acquired on either Leica LMD7000 or Leica DMI6000 microscopes (Leica Microsystems, Wetzlar, Germany) and processed using ImageJ software (NIH).

*Deparaffinization.* FFPE sections were deparaffinized by performing the following washes: Two times 10 min XEM-200 (Xylol substitute; Vogel, Giessen, Germany), 10 min 50 % XEM-200 (v/v) in ethanol, 5 min 100 % ethanol, 5 min 95 % ethanol, 5 min 70 % ethanol, 5 min 50 % ethanol, final wash with $H_2O$.

*Antigen retrieval.* Heat induced epitope retrieval (HIER) was performed using a conventional steamer (Gastroback, Hollenstedt, Germany). Sections were boiled in pre-heated (95°C to 100°C) Tris-EDTA buffer (table 15) for 30 min, cooled to room temperature and subjected either to chromogenic- or fluorescence-staining.

*3.3'-Diaminobenzidine (DAB) staining.* Following deparaffinization and HIER, the sections were rinsed for 5 min in 0.05 % Triton-X in PBS, followed by a PBS wash (5 min) and finally blocked with 10 % FCS and 1 % BSA in PBS for 1 h at room temperature. The primary antibodies were either incubated in 1 % BSA in PBS for 2 h at room temperature or overnight at 4°C. Sections were rinsed with PBS (three times 5 min), incubated with 0.3 % $H_2O_2$ in PBS for 15 min at room temperature followed by a wash with PBS (5 min). Secondary biotin-conjugated antibodies in 1 % BSA in PBS were applied for 30 min at room temperature and the PBS wash was repeated (three times 5 min). Streptavidin-conjugated peroxidase was incubated for 30 min at room temperature, followed by a final PBS wash (three times 5 min). DAB chromogen was

diluted 1:50 in DAB buffer (both DAKO) and incubated until DAB precipitate appeared. Reaction was stopped by rinsing slides with $H_2O$. If required, sections were incubated for 2 seconds in haematoxylin solution (Merck) and dehydrated by the following washes: 1 min 70 % ethanol, 1 min 95 % ethanol, 1 min 100 % ethanol, 1 min XEM-200. Sections were mounted with Eukitt® mounting medium (Sigma-Aldrich).

*Luxol fast blue (LFB) staining.* FFPE tissue sections were deparaffinized, hydrated to 95 % ethanol and incubated in LFB solution (table 16) over night at 60°C. Sections were rinsed in 95 % ethanol and subsequently in $H_2O$. Sections were destained by incubation in 0.05 % aqueous lithium carbonate solution (Sigma-Aldrich) for 5 seconds and a subsequent 10 seconds wash in 70 % ethanol (destaining was repeated as required). Sections were rinsed in $H_2O$, dehydrated and mounted with Eukitt® mounting medium.

*Fluorescence staining.* Following deparaffinization and HIER the sections were rinsed for 5 min in 0.05 % Triton-X in PBS, washed in PBS (5 min) and blocked with 10 % FCS and 1 % BSA in PBS for 1 h at room temperature. The primary antibodies were incubated as described for the DAB staining. Subsequently, fluorescent dye coupled antibodies with 1 µg/ml DAPI (Carl Roth) were applied for 30 min at room temperature. Sections were washed with PBS (three times 5 min) and mounted with Fluoromount G (SouthernBiotech).

*Tyramide signal amplification (TSA™).* For fluorescence staining of FGF1, additional signal amplification was needed. Therefore, the TSA Plus Biotin kit (PerkinElmer, Waltham, USA) was used according to manufacturer instructions. Briefly, sections were deparaffinized, HIER was performed as described, sections were incubated with 0.3 % $H_2O_2$ for 15 min at room temperature and blocked with TSA blocking reagent (PerkinElmer). FGF1 antibody was incubated for 1 h, sections were washed with PBS (three times 5 min) and a secondary biotinylated antibody was applied for 1 h at room temperature. Sections were washed with PBS (three times 5 min) and incubated with streptavidin-peroxidase for 30 min at room temperature. Following a PBS wash (three times 5 min), the signal was amplified by incubation with TSA reagent for 1 min. Sections were washed with PBS (three times 5 min) and the fluorescent dye-streptavidin construct was applied for 30 min at room temperature. Sections were washed (three times 5 min) and mounted with Fluoromount G.

### 3.2.8 Lymphocyte isolation from human tonsils

*Human tonsils.* Fresh human palatine tonsils (from tonsillectomies or tonsillotomies) were obtained from PD Dr. Klaus Stelter (Klinik und Poliklinik für Hals-Nasen-

Ohrenheilkunde, Klinikum LMU, Germany) and processed immediately after the surgery.

*Lymphocyte isolation.* After surgery, tonsils were transferred to ice-cold PBS supplemented with 1 % penicillin-streptomycin. Tissue was minced and single cell suspension was obtained by dissociating tissue through a 40 µm cell strainer (BD). Cells were centrifuged (300 g, 6 min, 4°C) and resuspended in ice-cold PBS. Cells were counted using a Neubauer hemocytometer. A maximum of $10^8$ cells were purified from a total of $2x10^8$ cells using magnetic anti-CD19 beads or anti-CD3 beads (Miltenyi, Bergisch Gladbach, Germany) for B cell depletion and T cell separation, according to manufacturer instructions.

### 3.2.9 Enzyme-linked immunosorbent assay

*ELISA.* For a complete list of ELISA kits used in this study see table 3. 96-well flat bottom MaxiSorp® plates (Nunc, Langenselbold, Germany) were used if pre-coated plates were not provided with the kit. Coating, incubation of cell supernatant and detection was performed according to manufacturer instructions. If substrate was not supplied with the kit, 3.3',5.5'-Tetramethylbenzidine (TMB) solution (Sigma-Aldrich) was used and color reaction was stopped by adding one volume of 1 mol/l $H_2SO_4$. Absorption was measured with a Wallac Victor$^2$ 1420 multilabel counter (PerkinElmer) at 450 nm and 540 nm, respectively.

*MMP9 activity assay.* To measure active MMP9 (naturally occurring) or total active MMP9 (following activation with APMA), an ELISA-based MMP9 activity assay (QuickZyme) was used according to manufacturer instruction. Absorption was measured with a Wallac Victor$^2$ 1420 multilabel counter (PerkinElmer) at 405 nm after 1 h and 4 h incubation, respectively.

### 3.2.10 Flow cytometry

*Flow cytometry staining and data analysis.* Cells were transferred into 96-well V-bottom plates (Nunc), centrifuged at 280 g for 5 min at 4°C and washed once with 200 µl flow cytometry buffer (table 17). Cell pellet was resuspended in 50 µl/well flow cytometry buffer containing directly labeled antibodies (table 1) and incubated for 20 min at 4°C in the dark. Cells were washed three times and resuspended in 200 µl flow cytometry buffer. Fluorescence was measured using a FACSverse™ flow cytometer (BD) and data were analyzed with FlowJo 7.6 software (TreeStar, Ashland, USA).

# 4 RESULTS

## 4.1 *IN VITRO* MYELINATING CULTURE

### 4.1.1 Generation of *in vitro* myelinating cultures

The method for the generation of *in vitro* myelinating cultures was originally developed for cells obtained from embryonic mouse spinal cords[196] and modified for cells isolated from embryonic rat spinal cords in the laboratory of Susan Barnett[58]. The aim was to establish this method in our laboratory as a stable, reproducible and easy to quantify *in vitro* system, which could be used for determining effects of external stimuli on neurons and glial cells. Having established the *in vitro* myelinating culture system, it was used to determine effects of FGF1 on myelination and neuronal growth in an independent study in our laboratory (Mohan et al., in preparation).

The changes in cell growth and morphology during the maturation of the *in vitro* myelinating cultures were followed using ICC. Antibodies detecting either neurofilament in axons (SMI-310) or MOG (Z2), a myelin protein which is specifically expressed on the outermost layer of the myelin sheath as well as in oligodendrocytes, were applied.

A timeline indicating preparation and growth of the myelinating cultures (based on previously published data[196] and results of the present study) is given in figure 8, A. To generate the astrocyte monolayer, cells were grown for 14 days *in vitro* (DIV). After seeding of the spinal cord cells, 28 DIV were needed to obtain fully myelinated cultures. After seeding, neuronal processes formed within two weeks *in vitro,* accompanied by the proliferation of OPCs in the presence of insulin in the cell culture medium[196]. During this time only few oligodendrocytes with short processes (figure 8, B; 10 DIV, inset) could be observed. Withdrawal of insulin supported the differentiation of oligodendrocytes, the formation of processes and the wrapping of axons (figure 8, B; 63x 28 DIV). An increase in myelination was especially detected between 15 and 24 DIV (figure 8, A and B). Myelination reached a maximum between 24 and 28 DIV and cultures were used for experiments during this period. At later time points, cell death of astrocytes comprising the feeder layer was frequently observed and caused the subsequent death of neurons and oligodendrocytes (figure 8, B; 28 DIV). Therefore, the *in vitro* myelinating culture was not used for experiments at time points later than 28 DIV.

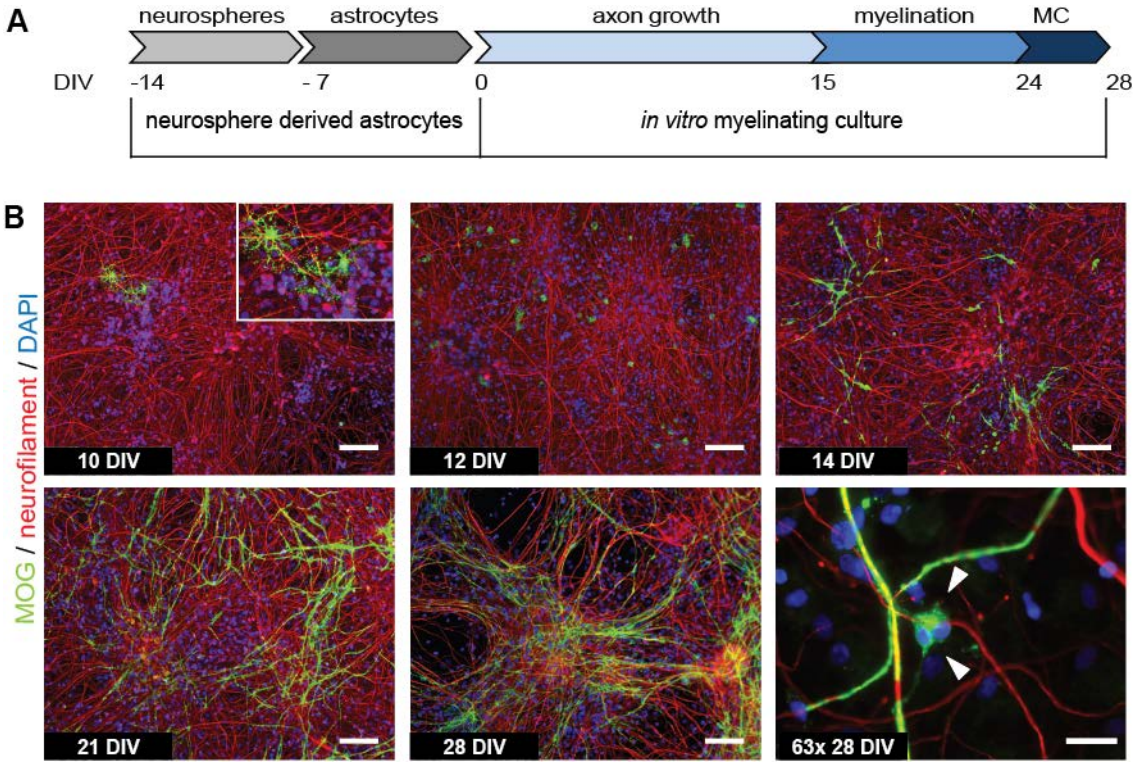


Figure 8: Generation of *in vitro* myelinating cultures

DIV: days *in vitro*; MC: *in vitro* myelinating cultures
**(A)** Timeline: Generation of in vitro myelinating cultures. Neurosphere-derived astrocytes were generated 14 days prior to the seeding of spinal cord cells. After having formed a confluent monolayer, the rat spinal cord cells were seeded on top of the astrocyte monolayer (0 DIV). Between 0 and 15 DIV neuronal processes and axons formed a dense mesh. This was followed by a phase of extensive myelination. Between 15 and 24 DIV myelination increased and peaked. Between 24 and 28 DIV, *in vitro* myelinating cultures were used for experiments. **(B)** Representative images of different time points after seeding of spinal cord cells. Neurons and axonal processes were visualized using a neurofilament-specific antibody (SMI-310, red). Oligodendrocytes and myelin were stained with a MOG-specific antibody (Z2, green). Nuclei were stained with DAPI (blue). From 10 to 12 DIV reticulated axonal processes could be observed. Only few immature oligodendrocytes (inset in 10 DIV) were detected. The number of oligodendrocytes increased over time (12 DIV). Insulin deprivation from the cell culture medium at 12 DIV resulted in maturation of oligodendrocytes and increased myelination of axonal processes (14 to 28 DIV). An enhanced cell death was observed at time points later than 28 DIV. Oligodendrocyte processes ensheathing axons could be observed at higher magnification (63x 28 DIV; arrowheads). Scale bars represent 50 µm (10x magnification) and 10 µm (63x magnification), respectively.

### 4.1.2 Quantification of axonal density and myelination

For the simple applicability of *in vitro* myelinating cultures, it is crucial to develop a rapid and easy to use method for the quantification of changes in myelination and axonal density. MetaMorph software was used to establish an automated quantification method in which 16-bit grayscale images, acquired with a Zeiss AxioVert200M microscope, were transformed into binary pictures. The binary pictures were corrected according to the shape factor and area of the objects. Subsequently, pixel values of the binary pictures could be used to calculate axonal density and myelination of the *in vitro* myelinating cultures (figure 9, A).

The *in vitro* myelinating cultures should be used as a bioassay to identify effects of external stimuli such as FGF1. To test, whether the quantification method allowed the detection of differences in axonal density and myelination caused by external stimuli, a previously established experiment was performed[58]. Cultures were treated with antibodies and complement to evaluate complement dependent degradation of axons and myelin. Besides appropriate isotype controls, antibodies targeting MOG (Z2 and 8-18C5) as well as pan-neurofascin (A12/18.1) were used. MOG is localized at the outermost myelin sheath, whereas, the pan-neurofascin antibody detects isoforms 155 and 186 present on oligodendrocytes and neurons. For visualization, antibodies detecting neurofilament (SMI-310) and MOG (Z2) were used (figure 9, B).

The result of the quantification of one representative experiment is shown in figure 9, C. The axonal density in medium treated control cultures was 37 ± 4.5 % with a myelination of 11.4 ± 1.5 % (figure 9, C; column 1). The treatment of myelinating cultures with the MOG-specific antibodies Z2 and 8-18C5 plus complement resulted in a complete degradation of myelin (figure 9, C, column 6 and 7). A representative image of Z2-mediated complement dependent degradation of myelin is shown in figure 9, B (63x Z2). Treatment with the pan-neurofascin antibody A12/18.1 depleted axons as well as myelin (figure 9, C; column 8). No reduction of myelin and axons was seen for complement without antibody and for the isotype controls (figure 9, C; column 2, 4 and 5). Z2 and heat-inactivated complement induced a slight demyelination (figure 9, C, column 3). The increase in axonal density seen in IgG1 treated samples (figure 9, C, column 4) resulted most likely from an above average cell density and was not reproducible in subsequent experiments (not shown).

Taken together, an *in vitro* myelinating culture system was established and a quick and easy to use method to assess changes in myelination as well as axonal density was developed. Reliability of the quantification method and the possibility of manipulating the system by application of external stimuli, were proven by antibody-mediated complement dependent demyelination and axonal loss.

The impact of FGF1 on *in vitro* myelinating cultures was tested in an independent study performed in our laboratory (Mohan et al, in preparation).

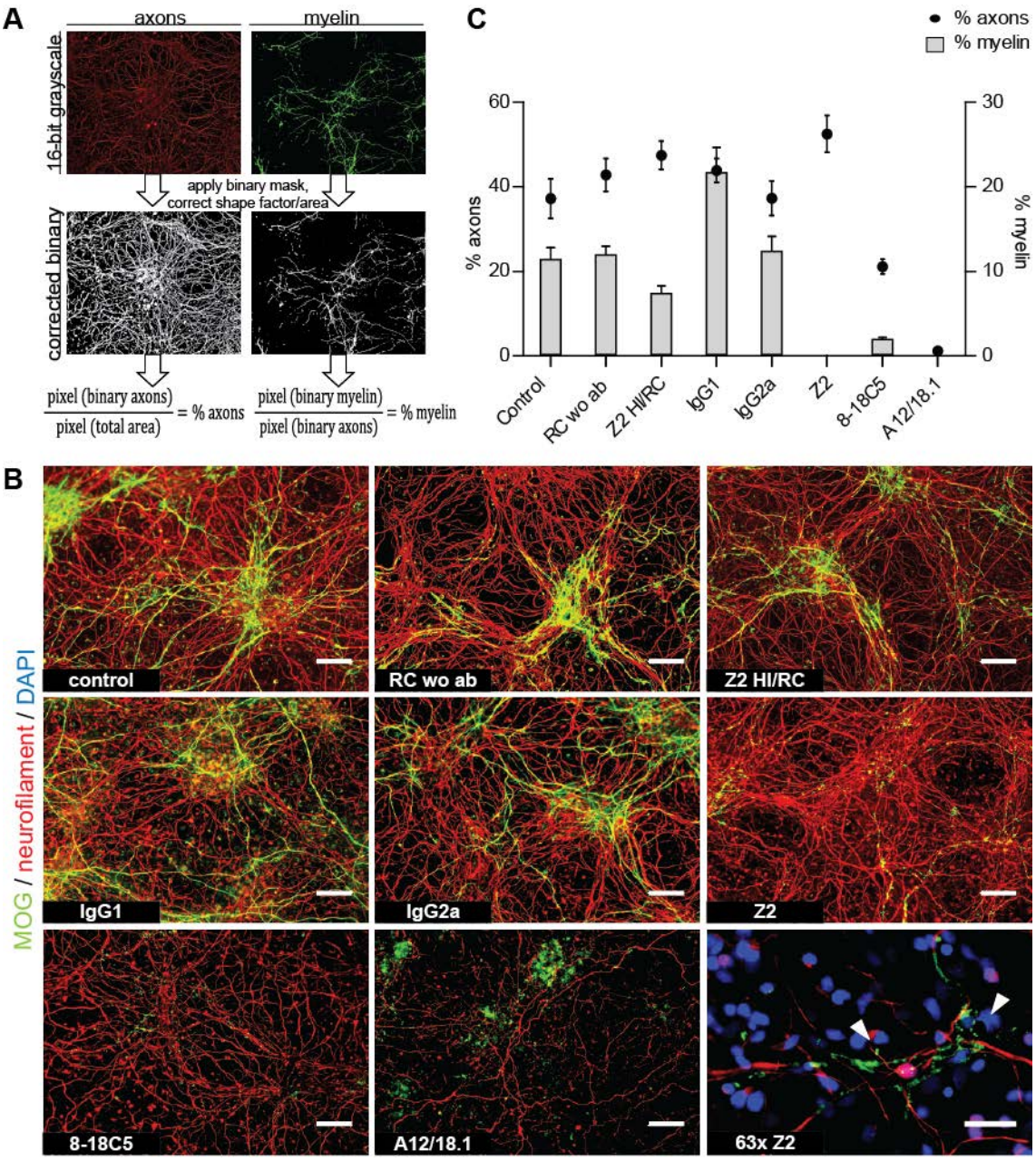


Figure 9: Quantification of antibody-mediated complement dependent effects on *in vitro* myelinating cultures

RC wo ab: rabbit complement without antibody; HI/RC: heat-inactivated rabbit complement
**(A)** Scheme for the quantification of axonal density and myelination. **(B and C)** *In vitro* myelinating cultures were treated with antibodies targeting neurofascin (A12/18.1) or MOG (Z2 and 8-18C5) plus complement. Additionally, control cultures were treated with: Medium (control), isotype controls plus complement (IgG1, IgG2a), Z2 plus heat-inactivated complement (Z2 HI/RC). **(B)** Representative images of antibody-mediated complement dependent effects on *in vitro* myelinating cultures. Neurons and axonal processes were stained with a neurofilament-specific antibody (red). Oligodendrocytes and myelin were stained with a MOG-specific antibody (green). In 63x magnification nuclei are visualized with DAPI (blue). Degradation of myelin can be observed (arrowheads). Scale bars represent 50 µm (10x magnification) and 10 µm (63x magnification). **(C)** Quantification of antibody-mediated complement dependent effects. Treatment with Z2 and 8-18C5 abolished myelin. Axons as well as myelin were completely depleted by treatment with A12/18.1 and complement. The result represents the mean of 10 images acquired from 3 replicates in one representative experiment. Error bars show SEM.

## 4.2 FGF1-MEDIATED EFFECTS IN HUMAN ASTROCYTES

The second part of the present study can be considered as a follow up study of work which was previously performed in our laboratory (Mohan et al., in preparation). In the work of Mohan et al., a transcript profiling of different macro-dissected MS lesions was performed and FGF1 was found to be upregulated in remyelinated areas, suggesting a role of FGF1 in the regulation of myelination. The *in vitro* myelinating cultures, established as described before, were used to decipher the effects of FGF1 on the regulation of myelination *in vitro*. FGF1 turned out to contribute to enhanced myelination (Mohan et al., in preparation). Based on this finding, the present work aimed at the identification of additional functions of FGF1 considering *FGF*-expressing astrocytes as target cells.

### 4.2.1 Characterization of primary human astrocytes as a target of FGF1 stimulation

#### 4.2.1.a RNA level of *FGFRs* in primary human astrocytes

Primary human astrocytes were used as cell culture system to elucidate potential effects of FGF1. RT-qPCR was used to determine the RNA levels of *FGFR1–FGFR4*. The highest transcript level was detected for *FGFR1*. The *FGFR4* level was approximately 7-fold lower compared to *FGFR1*. *FGFR2* and *FGFR3* were barely detectable (figure 10). No difference in the *FGFR* RNA levels could be detected for cells kept in serum-free medium (for FGF1 stimulation) or DMEM supplemented with 10 % FCS (for routine cell culture; not shown).

#### 4.2.1.b *HMOX1* level as an indicator for FGF1 responsiveness

Heparin is well known to stabilize the interaction of various FGFs with their receptors[72, 220], to induce oligomerization[178] and to increase the stimulation efficiency[168]. Therefore, FGF1 together with heparin was applied to stimulate primary human astrocytes. The level of *HMOX1* RNA was used as a positive control to establish optimal stimulation conditions as *HMOX1* has previously been shown to be upregulated following FGF1 stimulation of astrocytes[211]. 5 U/ml heparin were incubated with either 10 ng/ml or 50 ng/ml FGF1 for 8 h and 24 h, respectively. Heparin alone did not result in an increase of *HMOX1* RNA compared to serum-free medium treated control cells (figure 11). In astrocytes, treated additionally with either 10 ng/ml or 50 ng/ml FGF1, the *HMOX1* level was approximately 3.5-fold increased (figure 11). Although, stimulation with 10 ng/ml and 50 ng/ml FGF1 resulted in an elevated *HMOX1* level, no further induction could be seen at the higher concentration. Therefore, in subsequent experiments cells were stimulated with 5 U/ml heparin and 10 ng/ml FGF1.

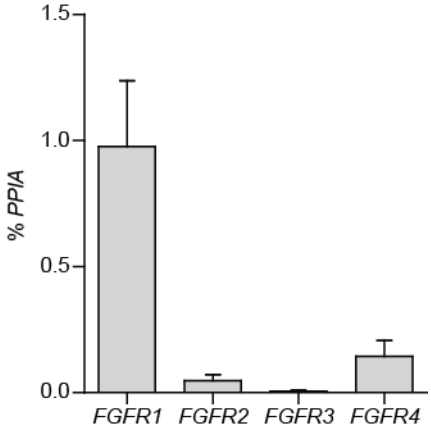


Figure 10: RNA level of *FGFRs* in primary human astrocytes

Relative RNA levels of *FGFR1* – *FGFR4* in primary human astrocytes (% *PPIA*, housekeeping gene). Highest level was detected for *FGFR1*. Lower RNA levels were detected for *FGFR4*. RNA of *FGFR2* and *FGFR3* was barely detectable. Results represent the mean of three independent experiments; error bars show SEM.

Taken together, of all FGFRs tested, *FGFR1* exhibited the highest RNA level. Using the *HMOX1* RNA level as positive control, 10 ng/ml FGF1 and 5 U/ml heparin were determined to be suitable for stimulating astrocytes. Heparin without FGF1 did not impact the *HMOX1* level.

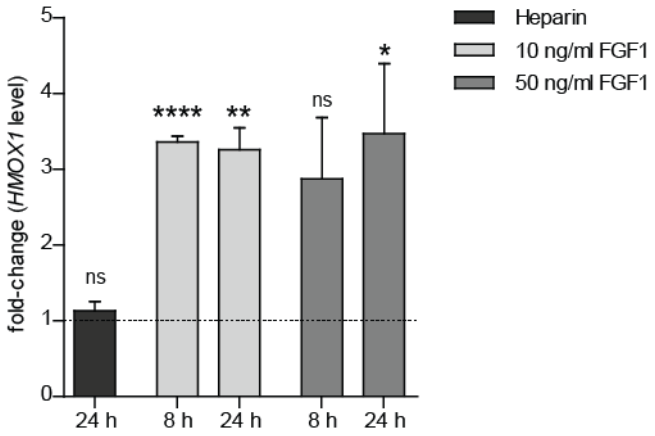


Figure 11: *HMOX1* level as an indicator for FGF1 responsiveness

ns: not significant; p≤0.05 (*); p≤0.01 (**); p≤0.001 (***); p≤0.0001 (****)
Stimulation of primary human astrocytes with heparin and FGF1. 5 U/ml heparin were incubated with either 10 ng/ml or 50 ng/ml FGF1 for 8 h and 24 h, respectively. Heparin alone did not increase the *HMOX1* RNA level compared to astrocytes in serum-free medium. In astrocytes, additionally treated with either 10 or 50 ng/ml FGF1, *HMOX1* levels were approximately 3.5-fold increased. Results represent the mean of n=4 (8 h, 10 ng/ml and 50 ng/ml FGF1), n=5 (heparin and 24 h 10 ng/ml FGF1) and n=6 (24 h 50 ng/ml FGF1) independent experiments. T-test was used to calculate the significance of fold-changes; error bars show SEM.

### 4.2.2 Transcriptome microarray analysis

Having determined suitable stimulation conditions and a proper control gene, the effects of FGF1 stimulation on primary human astrocytes were investigated using an Affymetrix GeneChip® Human Gene 1.0 ST array. The microarray screening service was provided by IMGM laboratories and the data was analyzed in collaboration with the laboratory of Cinthia Farina. The results of the Affymetrix GeneChip® Human Gene 1.0 ST array, as obtained from the IMGM laboratories, are shown in 9.1.

#### 4.2.2.a Transcriptome microarray data analysis

For analyzing differentially expressed genes (DEGs) significantly altered after FGF1 stimulation, the RNA levels of medium-treated and FGF1-stimulated samples were compared. After normalization and filtering, the data were analyzed by principal component analysis and hierarchical sample clustering methods. No outliers were identified (hierarchical tree diagram in figure 12, A). DEGs were further analyzed as described in 3.2.5. A total of 272 DEGs after 8 h and 895 DEGs after 24 h of FGF1 stimulation was detected (figure 12, B and C). Approximately 82 % (225 DEGs) of the genes regulated after 8 h were regulated in the same direction after 24 h. None of the identified genes was regulated in opposite directions at two different time points. After 8 h the majority of DEGs (approximately 95 %) displayed fold-changes between 1.4- to 3.0-fold and 0.7- to 0.3-fold, respectively (figure 12, C). A similar distribution was obtained after 24 h. However, the number of DEGs which were more than 4.0-fold and less than 0.25-fold regulated increased from 1 to 8 (DEGs upregulated) and from 0 to 2 (DEGs downregulated), respectively (figure 12, C).

In summary, by comparing heparin-treated with FGF1-stimulated human astrocytes at 8 h and 24 h, a total of 272 (8 h) and 859 (24 h) DEGs was identified. An intersection of 225 DEGs was expressed after 8 h and 24 h in equal directions.

#### 4.2.2.b Genes regulated in astrocytes upon FGF1 treatment

The interpretation of a list of DEGs is facilitated if the genes exhibit similarities, e.g., in their functional annotation. A commonly used method, to handle large sets of data such as obtained from a transcriptome microarray analysis, is to perform an enrichment analysis to identify significantly represented pathways or gene ontology terms. Therefore, an enrichment analysis for FGF1-mediated pathways, processes, metabolic networks and for gene ontology terms was performed. This analysis pointed to an impact of FGF1 on pathways and processes involved in cell cycle regulation (not shown).

To get a further impression of FGF1-mediated effects in human astrocytes, the focus was set on genes which were found to be upregulated at 8 h and 24 h (115 DEGs, for a complete list see 9.2). Within this subset, genes with known functions in MS pathology were further analyzed. 8 DEGs with implications in MS were identified (figure 13, A and 9.2). These genes code for proteins which could be grouped into the following categories: (1) proteins, known to be elevated in response to acute inflammation (*PTX3, IL8, HMOX1, PTHLH*), (2) proteins with proinflammatory and immune modulatory roles (*IL8, KCNN4, SPHK1*), (3) proteins, impacting lymphocyte migration or the constitution of the ECM (*NT5E, IL8*) and (4) proteins with an established protective function in MS by the support of remyelination (*LIF, IL8, PTX3*). Four of them have already been identified to be elevated in serum and CSF of MS patients and/or EAE models (*PTX3, IL8, SPHK1* and *LIF*). Changes in the RNA levels of these genes at 8 h and 24 h as determined by the transcriptome microarray analysis are shown in figure 13, A and C.

In summary, among the 115 DEGs which were elevated in response to FGF1 stimulation of human astrocytes after 8 h and 24 h, 8 DEGs with established functions in MS were identified and selected for further validations.

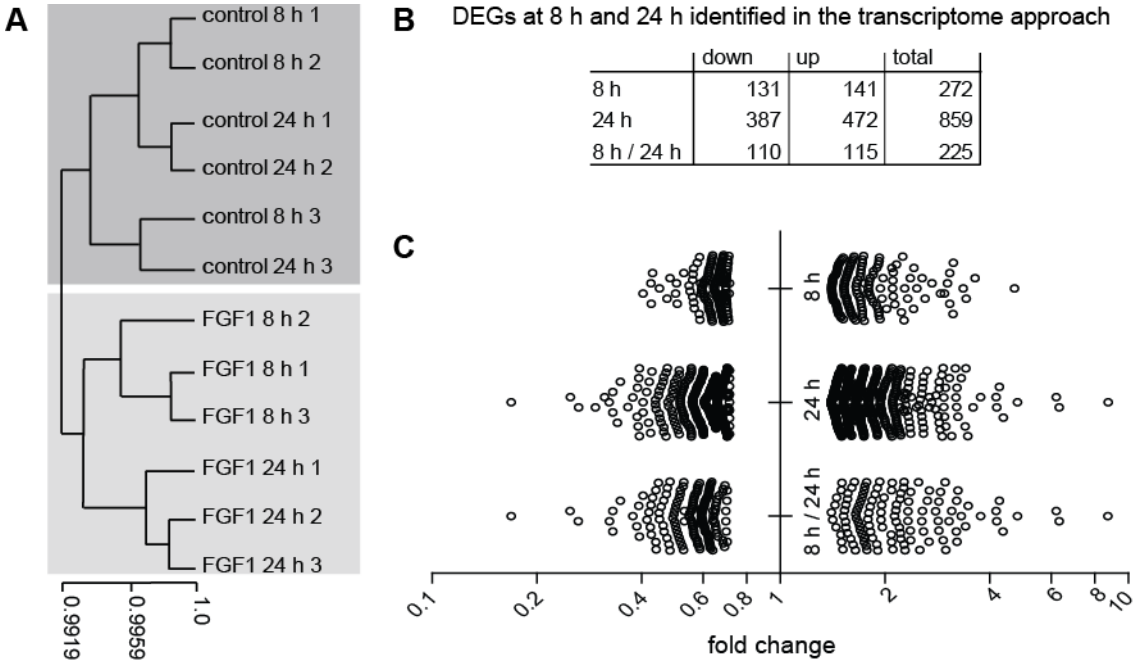


Figure 12: Transcriptome microarray analysis of FGF1-stimulated human astrocytes

**(A)** Hierarchical tree diagram. Applying the hierarchical tree clustering method, the samples could be divided in two distinct groups representing untreated control samples and FGF1-stimulated samples. No outliers were identified. **(B)** Total number of genes which were found to be regulated at 8 h, 24 h and at both time points (8 h / 24 h). None of the genes was found to be regulated in opposite directions at two different time points. Approximately 82 % of the DEGs found to be regulated after 8 h were also detected after 24 h. **(C)** Fold-changes in the RNA level of DEGs at 8 h and 24 h. Approximately 95 % of all DEGs displayed changes in the RNA level between 1.4- to 3.0-fold and 0.7- to 0.3-fold, respectively. The total number of DEGs altered more than 4.0-fold and less than 0.25-fold increased at 24 h. In “8 h / 24 h” the fold-changes detected at 24 h are depicted.

#### 4.2.2.c Validation of the transcriptome microarray analysis

The results, obtained from the transcriptome microarray analysis were validated by determining the RNA levels of DEGs with implications in MS (figure 13, A). Using RT-qPCR, an induction could be demonstrated for all of them at 8 h and 24 h (figure 13, B). Due to variations between independent replicates, not all tested genes appeared to be significantly altered at both time points (figure 13, B). Direct comparison of fold-changes in the RNA levels detected in the transcriptome- and the RT-qPCR-approach revealed a strong correlation of results. Fold-changes in RNA levels determined by RT-qPCR were equal to or higher than the fold-changes obtained from the transcriptome approach (figure 13, C).

Taken together, results obtained from the transcriptome microarray analysis could be validated for genes with known implications in MS by RT-qPCR. By comparing the fold-changes in RNA levels detected in the different approaches, a strong correlation was found.

### 4.2.3 Secretome analysis

#### 4.2.3.a Identification of glycosylated and secreted proteins

Besides the transcriptome microarray analysis a secretome analysis was performed to unravel FGF1-mediated effects in human astrocytes which might not have become apparent by screening the RNA levels. The secretome analysis comprised the labeling of secreted and glycosylated proteins with the recently established SPECS method[99] and the subsequent analysis of these proteins using mass spectrometry. 303 proteins were identified to be regulated in the cell culture supernatant of FGF1-treated human astrocytes (figure 14) of which 72 proteins were significantly changed (for a complete list of significantly induced proteins see 9.3). 33 out of 72 proteins were increased and 39 out of 72 proteins were decreased. In average, proteins were altered ± 3.32-fold compared to heparin-treated control samples. 19 out of 72 proteins exceeded this average (>|3|-fold). Of the 19 proteins 11 were detected to be up- and 8 were down-regulated (figure 14; labeled dots).

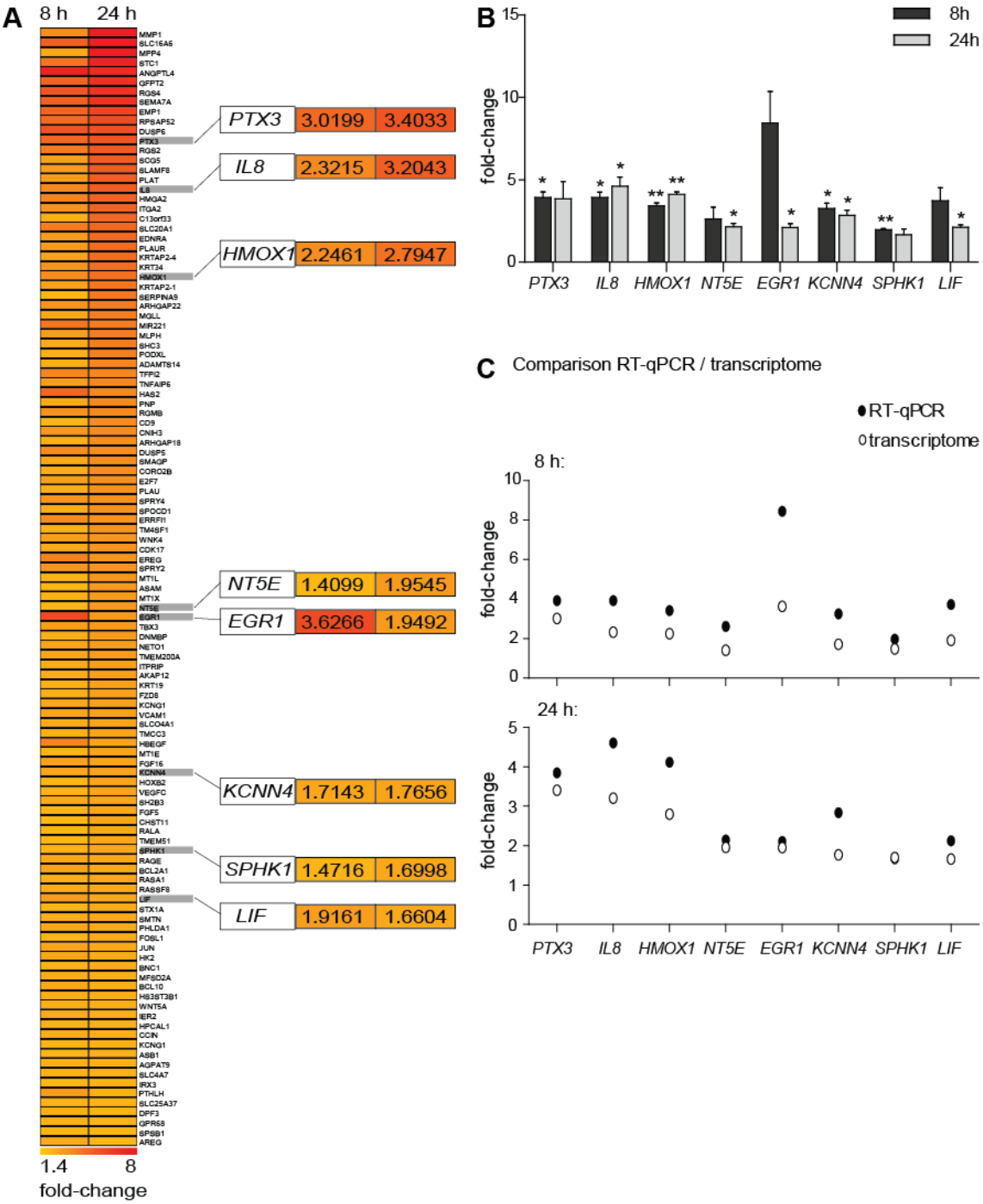


Figure 13: Validation of transcriptome microarray data

p≤0.05 (*); p≤0.01 (**)
**(A**) Elevated DEGs identified in the transcriptome microarray analysis after 8 h and 24 h FGF1 stimulation. DEGs chosen for validation using RT-qPCR are highlighted on the right. The fold-changes in RNA levels detected at 8 h and 24 h are stated. **(B)** Validation of transcriptome results using RT-qPCR. Elevation of the RNA level was proven for all tested DEGs. Results represent the mean of three independent samples. T-test was used to calculate the significance of fold-changes, error bars show SEM. **(C)** Comparison of the fold-changes in RNA levels detected in the transcriptome and the RT-qPCR approach. The fold-changes detected by RT-qPCR were higher than or equal to values of the transcriptome microarray analysis.

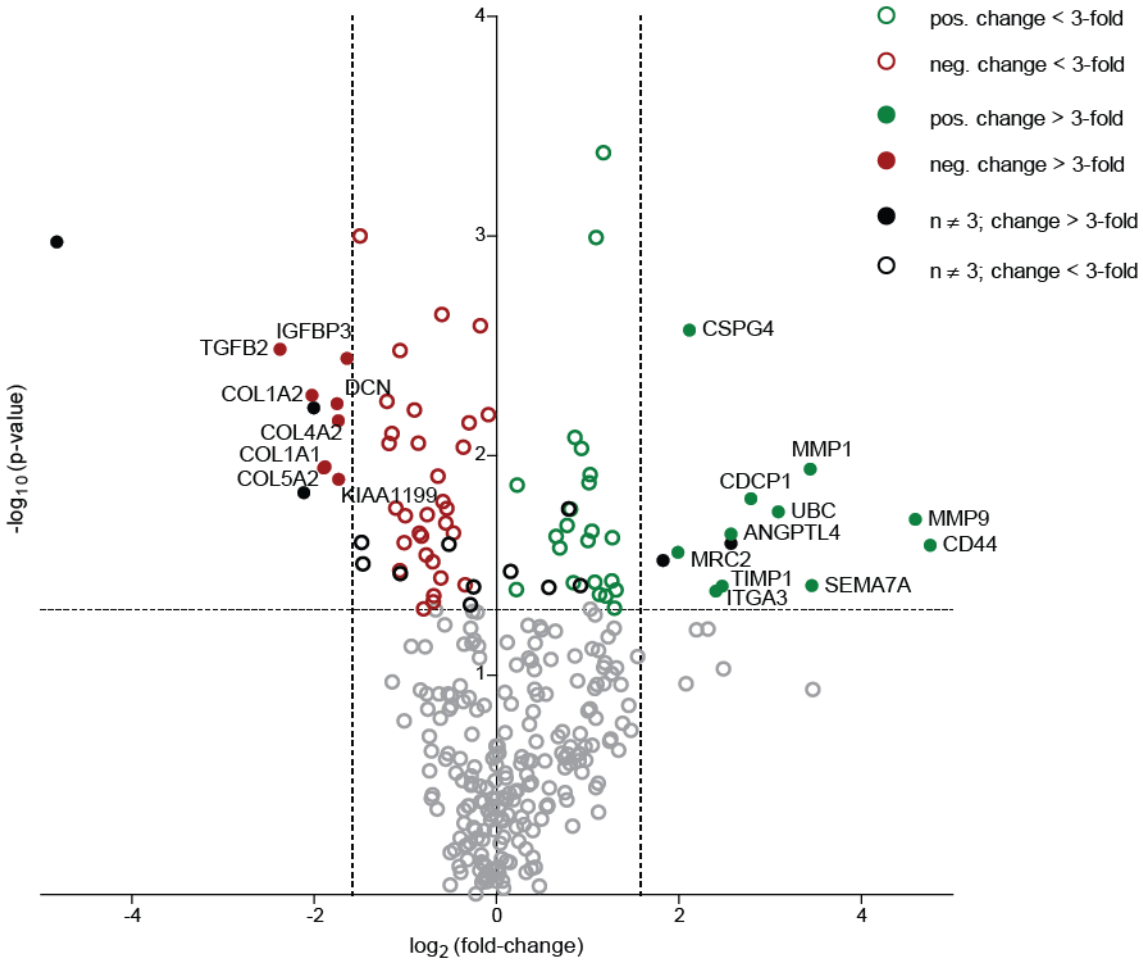


Figure 14: Glycosylated proteins in supernatant of FGF1-treated astrocytes

Proteins identified in the cell culture supernatant of FGF1-treated human astrocytes. Horizontal dashed line determines the threshold for p<0.05. Vertical dashed lines represent the average protein induction (|3|-fold). Black circles and dots: proteins identified in two out of three independent experiments (n≠3). Green circles: upregulation < 3-fold. Red circles: downregulation < 3-fold. Green dots: upregulation > 3-fold. Red dots: downregulation > 3-fold. Labels of proteins regulated >|3|-fold are included.

### 4.2.3.a Grouping of induced proteins based on gene ontology

The FGF1-regulated proteins were grouped using a gene ontology enrichment tool[31] (3.2.6). Twelve specific gene ontology terms were identified which comprised at least five of the proteins detected in the secretome approach (figure 15, A). Proteins belonging to the identified gene ontology terms are listed in table 18.

Three out of twelve identified gene ontology groups were directly linked to ECM degradation and ECM adhesion. Those were: “collagen catabolic process”, “cell-matrix adhesion” and “ECM disassembly”. Furthermore, FGF1 signaling led to an induction of proteins involved in the biological process of “cell migration” and “chemotaxis”. Proteins belonging to these groups largely overlapped with those involved in “axon guidance” (compare table 18). In addition, FGF1 treatment led to an induction of proteins participating in “wound healing” which also comprised proteins involved in “blood coagulation” and “platelet activation” (compare table 18). Finally, proteins participating in “blood vessel development”, “enzyme linked receptor protein signaling pathways”

and in the “response to growth factor stimuli” were detected to be mediated by FGF1 treatment of human astrocytes (all summarized in figure 15, A).

The focus was set on proteins which stood out because of their strong FGF1-dependent up- or downregulation (alteration >|3|-fold; compare figure 14). This group comprised 19 proteins of which 11 were up- and 8 were downregulated. Interestingly, ≥75 % of the proteins which were >|3|-fold regulated belonged to the two gene ontology groups “collagen degradation” and “ECM disassembly” (figure 15, B). Within other gene ontology groups, proteins >|3|-fold regulated represented 25 % to 47 % of the proteins (figure 15, B).

This suggests that FGF1 stimulation of human astrocytes mainly has an impact on the degradation and the disassembly of the ECM. Proteins upregulated >3-fold in these groups were: MMP1, MMP9 and TIMP1 (a modulator of MMPs). Proteins, downregulated >3-fold in these groups were: COL1A1, COL1A2, COL4A2 and COL5A2 (compare figure 14).

Taken together, proteins detected in the secretome analysis could be assigned to twelve specific gene ontology groups using a gene ontology enrichment tool. The focus was set on proteins which were induced above average in response to FGF1 treatment (>|3|-fold). They were found to be disproportionately represented in the gene ontology groups “collagen catabolic process” and “ECM disassembly”. ECM degrading enzymes such as MMP1 and MMP9, as well as the MMP regulator TIMP1 were strongly enhanced, whereas, essential constituents of the ECM (COL1A1, COL1A2, COL4A2, and COL5A2) were diminished.

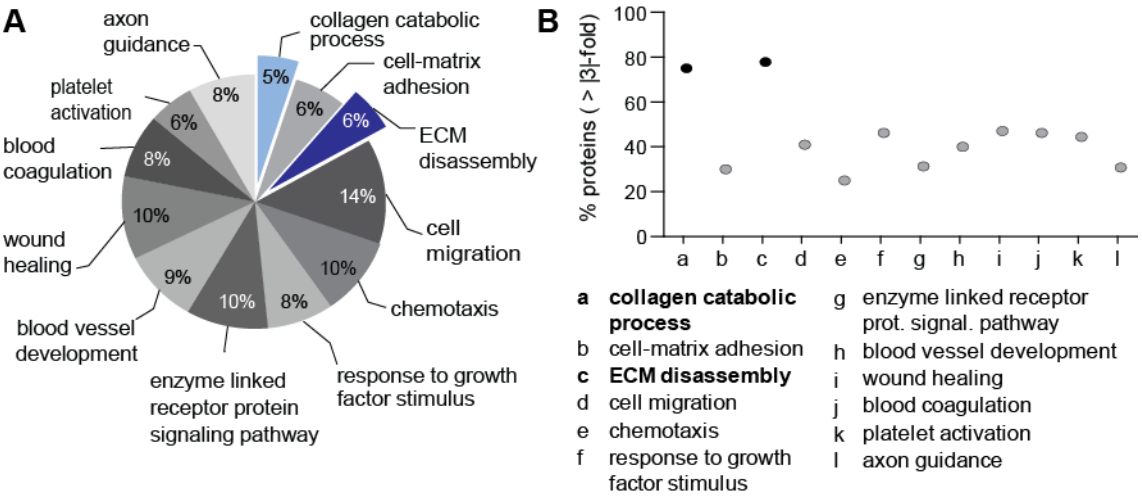


Figure 15: Classification of proteins according to their gene ontology

**(A)** Gene ontology grouping of induced proteins. **(B)** Percentage of proteins which were induced above average (≥|3|-fold) belonging to the different gene ontology groups. The biological functions “collagen catabolic processes” and “ECM disassembly” peaked out because ≥75 % of the proteins in these groups were more than ≥|3|-fold induced in response to FGF1 treatment of human astrocytes.

#### 4.2.3.b RNA levels of proteins identified in the secretome approach

To validate the secretome results, the RNA levels of strongly induced proteins belonging to the ontology groups “collagen catabolic process” and “ECM disassembly” were determined by RT-qPCR. Furthermore, as none of the collagens was detected to be regulated in the transcriptome approach, the question should be answered whether the reduction of collagens could result from increased degradation instead of a decrease in RNA levels. Therefore, the RNA levels of *MMP1*, *MMP9, TIMP1* and of the collagens *COL1A1*, *COL1A2*, *COL4A2* and *COL5A2* were determined.

Table 18: Grouping of induced proteins based on gene ontology

| Gene ontology grouping | Genes/proteins |
|---|---|
| Collagen catabolic process | COL1A1, COL6A1, COL5A2, MMP9, CTSB, MMP1, COL1A2, COL4A2 |
| Cell-matrix adhesion | CTGF, ITGA3, UCC1, SERPINE1, THBS1, ITGB1, CSF1, NID1, CDH13, CD44 |
| ECM disassembly | COL1A1, COL6A1, COL5A2, MMP9, CTSB, MMP1, TIMP1, COL1A2, COL4A2 |
| Cell migration | TGFB2, CTGF, COL1A1, ITGA3, MET, SLC3A2, CSPG4, SERPINE1, IGFBP3, MMP9, LRP1, THBS1, ITGB1, CSF1, AXL, MMP1, PTK7, TIMP1, CDH13, COL1A2, NRP1, MYH9 |
| Chemotaxis | TGFB2, COL6A1, MET, BOC, COL5A2, SERPINE1, SEMA7A, THBS1, ITGB1, NEO1, ALCAM, GPC1, CDH13, COL4A2, NRP1, MYH9 |
| Response to growth factor stimulus | TGFB2, CTGF, COL1A1, UBC, SERPINE1, NDST1, THBS1, ITGB1, GPC1, COL1A2, COL4A2, NRP1, CD44 |
| Enzyme linked receptor protein signaling pathway | TGFB2, CTGF, UBC, CSPG4, SERPINE1, IGFBP3, NDST1, LRP1, PDGFC, THBS1, AXL, FSTL3, GPC1, CDH13, COL1A2, NRP1 |
| Blood vessel development | TGFB2, CTGF, COL1A1, CSPG4, SERPINE1, ANGPTL4, LRP1, THBS1, ITGB1, CDH13, COL1A2, COL4A2, NRP1, LOX, MYH9 |
| Wound healing | TGFB2, ALDOA, COL1A1, ITGA3, SLC3A2, SERPINE1, ACTN4, DCN, THBS1, ITGB1, AXL, MMP1, PTK7, TIMP1, COL1A2, LOX, CD44 |
| Blood coagulation | TGFB2, ALDOA, COL1A1, ITGA3, SLC3A2, SERPINE1, ACTN4, THBS1, ITGB1, AXL, MMP1, TIMP1, COL1A2 |
| Platelet activation | TGFB2, ALDOA, COL1A1, SERPINE1, ACTN4, THBS1, AXL, TIMP1, COL1A2 |
| Axon guidance | TGFB2, COL6A1, MET, BOC, COL5A2, SEMA7A, ITGB1, NEO1, ALCAM, GPC1, COL4A2, NRP1, MYH9 |

The relative RNA levels of the four collagens were determined in untreated human astrocytes. The highest RNA level was found for *COL1A1*, followed by *COL1A2* and *COL4A2*. Minor levels of *COL5A2* were detected (figure 16, A). The changes in RNA levels after FGF1 stimulation were detected at three different time points which represented the stimulation conditions used in the transcriptome microarray analysis (8 h, 24 h) and the secretome analysis (48 h), respectively. For *COL1A1*, *COL1A2* and *COL4A2* a stepwise decrease in RNA upon increasing stimulation periods could be demonstrated (figure 16, B). The RNA level of *COL4A2* was detected to be significantly altered only after 48 h of FGF1 stimulation, whereas, *COL1A1* and *COL1A2* displayed significant alterations after 24 h. The RNA level of *COL5A2* was significantly reduced

after 24 h but did not further decrease upon longer FGF1 incubation (figure 16, B). None of the collagens was significantly altered after 8 h.

RNA levels of *MMP1*, *MMP9* and *TIMP1* were also determined. Upon FGF1 treatment RNA levels of all three genes increased at 8 h, 24 h and 48 h (figure 16, C). However, due to strong alterations in fold-changes detected in independent experiments, significance could not be proven at all time points (figure 16, C).

Taken together, data obtained from the secretome analysis could be validated by determining the RNA levels of *MMP1*, *MMP9* and *TIMP1* as well as of *COL1A1*, *COL1A2*, *COL4A2* and *COL5A2*. Furthermore, the decrease in collagen protein could be assigned to a decrease of collagen RNA and might not only result from increased collagen degradation.

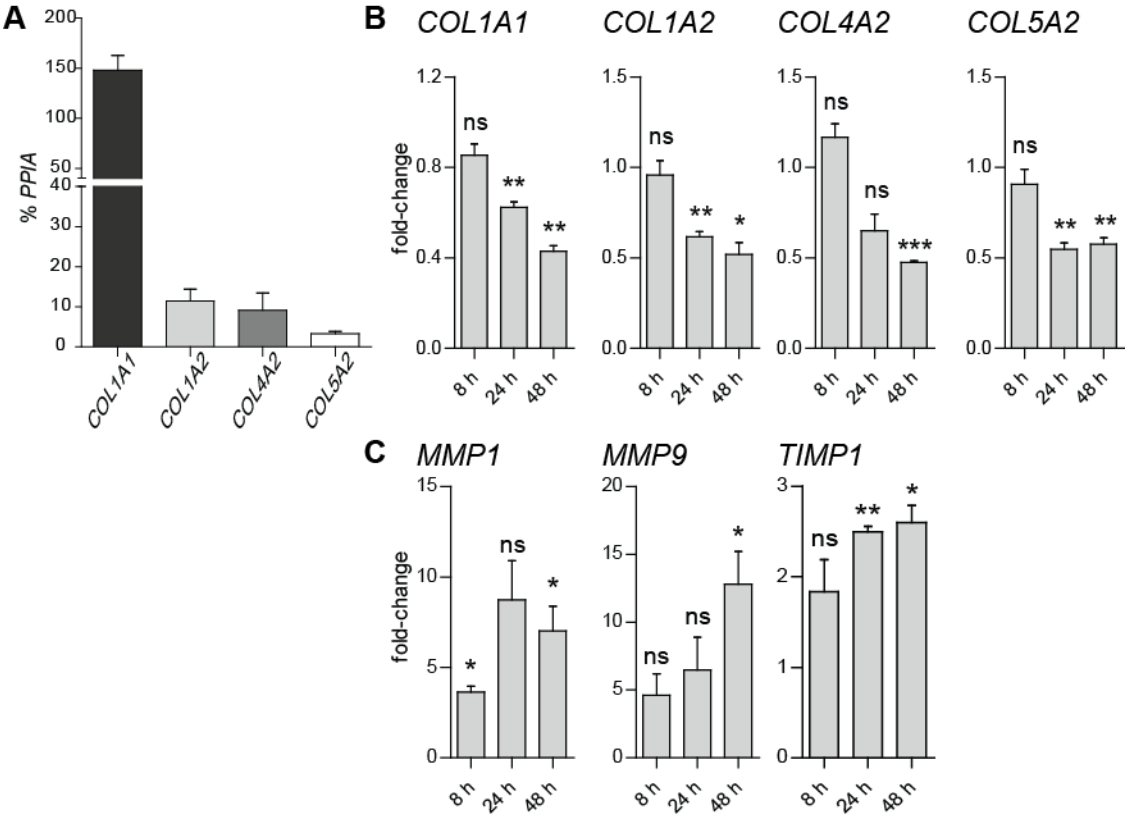


Figure 16: RNA levels of proteins identified in the secretome approach

ns: not significant; p≤0.05 (*); p≤0.01 (**); p≤0.001 (***)
**(A)** Relative RNA levels of *COL1A1*, *COL1A2*, *COL4A2* and *COL5A2* in untreated human astrocytes (% *PPIA*, housekeeping gene). Results represent the mean of three independent experiments; error bars show SEM. **(B)** Changes in the RNA level of collagens after 8 h, 24 h and 48 h FGF1 treatment of human astrocytes. *COL1A1*, *COL1A2* and *COL4A2* RNA levels decreased over time. *COL4A2* was significantly altered only after 48 h. *COL5A2* was significantly downregulated after 24 h and did not further decrease at 48 h. None of the collagens was significantly altered at 8 h. **(C)** Changes in the RNA level of *MMP1*, *MMP9* and *TIMP1* after 8 h, 24 h and 48 h of FGF1 treatment in human astrocytes. RNA levels were found to be upregulated at all three time points. Results represent the mean of three independent experiments. T-test was used to calculate the significance of fold-changes, error bars show SEM.

### 4.2.3.c MMP9 protein concentration and enzymatic activity

To answer the question whether the reduction of collagens can be partly attributed to the increased degradation by an elevated expression of MMPs, an MMP9 activity assay was performed. MMP9 is known to degrade collagen IV and collagen V[171] and does play an important regulatory role in the penetration of lymphocytes into the CNS[3].

To determine the protein concentration of MMP9 in the cell culture supernatant and to distinguish between active MMP9 and its inactive pro-enzyme, a MMP9 activity assay was applied after 48 h FGF1 treatment. In this ELISA-based activity assay the cleavage of pro-MMP9 into active MMP9 is catalyzed by AMPA. The concentration of active MMP9 is subsequently determined by degradation of a MMP9 substrate. Without AMPA, no MMP9 activity was detected in the cell culture supernatant of FGF1-treated astrocytes and heparin-treated controls (figure 17). AMPA-dependent cleavage of pro-MMP9 resulted in a significant increase of active MMP9 in FGF1-treated samples. An average concentration of 1300 pg/ml active MMP9 was measured. It was concluded that MMP9 protein, elevated in human astrocytes in response to FGF1, was present as zymogen in the cell culture supernatant. A minor level of MMP9 protein could also be detected in heparin-treated control samples (figure 17).

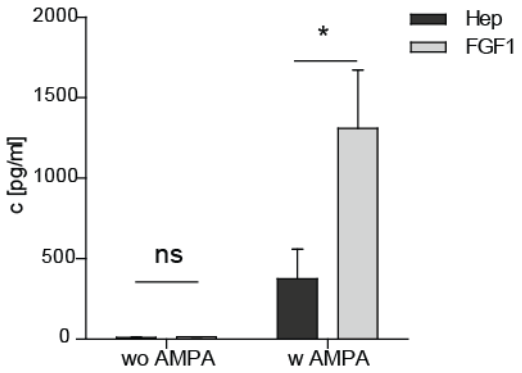


Figure 17: MMP9 protein concentration based on enzymatic activity

p≤0.05 (*); Hep: heparin-treated astrocytes; FGF1: FGF1-stimulated astrocytes
Protein concentration of active MMP9 in the cell culture supernatant of human astrocytes stimulated with FGF1 for 48 h. Inactive pro-MMP9 was activated by AMPA-dependent cleavage. MMP9 concentration was determined by means of its substrate degrading activity. Without AMPA, MMP9 activity was neither detected in heparin-treated control samples nor in FGF1-treated samples. AMPA-dependent cleavage of MMP9 significantly increased MMP9 activity in the FGF1-treated samples. Results represent the mean of three independent experiments. T-test was used and concentrations of active MMP9 were $\log_{10}$-transformed to converge to normal distribution, error bars show SEM.

Taken together, MMP9 present in the cell culture supernatant of FGF1-treated astrocytes was detected to be inactive by using an MMP9 activity assay. AMPA-dependent activation of MMP9 demonstrated a significantly increased concentration of active MMP9 in FGF1-treated astrocytes compared with control samples.

### 4.2.4 Comparison of secretome and transcriptome results

Proteins identified after 48 h in the cell culture supernatant of FGF1-treated primary human astrocytes, were compared with results obtained from the transcriptome microarray analysis after 8 h and 24 h, respectively. Of 72 proteins significantly changed in the secretome approach, 15 were also found to be regulated on the RNA level in the transcriptome microarray analysis. 14/15 proteins were regulated in equal directions on the RNA level. The regulation of RNA and protein levels of PTK7 was found to be the only exception (table 19; figure 18). Inactive tyrosine-protein kinase 7 which is encoded by the *PTK7* gene, found to be 2.13-fold elevated in the cell culture supernatant, whereas, the corresponding RNA level was 1.41-fold decreased at 24 h (table 19, figure 18). However, as changes on the protein and RNA level were rather low, the relevance of this discrepancy remains elusive.

Table 19: Proteins detected to be altered in the secretome as well as in the transcriptome approach

| Protein name | ACCN (UniProt KB) | Gene name | FC Sec 48 h | FC Trans 8 h | FC Trans 24 h |
|---|---|---|---|---|---|
| CD44 antigen | P16070 | CD44 | 26.99 | - | 1.53 |
| Semaphorin-7A | O75326 | SEMA7A | 10.98 | 3.13 | 4.17 |
| Interstitial collagenase | P03956 | MMP1 | 10.84 | 2.23 | 8.74 |
| CUB domain-containing protein 1 | Q9H5V8 | CDCP1 | 6.90 | - | 2.00 |
| Angiopoietin-related protein 4 | Q9BY76 | ANGPTL4 | 5.94 | 4.71 | 4.37 |
| Metalloproteinase inhibitor 1 | P01033 | TIMP1 | 5.30 | - | 1.51 |
| Neuropilin-1 | O14786 | NRP1 | 2.18 | - | 1.64 |
| Inactive tyrosine-protein kinase 7 | Q13308 | PTK7 | 2.13 | - | -1.41 |
| Follistatin-related protein 3 | O95633 | FSTL3 | -1.51 | - | -1.40 |
| Calsyntenin-2 | Q9H4D0 | CLSTN2 | -1.69 | - | -1.50 |
| Serine protease 23 | O95084 | PRSS23 | -1.80 | - | -1.56 |
| Heparan sulfate N-deacetylase/N-sulfotransferase 1 | P52848 | NDST1 | -1.87 | - | -1.41 |
| Stanniocalcin-2 | O76061 | STC2 | -2.82 | - | -1.81 |
| Protein KIAA1199 | Q8WUJ3 | KIAA1199 | -3.69 | -1.45 | -4.01 |
| Transforming growth factor beta-2 | P61812 | TGFB2 | -5.19 | - | -1.93 |

ACCN: Accession number; FC: fold-change; Sec: Secretome; Trans: Transcriptome; Protein/RNA levels altered in opposite directions are double underlined.
15 out of 72 proteins identified in the secretome approach were detected to be regulated in the transcriptome microarray analysis.

For 11/15 proteins, changes in RNA expression could be detected after 24 h. 4/15 proteins exhibited changes in RNA expression already at 8 h. Those were: Semaphorin 7A, interstitial collagenase, angiopoietin-related protein 4 and protein KIAA1199 (table 19, figure 18).

Most of the identified proteins and corresponding RNAs were altered in the same direction (qualitative correlation). In contrast, the fold-changes of RNA and protein induction did not correlate (no quantitative correlation). That means, a high induction on the RNA level did not always lead to a high induction on the protein level and vice versa (figure 18). This becomes obvious considering the fold-changes in protein and RNA levels of CD44 (figure 18) which is a proteoglycan implicated in several adhesion events. CD44 peaked out in the secretome approach as it was highly induced (26.99–fold), whereas, the *CD44* RNA level was barely elevated in the transcriptome microarray analysis (1.53–fold at 24 h). The reason why CD44, a membrane bound protein, is found to be elevated in the secretome approach is unknown. A possible explanation, however, could be the enhanced cleavage of cell surface bound CD44.

The quantitative differences between protein and RNA levels could result from different incubation times used in the transcriptome (8 h, 24 h) and the secretome approach (48 h). Therefore, it was determined whether fold-changes of protein and RNA levels quantitatively correlated at 8 h and 24 h, respectively. Protein concentrations of three different proteins were determined in the cell culture supernatant at 8 h and 24 h. Those were: (1) LIF, which displayed an increase of the RNA level at 8 h (1.92-fold) and 24 h (1.66-fold) in the transcriptome approach. (2) IL11, which was slightly elevated at 8 h (1.45-fold) and was not detected at 24 h in the transcriptome approach. (3) MMP9, which was not detected in the transcriptome approach (8 h, 24 h) but in the secretome approach (48 h).

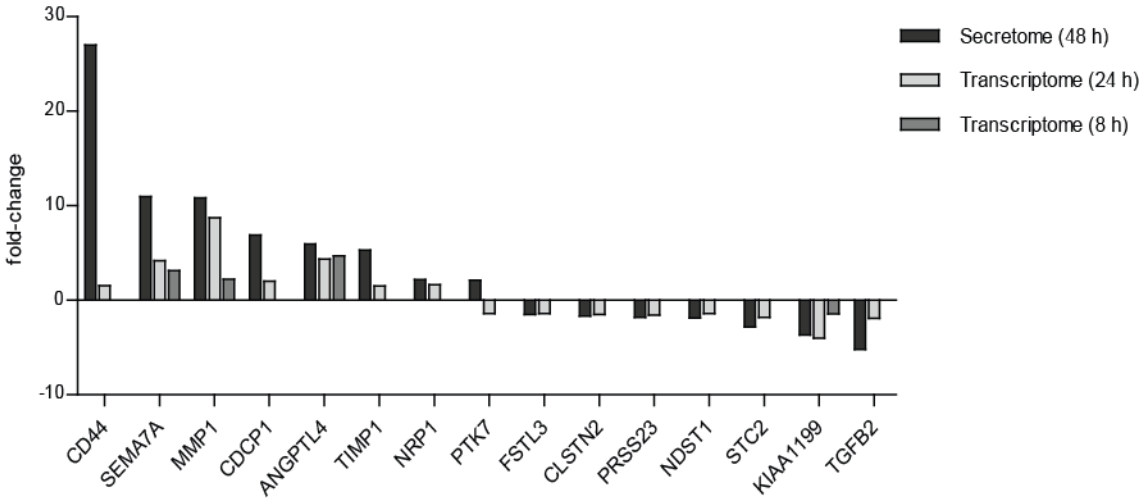


Figure 18: Comparison of FGF1-induced changes in RNA and protein levels

RNA and protein levels were found to be altered in equal directions for 14/15 proteins identified in the secretome and the transcriptome approach (qualitative correlation). PTK7 constituted the only exception. No correlation was found for the fold-changes of protein and RNA levels (no quantitative correlation).

Using ELISA, we found protein levels of LIF, IL11 and MMP9 to be significantly elevated at 8 h and to be further increased at 24 h (figure 19, A). Direct comparison of

the fold-changes detected for the RNA level (transcriptome approach) and the protein level (ELISA) revealed no quantitative correlation at 8 h and 24 h (figure 19, B). Therefore, the difference between changes in RNA and protein levels is not exclusively caused by the different incubation times used in the secretome and the transcriptome approach.

Taken together, of 72 proteins which were identified to be altered in the secretome approach, 15 were also found to be regulated in the transcriptome approach. For 14/15 proteins, the protein and RNA levels were altered in equal directions (qualitative correlation). However, no correlation of the fold-changes of RNA and protein levels was found (no quantitative correlation). To exclude, that this was due to different incubation times used in the transcriptome (8 h, 24 h) and the secretome approach (48 h), the protein concentrations of LIF, IL11 and MMP9 were determined at 8 h and 24 h. No correlation of the fold-changes of RNA and protein levels could be detected at 8 h and 24 h.

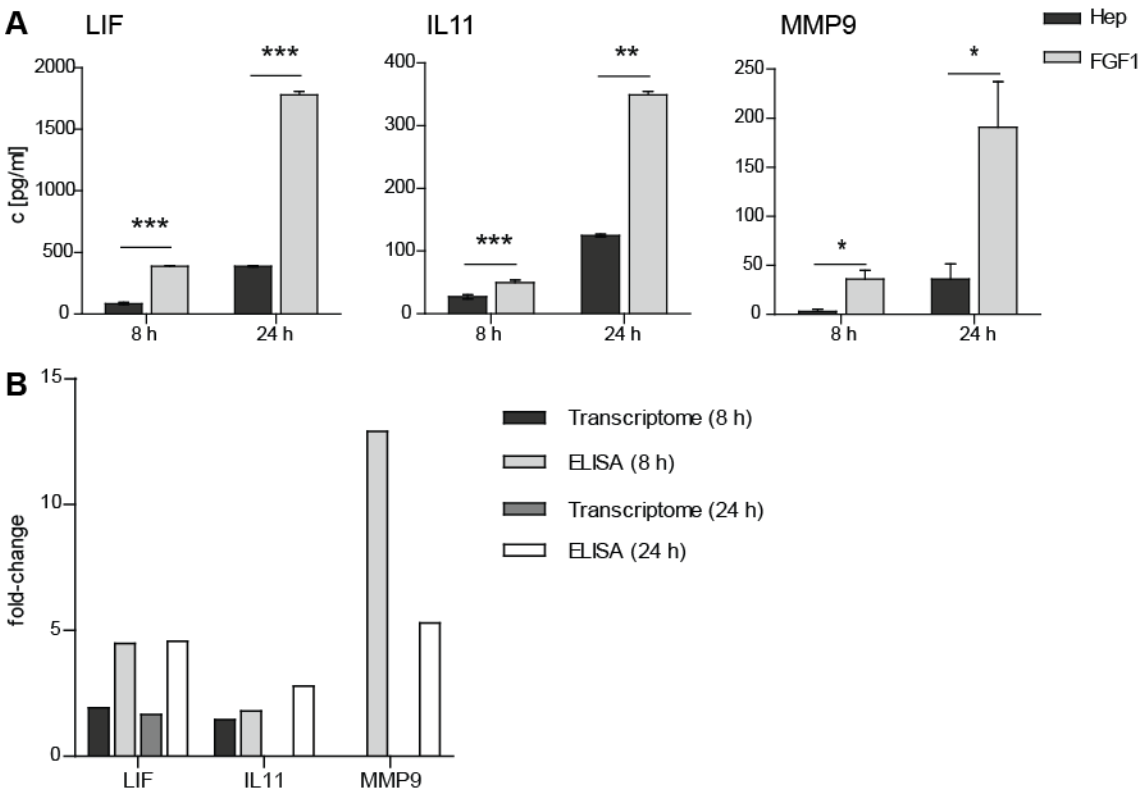


Figure 19: Protein and mRNA levels of LIF, IL11 and MMP9 at 8 h and 24 h

p≤0.05 (*); p≤0.01 (**); p≤0.001 (***); Hep: heparin-treated astrocytes; FGF1: FGF1-stimulated astrocytes
**(A)** Protein concentration of LIF, IL11 and MMP9 in the cell culture supernatant of astrocytes after 8 h and 24 h of FGF1 stimulation. FGF1 treatment significantly elevated protein concentrations at 8 h and 24 h. LIF and IL11: Results represent the mean of three independent samples. MMP9: Results represent the mean of three independent experiments. Concentrations of MMP9 were $\log_{10}$-transformed to converge to normal distribution. T-test was used; error bars show SEM. **(B)** Comparison of FGF1-induced fold-changes of RNA and protein levels. No correlation was found for the fold-changes of protein and RNA levels at 8 h and 24 h.

## 4.3 FGF1-POSITIVE CELLS IN MS LESIONS

### 4.3.1 Characterization of FGF1-positive cells in control brain and MS lesions

FGF1 is known to exhibit widespread functions in the developing as well as in the adult brain and is expressed by various cell types in the CNS, predominantly by neurons but also by glial cells[153]. In the transcriptome and secretome analysis, FGF1 was found to mediate the induction of a multitude of genes and proteins in human astrocytes, pointing to diverse functions of FGF1 in mediation of inflammation, tissue repair mechanisms as well as the disintegration of extracellular matrix. To evaluate functions of FGF1 in MS lesion environment, IHC was used to characterize different FGF1-positive cell types in human control brain and MS lesions. FGF1 in gray and white matter of control brain, NAWM of MS brain, remyelinated lesions, demyelinated lesions and in active lesions was analyzed.

To determine FGF1-positive cells contributing to high levels of FGF1 in normal brain, post-mortem FFPE brain specimens from healthy controls were stained. In white matter, FGF1 staining was detected in glial cells, which according to the morphology, were oligodendroglia (figure 20, A). FGF1-positive oligodendroglia were also detected in NAWM surrounding MS lesions (figure 20, B). However, not all the oligodendroglia detected in white matter of control brain and in NAWM of MS lesions were FGF1-positive. Often, FGF1-positive oligodendroglia were found to be focally accumulated, whereas, other parts of the control white matter and the NAWM were free from FGF1 staining. Besides oligodendroglia, neurons of the cortical gray matter were found to be FGF1-positive in control brain (figure 20, C) and in gray matter parts of MS lesions (not shown). As for oligodendroglia, FGF1 staining was found only in a subset of neurons. No staining was detected using an IgG1 isotype control (not shown).

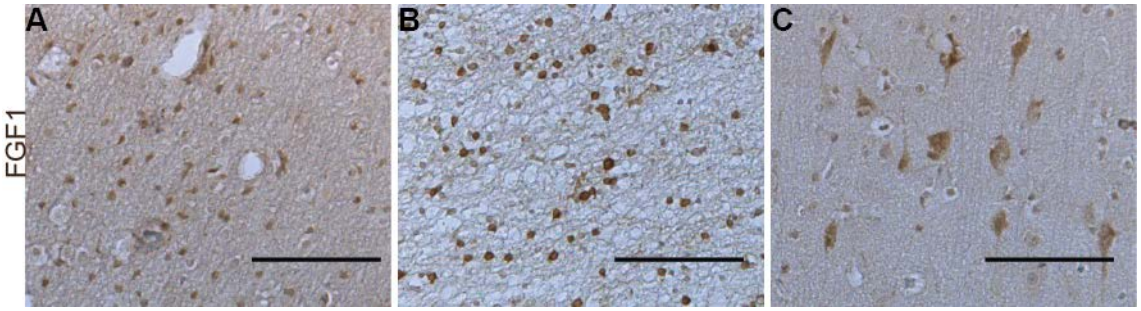


Figure 20: FGF1-positive oligodendroglia and neurons

FGF1 (DAB) staining of post-mortem FFPE brain specimens obtained from healthy controls and MS patients. **(A)** FGF1-positive cells with oligodendroglial morphology in control brain white matter. **(B)** FGF1-positive cells with oligodendroglial morphology in the NAWM of a MS lesion. **(C)** FGF1-positive neurons in gray matter of control brain. Scale bars represent 100 µm.

FGF1 appeared to be regulated in MS lesions as previously detected in our laboratory (Mohan et al., in preparation). Particularly, it was upregulated in remyelinated lesions compared to demyelinated lesions and NAWM. Seven post-mortem MS tissue specimens containing remyelinated lesions were stained (listed in table 14). The overview of a representative lesion (Nbb 03-074 # 3) is shown in figure 21. In the remyelinated as well as demyelinated areas, cells with ramified processes were FGF1-positive (figure 21, A, a and b). However, density of FGF1-positive cells was largely reduced in demyelinated compared to remyelinated parts of the lesion (figure 21, A, a and b). As expected, double staining of FGF1 with the astrocyte marker GFAP revealed these cells to be hypertrophic astrocytes forming a compact glial scar (figure 21, B, a-c). Nevertheless, not all reactive astrocytes exhibited FGF1 staining. Some astrocytes, with a rather mild hypertrophic phenotype localized in the NAWM were found to be GFAP-positive but FGF1-negative (figure 21, C, a-c).

In addition, active and chronic active MS lesions were investigated for FGF1-positive cells. A LFB and HE stain of a representative chronic active lesion as well as the corresponding staining of macrophages and microglia is shown in figure 22, A and B. FGF1-positive macrophages and microglia were identified by double staining of FGF1 with the pan-macrophage marker Iba-1 (figure 22, C). Comparable to the observations made for neurons, oligodendroglia and astrocytes, not all the microglia and macrophages present in the lesion were FGF1-positive. FGF1-negative Iba1-positive cells could be observed (not shown). The distribution of FGF1-positive and negative cells was independent of the lesion type (active or chronic active).

Analyzing active MS lesions with a high number of perivascular infiltrates, a prominent FGF1 staining was detected in some lymphocytes residing in these perivascular cuffs (figure 23). Double staining of FGF1 with T cells (CD3) and B cells (CD20) markers, revealed FGF1 expression in both cell types (figure 23, B and C). Compared to T cells the number of B cells in active MS lesions is rather small. Nevertheless, in some of the observed lesions a substantial number of B cells were present within the perivascular cuffs (figure 23, C).

Taken together, various FGF1-positive cell types in control brain as well as in different types of MS lesions were detected. Subsets of oligodendroglia in white matter of control brain and NAWM in MS lesions were shown to express FGF1. Additionally, subsets of neurons in gray matter of control brain were FGF1-positive. Hypertrophic astrocytes were found to be FGF1-positive in re- as well as in demyelinated lesions. In (chronic) active lesions, Iba-1/FGF1-double positive macrophages and microglia were observed. Furthermore, double staining with CD3 and CD20 revealed FGF1-positive T and B cells in perivascular cuffs of active lesions.

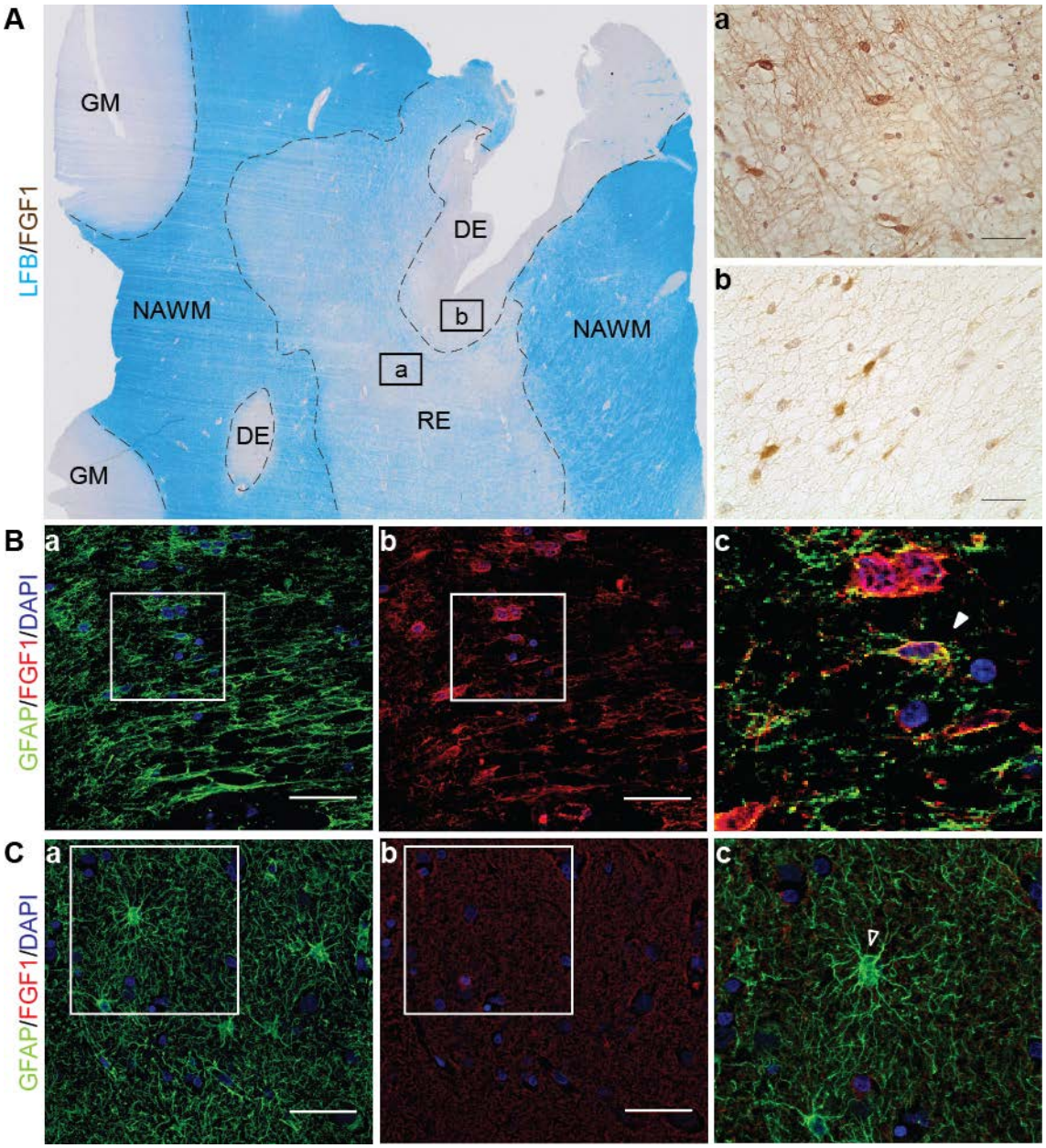


Figure 21: FGF1-positive astrocytes in re- and demyelinated MS lesions

**(A)** LFB staining of a representative post-mortem MS tissue specimen containing gray matter (GM), normal appearing white matter (NAWM), remyelinated (RE) as well as demyelinated (DE) areas. Images (a) and (b) were acquired in box-highlighted areas. (a) DAB staining of FGF1 in remyelinated lesions. Cells forming a dense mesh of ramified processes were FGF1-positive. (b) DAB staining of FGF1 in demyelinated lesions. Cells with ramified processes were FGF1-positive. Cell count was decreased compared to remyelinated lesions. Scale bars represent 25 µm. **(B)** Fluorescence staining of GFAP and FGF1. (a) GFAP and DAPI (b) FGF1 and DAPI (c) merged and magnified image of the boxes highlighted in (a) and (b). Arrowhead indicates a double positive astrocyte. **(C)** Hypertrophic astrocytes in NAWM surrounding MS lesions. (a) GFAP and DAPI (b) FGF1 and DAPI (c) merged and magnified image of the boxes highlighted in (a) and (b). Open arrowhead indicates a GFAP-positive, FGF1-negative cell. Scale bars in **(B)** and **(C)** represent 50 µm.

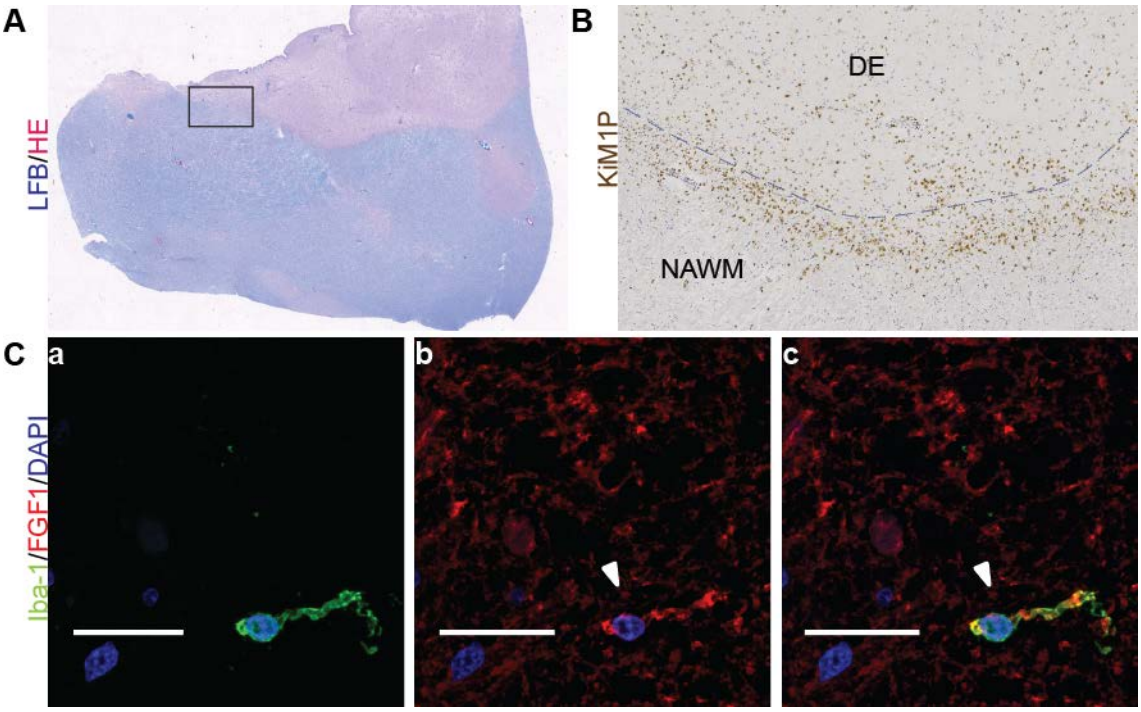


Figure 22: FGF1-positive macrophages and microglia

**(A)** LFB and HE stain of a representative chronic active lesion. **(B)** KiM1P-positive macrophages and microglia at the rim of the lesion. Image was acquired in the box-highlighted area in **(A)**. **(C)** FGF1 and Iba-1 double staining of macrophages and microglia at the lesion rim. (a) Iba-1 and DAPI (b) FGF1 and DAPI (c) merged image. Arrowheads indicate a double positive cell. Scale bars represent 25 µm.

### 4.3.2 FGF1 in adenoids and in CD3-positive T cells from human tonsils

So far, only few studies reported about FGF1 expression in lymphocytes. Therefore, it was investigated whether FGF1-positive lymphocytes could also be detected in lymphatic tissues. Using FFPE sections of human adenoids, FGF1-positive cells were found to be mainly located in germinal centers (figure 24, A, a). Germinal centers represent the site of B cell proliferation and differentiation. Therefore, they are rich in B cells and low in T cells (figure 24, A, b). Double staining with CD3 (figure 24, B), CD20 (figure 24, C) as well as the macrophage marker CD68 (figure 24, D) revealed that FGF1 staining colocalized with CD3 and no double staining was detected for CD20 or CD68 (figure 24, B-D).

The results obtained from FGF1 staining in human adenoids were confirmed by determining the *FGF1* RNA level in human tonsils. Lymphocytes were isolated from human tonsils immediately after surgery. CD3 and CD19-positive lymphocytes were purified using magnetic beads and purity of the isolated fractions was checked by flow cytometry. CD3-positive T cells could be isolated with a purity of 95 %. 83 % of the cells were CD4-positive and 16 % of the cells revealed to be CD8-positive (not shown). For CD19-positive B cells a purity of 96 % was obtained (not shown). RNA was isolated from purified B and T cells and FGF1 levels were determined using RT-qPCR. The relative RNA level of *FGF1* in lymphocytes was low and did not exceed $6x10^{-3}$ % *PPIA*

(figure 25). The low level of *FGF1* matched the IHC findings in which of a small subpopulation of CD3-positive cells was found to be FGF1 positive. Relative *FGF1* levels varied between tonsils from different patients. In accordance with IHC results, T cells contributed the major part of the detected *FGF1* level in human tonsils (figure 25).

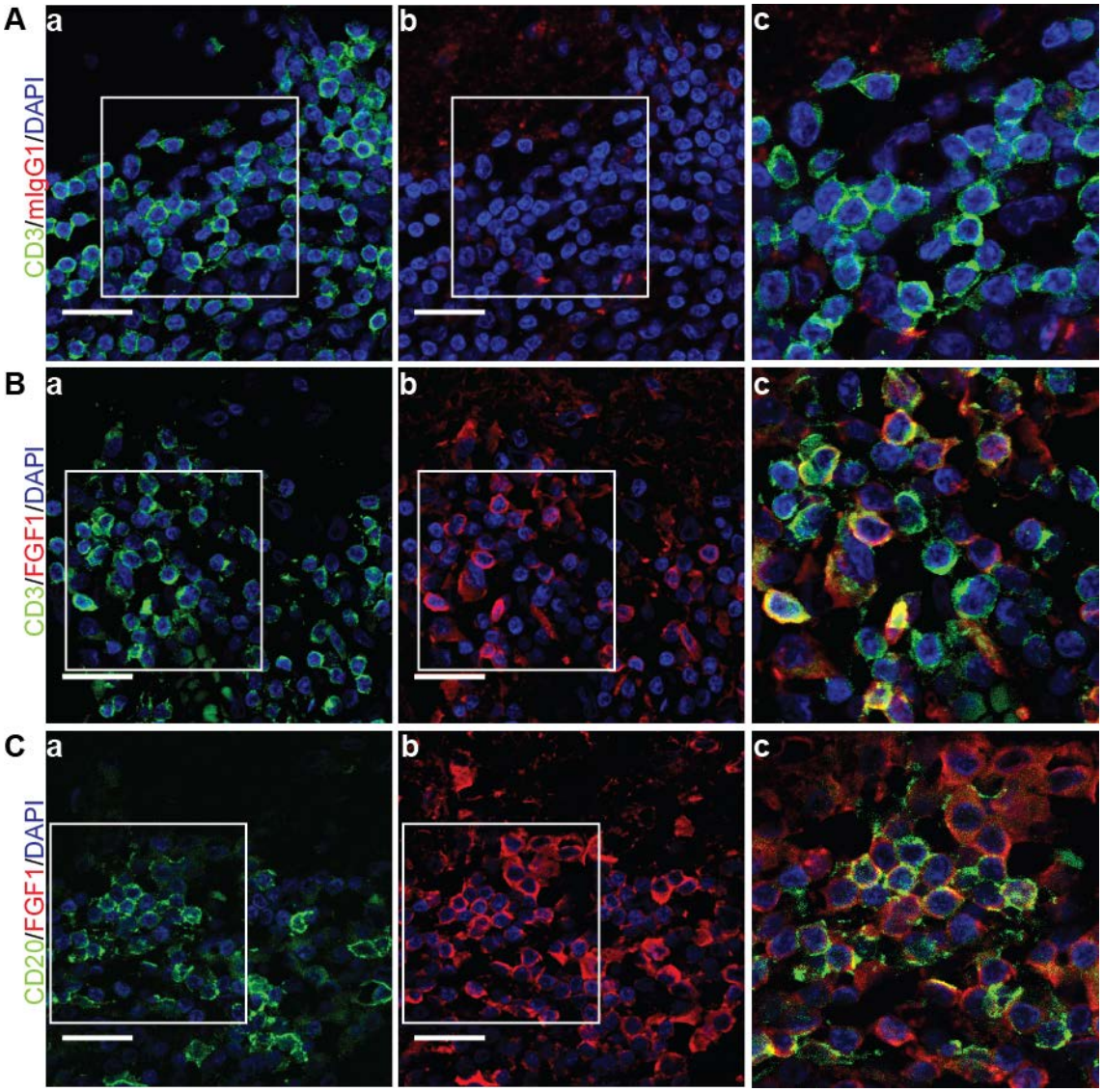


Figure 23: FGF1-positive T cells and B cells in perivascular cuffs of active lesions

**(A)** Mouse IgG1 isotype control for FGF1 (a) CD3 and DAPI (b) mouse IgG1 isotype control and DAPI (c) merged and magnified image of the boxes highlighted in (a) and (b). **(B)** FGF1-positive T cells. (a) CD3 and DAPI (b) FGF1 and DAPI (c) merged and magnified image of the boxes highlighted in (a) and (b). **(C)** FGF1-positive B cells. (a) CD20 and DAPI (b) FGF1 and DAPI (c) merged and magnified image of the boxes highlighted in (a) and (b). Scale bars represent 25 µm.

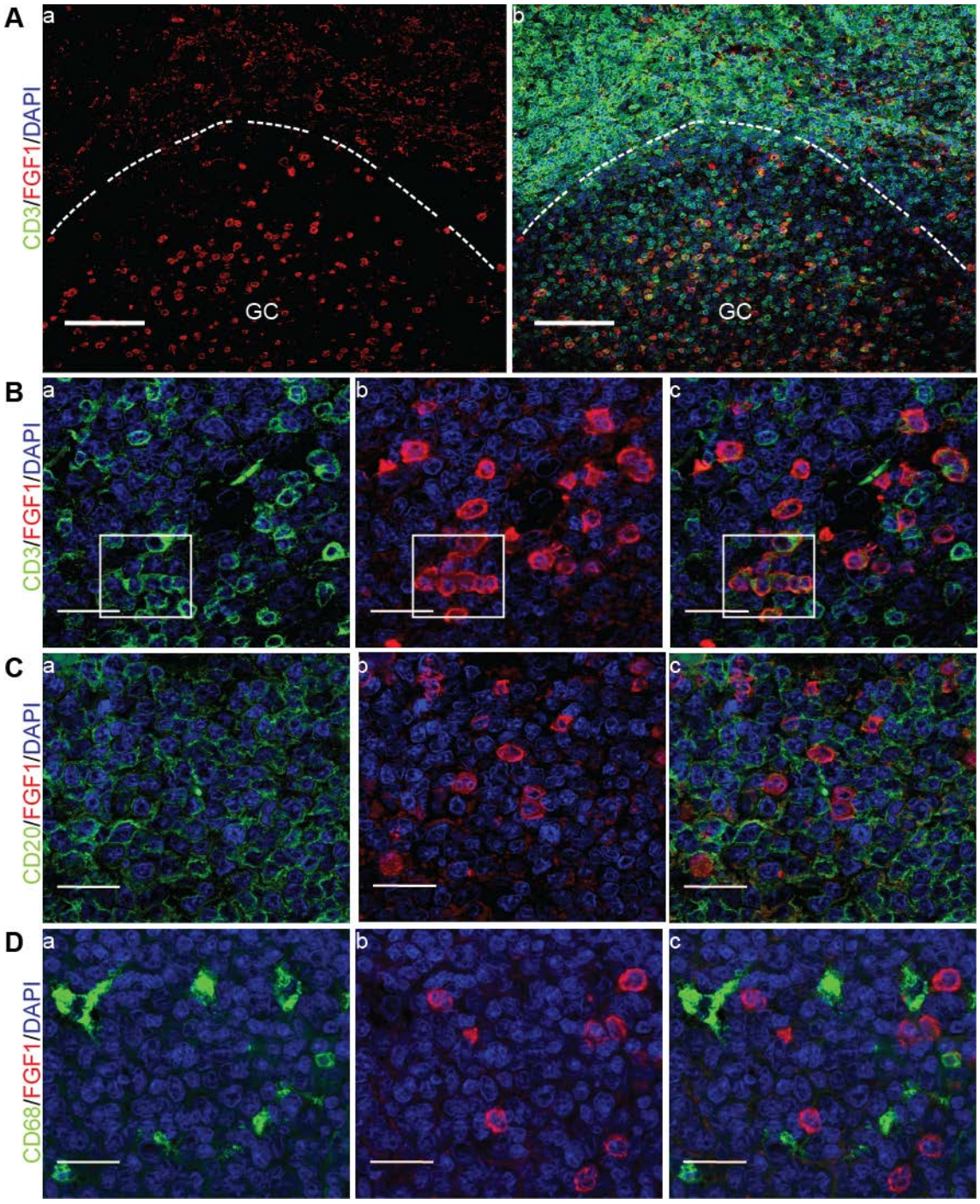


Figure 24: FGF1-positive T cells in the germinal center of human adenoids

**(A)** FGF1 and CD3 staining of human adenoids. (a) FGF1-positive cells were mainly detected in germinal centers (GC) (b) merged image of FGF1 and CD3 staining in GC. Nuclei were stained with DAPI (blue). Scale bars represent 100 µm. **(B)** FGF1-positive T cells. (a) CD3 and DAPI (b) FGF1 and DAPI (c) merged image of (a) and (b). Boxes highlight CD3/FGF1-double positive T cells. **(C)** FGF1-negative B cells (a) CD20 and DAPI (b) FGF1 and DAPI (c) merged image of (a) and (b). No colocalization of FGF1 and CD20 was detected. **(D)** FGF1-negative macrophages (a) CD68 and DAPI (b) FGF1 and DAPI (c) merged image of (a) and (b). No colocalization of FGF1 and CD68 was detected. Scale bars in **(B)** – **(D)** represent 25 µm.

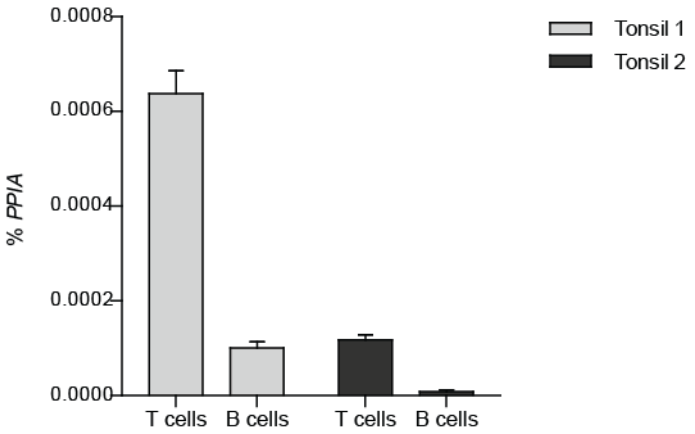


Figure 25: Relative *FGF1* levels in lymphocytes purified from tonsils

Relative *FGF1* RNA levels in B and T cells isolated from human tonsils (% *PPIA*, housekeeping gene). Approximately 95 % purity was obtained for T and B cells fractions determined by flow cytometry (not shown).The *FGF1* RNA level in T cells exceeded the *FGF1* level in B cells. Results from two independent experiments are shown. Error bars show SD of 6 technical replicates.

Taken together, by double staining of human adenoid tissue with FGF1 and antibodies specific for T cells, B cells and macrophages, FGF1-positive T cells were found to be mainly localized within germinal centers. This finding could be substantiated by isolation of B cells and T cells from fresh human tonsils and the subsequent quantification of the relative *FGF1* level using RT-qPCR. The *FGF1* RNA level in T cells exceeded the *FGF1* level detected in B cells.

# 5 DISCUSSION

## 5.1 *IN VITRO* MYELINATING CULTURE

*In vitro* myelinating cultures were originally derived from mouse spinal cords[196] and later modified for cells isolated from rats[58]. These *in vitro* myelinating cultures were established in our laboratory. Furthermore, using MetaMorph software a rapid and easy to use quantification method was developed to determine changes in myelination as well as axonal density induced by external stimuli. Reliability of the quantification method was checked by reproducing antibody-mediated complement dependent demyelination or axonal loss, as described before[58].

In accordance with the work of Elliot et al.[58], the effect seen for different CNS-specific antibodies was highly selective. The results obtained for the anti-MOG antibodies (Z2 and 8-18C5) as well as for isotype controls (IgG1, IgG2a) were comparable to published results[58]. A minor difference was detected in effects mediated by the neurofascin antibody A12/18.1. In the present study, A12/18.1 induced 100 % loss of both, myelin and axons. Elliot et al.[58], in contrast, found a complete abolishment of myelin but only a reduction in axonal density of around 40 %. Furthermore, in the present study Z2 plus heat-inactivated complement induced a slight demyelination, in contrast, in[58] no demyelination was seen. A possible explanation for these differences is the usage of complement from a different source (rabbit complement instead of fresh rat serum) and in a higher final concentration (2.5 % instead of 1 % complement in medium). In our system, total loss of axons and/or myelin could already be detected after 90 min, whereas, incubation times of 3-4 h were reported before[58]. Nonetheless, toxicity of the complement itself can be excluded as complement alone did not affect myelinating cultures. Demyelination in samples treated with Z2 plus heat-inactivated complement might be caused by incomplete inactivation. Therefore, differences between the present work and previously published results[58] can most likely be traced back to variations in the conduction of the experiments and do not account for invalidity of the quantification approach. It is important to mention, however, that quality and reproducibility of screenings strongly depend on the quality of the cultures. Variations in axonal density and myelination might be observed between independent replicates. To obtain reliable and reproducible results, an adequate number of replicates and independent experiments for each condition must be used.

In summary, by introducing this culture system in combination with a quantification method, a valuable tool to study effects of externally applied factors was obtained. This was demonstrated by antibody-mediated complement dependent cell damage. To shed

light on potential functions of FGF1 on different CNS cells, myelinating cultures were stimulated with FGF1. Thereby, FGF1 was found to promote myelination (Mohan et al., in preparation).

## 5.2 FGF1-MEDIATED EFFECTS IN HUMAN ASTROCYTES

In a study previously performed in our laboratory (Mohan et al., in preparation) transcript profiling of macro-dissected tissue of different types of MS lesions was conducted. FGF1 was one the factors identified to be differentially expressed in distinct lesion types. In particular, it was found to be upregulated in re- compared to demyelinated lesions as well as compared to control white matter. This raised the question of the role of FGF1, known to be abundantly expressed in adult brain[153], in the context of MS lesion formation and/or repair.

As FGFRs are expressed on a variety of cells in the CNS, including oligodendrocytes, neurons and astrocytes, FGF1 can have a multitude of regulatory functions. Astrocytes are important mediators in MS lesion formation and can exert beneficial but also detrimental functions[216]. To unravel the FGF1-mediated effects in astrocytes, the focus of the second part of this study was set on FGF1-induced changes in RNA and protein levels in astrocytes and how these could impact MS pathology.

### 5.2.1 Characterization of primary human astrocytes as a target of FGF1 stimulation

Astrocytes are known to express different FGFRs on their surface and can be activated by FGF1[41]. Using RT-qPCR the expression of *FGFR1* - *FGFR4* in primary human astrocytes was evaluated. The highest RNA level was detected for *FGFR1*. However, low levels of *FGFR2*, *FGFR3* and *FGFR4* could also be demonstrated. The presence of *FGFR1* on human astrocytes is in accordance with studies of Balaci[14] and Stachowiak[179] who used northern blot analysis, immunoprecipitation and immunocytochemistry to demonstrate FGFR1 expression in fetal human astrocytes as well as in astrocytes derived from adult trauma patients. The decreased sensitivity of both techniques used in these studies compared to RT-qPCR might account for the absence of FGFR2 and FGFR3[14] and FGFR2 – FGFR4[179], respectively. Supporting data comes also from studies with rodents in which expression of *FGFR1* in rat-derived astrocytes[18] as well as in brain from adult rats[152] was shown. Interestingly, FGFR1 was described to be upregulated in astrocytes in response to brain injury[152] and transient ischemia[188]. Nonetheless, there are also studies based on IHC which report the presence of FGFR2[42] and FGFR3[15] in adult rat brain. These studies, however, did not

consider expression of other FGFR subtypes. These previous findings strongly support the assumption that also in the adult brain astrocytes do express different types of FGFRs and findings gained from *in vitro* work with fetal human astrocytes can, with the usual limitations, be transferred to conditions in adult cells.

*HMOX1* was previously shown to be upregulated in rat astrocytes in response to FGF1 stimulation[211]. In the present study the *HMOX1* RNA level was chosen as a positive control for the stimulation of human astrocytes with FGF1. A FGF1 concentration of 10 ng/ml in presence of 5 U/ml heparin led to a 3.5-fold increase of *HMOX1* RNA levels at 8 h and 24 h, respectively. Heparin without FGF1 did not have any impact on the *HMOX1* level and a higher concentration of FGF1 (50 ng/ml) did not further enhance *HMOX1* RNA levels. In the study of Vargas et al.[211], the *HMOX1* elevation was most pronounced at 4 h, and decreased with increasing incubation times, resulting in non-significant elevation after 24 h. In contrast, in the present study, elevation of *HMOX1* did not decrease at longer incubation and was still significant at 24 h. The reason for this difference is unclear. However, one might speculate that the interaction of recombinant human FGF1, used in both the studies, is more stable with human FGFRs than with rat FGFRs. This might lead to prolonged binding and stimulation and therefore to prolong elevation of *HMOX1* in human astrocytes. Regardless, as the *HMOX1* RNA level was significantly elevated at the indicated time points, it served as a suitable control for FGF1 stimulation of primary human astrocytes.

### 5.2.2 Transcriptome microarray analysis

To discover FGF1-mediated functions in human astrocytes, a transcriptome microarray analysis was performed. Human astrocytes were incubated for either 8 h or 24 h with FGF1 and differential gene expression was evaluated. A total of 272 (8 h) and 859 (24 h) DEGs were identified of which 115 were upregulated at 8 h as well as 24 h. Within this subset of 115 DEGs the focus was set on those, with established functions in MS. Namely, *PTX3*, *IL8*, *HMOX1*, *NT5E*, *EGR1*, *KCNN4*, *SPHK1* and *LIF*. FGF1-induced increase in the RNA levels was validated by RT-qPCR. An increased RNA level was detected for all selected genes at both time points. The congruent results obtained from the transcriptome microarray analysis and the RT-qPCR approach strongly argue for the validity of the array analysis.

It is possible that FGF1, by increasing the RNA levels of these factors, might also influence functions known to be mediated by the genes/proteins in MS. In the subsequent chapter, potential MS relevant aspects of PTX3, IL8, HMOX1, NT5E,

EGR1, KCNN4, SPHK1 and LIF are briefly summarized. A survey is also given in table 20.

*Pentraxin 3 (PTX3).* PTX3 is a prototypic long pentraxin which by binding to C1q can activate the complement cascade and might amplify inflammation and the innate immune response. It was shown to be induced during inflammation and by inflammatory cytokines[10, 22, 141]. In brain, PTX3 is not constitutively expressed. However, evidence was found for induction of *PTX3* in glial cells and neurons upon intracerebroventricular injection of LPS or IL1β[141]. In EAE, *PTX3* was elevated in response to inflammation[2] which correlates with the recent finding of elevated PTX3 plasma levels during the inflammatory response in MS and NMO[212]. Furthermore, PTX3 is known to bind specifically to FGF2 (not FGF1) and thereby inhibits its activity[158]. In EAE, FGF2 was shown to promote proliferation and to inhibit differentiation of OPCs[125]. Therefore, the FGF1-dependent elevation of *PTX3* might directly influence inflammation on the one hand and modulate remyelination by promoting differentiation of oligodendrocytes on the other hand.

*Interleukin 8 (IL8).* IL8 is an intensely studied CXC chemokine with known functions on degranulation of neutrophils and neutrophil transmigration[167]. It has also been described as chemo-attractant for monocytes, triggering their firm adhesion to endothelial cells[68]. It is expressed by a variety of cells in response to different inflammatory stimuli (for review see[167]) and is, therefore, often associated with inflammation. It acts via binding to two receptors, namely CXCR2 and CXCR1[167]. In astrocytes, IL8 production is upregulated in response to inflammatory stimuli such as TNFα and IL1β[8]. Furthermore, evidence was found for IL8-dependent production of MMPs in endothelial cells[106] which could promote ECM degradation and support cell migration. CXCR1 and CXCR2 were additionally found in an oligodendrocyte precursor cell line[132], in human oligodendrocytes *in vitro* and, importantly, upregulated on oligodendrocytes in MS lesions[136]. Their ligand IL8 was detected in astrocytes around active MS lesions[136]. Therefore, crosstalk between astrocytes and oligodendrocytes could be mediated by IL8 interaction with its receptors. This could be implicated in the recruitment or in proliferation of oligodendrocyte and thus in the regeneration of demyelinated lesions[132]. FGF1-mediated elevation of *IL8* in astrocytes, therefore, could be pro-inflammatory but could also have a modulating function in remyelination.

*Heme oxygenase 1 (HMOX1).* HMOX1 is responsible for the degradation of heme to biliverdin/bilirubin, free iron and carbon monoxide. In Alzheimer's as well as in Parkinson's disease it was found to be overexpressed in neurons and astrocytes[164]. In MS plaques, a disproportionately high number of HMOX1-expressing astrocytes was detected[124]. Evidence exists for a neuroprotective function of HMOX1 against different

toxic stimuli such as oxidative damage[43, 62, 191]. However, whereas the acute induction of HMOX1 is predominantly protective, persistent or repeated upregulation of the HMOX1 in astrocytes, oligodendroglia and possibly neurons may lead to cellular dysfunction in chronic degenerative and neuroinflammatory diseases. Thus, HMOX1 could contribute to pathological conditions[164, 180]. In active MS lesions, HMOX1 might be upregulated as a secondary response to inflammatory stimuli such as TNFα and IL1β[62, 124, 150]. Thereafter, the increase of HMOX1 in astrocytes could raise iron deposits in the vicinity of MS plaques[105, 124]. In EAE, increased levels of HMOX1 were reported in oligodendrocytes[105, 180]. Furthermore, evidence was provided that acute HMOX1 expression could confer cytoprotection against oxidative stress, whereas, long term induction exacerbated oxidative injury[180]. Therefore, FGF1-mediated elevation of *HMOX1* can initially be protective. However, it may also be detrimental in chronic MS.

*5' nucleotidase (CD73).* CD73 is a cell surface enzyme expressed by various cell types including subsets of lymphocytes[217], endothelial[95] as well as epithelial cells[184]. In the CNS, CD73 is also expressed by astrocytes, oligodendrocytes and microglia[227]. In astrocytes its expression was shown to be regulated by inflammatory factors[35]. During inflammation, ATP is released from damaged cells and cleaved to AMP in the extracellular environment. CD73 mediates the catalytic cleavage of AMP into adenosine. Extracellular adenosine is known to have strong immunosuppressive effects, whereas extracellular ATP acts proinflammatory[30]. Thereby, effects mediated by ATP and adenosine regulate the immune response and prevent an uncontrolled inflammation and a damage of healthy tissue[30]. Adenosine can also be directly protective in the CNS by regulating neuronal survival[156]. Furthermore, on peripheral blood lymphocytes CD73 has been shown to act as a costimulatory molecule and controls adhesion to endothelial cells[5]. In a study using *CD73*-/- mice it was found that these mice were highly resistant to induction of EAE[127]. In EAE, CD73 was not only found to regulate the entry of lymphocytes into the CNS but also generated extracellular adenosine by its enzymatic activity[127]. Besides immunosuppressive functions that might be mediated by FGF1-dependent elevation of *CD73* levels, CD73 could; also via adenosine signaling, increase lymphocyte migration into the CNS.

*Early growth response 1 (EGR1).* EGR1 is a zinc-finger transcription factor and functions as transcriptional regulator for differentiation and mitogenesis. Additionally, it is also known to induce expression of inflammatory factors in peripheral organs[218] or in the CNS in response to ischemia[205]. Therefore, amongst transcription factors which are known to be involved in brain damage, it is considered to be proinflammatory[222]. Furthermore, it appeared to be significantly elevated in a microarray based screening of the gene expression profile of MS brain lesions[130]. FGF1, by elevating the *EGR1*

RNA level, might be involved in the production of proinflammatory cytokines in astrocytes, thereby, modulating the immune response during neuroinflammation.

*Intermediate conductance $Ca^{2+}$-activated $K^+$-channel protein 4 (KCNN4).* The *KCNN4* gene codes for the voltage independent $K^+$-channel KCa3.1 which opens in response to minor increases in intracellular calcium levels[87]. Strong evidence was found that KCa3.1 can regulate activation and proliferation of certain T-lymphocyte subsets[70, 90]. Comparably little is known about KCNN4/KCa3.1 expression in the CNS. However, there are studies showing *in vitro* KCa3.1 expression on microglia[88] and *in vivo* upregulation in astrocytes after spinal cord injury[29]. Blocking of KCa3.1 resulted in an increased locomotor recovery and a reduced secondary damage as well as production of proinflammatory mediators such as TNFα, IL1β and iNOS[29]. Furthermore, blocking of KCa3.1 in EAE reduced clinical disability and also led to a reduction of proinflammatory chemokine/cytokine expression[151]. This suggests that KCNN4/KCa3.1 is important for inflammatory cytotoxicity and the FGF1-mediated elevation of the *KCNN4* RNA level in astrocytes might increase production of proinflammatory cytokines.

*Sphingosine kinase 1 (SPHK1).* SPHK1 is a critical enzyme in the synthesis of sphingosin-1-phosphate (S1P) from ceramide. It catalyzes the final, ATP-dependent phosphorylation of sphingosine[140]. S1P is a lysophospholipid which has been implicated as a crucial regulator in a broad range of physiological conditions, e.g., angiogenesis, vascular permeability, wound healing, apoptosis, cardiovascular function and immunity[177]. These functions are mediated by binding of S1P to its receptors S1P1–S1P5[34, 135]. Due to the clinical approval of fingolimod as oral therapy for MS, which targets S1PRs, the S1P/S1PRs pathway has also received increased attention in autoimmune diseases[33]. In the CNS, importance of S1P/S1PR signaling has been reported for several pathological conditions. This includes: Alzheimer's disease[190], ischemia[92], stress[85], pain[45], but also multiple sclerosis[100]. In healthy spinal cords S1P was mainly detected in neurons[93]. However, an increased synthesis was detected by reactive astrocytes and microglia upon tissue injury[11, 93]. S1P was also found to be elevated in the CSF of MS patients[100]. Additionally, an enhanced expression of SPHK1[63] as well as its receptors S1P1 and S1P3[208] was found on reactive astrocytes in tissue specimens of MS brain. Furthermore, fingolimod treatment of reactive primary human astrocytes led to a reduced expression of proinflammatory cytokines[208], suggesting that this effect might contribute to the clinical outcomes of fingolimod treatment. An upregulation of the *SPHK1* RNA level in astrocytes would therefore support a proinflammatory function of FGF1.

*Leukemia inhibitory factor (LIF).* LIF is a neurotrophic cytokine of the CNTF family which was not only shown to play a key role in neuronal but also in oligodendrocyte survival. It was found to support oligodendrocyte survival *in vitro*[21, 118] and *in vivo*[39, 89] and also reduced clinical severity in EAE[39]. Furthermore, LIF was released from astrocytes in response to ATP[81] and upon activation of TNFR2[64] and was shown to promote maturation of oligodendrocytes[64] and myelination[81]. Therefore, LIF gathered a lot of attention for the treatment of neurodegenerative diseases and autoimmune demyelination (see[148] for review). Besides its effects on neuronal and glial cells, it was found to interact with the immune system. Evidence was found for both pro- and anti-inflammatory effects of LIF. Deploying LIF deficient mice, it was found that proliferation of thymocytes was impaired upon ConA stimulation[61] and microglia/macrophage invasion was decelerated after spinal cord injury[185]. Furthermore, it was demonstrated to be an attractant for macrophages[185, 197]. On the other hand, endogenous and exogenous LIF was shown to reduce signs of inflammation in cutaneous inflammation induced by Freund's adjuvant[16, 226]. Only few studies applied LIF-/- mice to investigate its role in CNS inflammation. However, in MOG-induced EAE LIF deficiency resulted in an attenuation of the disease in the late phase and the maintenance of the inflammatory infiltrates was altered[107]. This adds an additional aspect to LIF-mediated functions and suggests that it might orchestrate T cell and macrophage responses in EAE. Taken together, besides its protective role, LIF also seems to act as an immunomodulator. FGF1 stimulation of human astrocytes increased the *LIF* transcript level and the secretion of LIF in the cell culture supernatant (figure 19). Depending on the lesion type, present cells and cytokine levels, FGF1 could mediate different functions by enhancing the RNA level of *LIF* in astrocytes.

In summary, by FGF1 treatment of human astrocytes and a transcriptome microarray analysis, a wide range of mediators which are implicated in MS lesion development were identified and validated. Known effects which are mediated by these FGF1-mediated factors could roughly be grouped into two categories: The regulation of myelination and the modulation of inflammation.

FGF1 was found to promote myelination in the *in vitro* myelinating culture system established in the present study as well as remyelination in a slice culture model (collaboration with T. Kuhlmann, Mohan et al., in preparation). The mechanisms behind FGF1-promoted myelination are not yet clear. In this study three mediators were identified which might promote myelination and were induced in astrocytes in response to FGF1, namely, *LIF*, *IL8* and *PTX3*. This suggests a contribution of these factors to FGF1 effects on myelination.

In addition to regulating myelination, data indicated that FGF1 modulates inflammation and might trigger the complex response of astrocytes to tissue damage. The astrocyte response to FGF1 mirrors multiple aspects of the response to proinflammatory stimuli such as TNFα and IL1β (table 20). This finding is in agreement with the work of Lee et al[103], who demonstrated that FGF1 stimulation of cultured astrocytes and microglia enhanced LPS and/or IFNγ-mediated neurotoxicity by increasing the expression of proinflammatory cytokines (TNFα and INFβ).

Table 20: FGF1-dependent regulation of genes with implications in MS

| Gene name | Protein | Protein function | Implications in neuroinflammation / MS / EAE |
|---|---|---|---|
| PTX3 | Pentraxin 3, long | - Innate resistance to pathogens | - *PTX3* is induced during the active phase of EAE[2]<br>- PTX3 is elevated in serum of in MS and NMO patients[212] |
| IL8 | Interleukin 8 (CXCL8) | - Chemokine<br>- Mediator of tissue damage in acute inflammation<br>- Chemo-attractant for monocytes[68] | - Increased levels in MS[112]<br>- Produced by astrocytes upon TNFα and IL1β treatment[8]<br>- Can stimulate MMP2 and MMP9 synthesis[106]<br>- Found on astrocytes in active MS lesions[136]<br>- Upregulation of CXCR1 and CXCR2 on oligodendrocytes in MS lesions[136] |
| HMOX1 | Heme oxygenase 1 | - Microsomal enzyme<br>- Degradation of heme groups to yield biliverdin, iron, and carbon monoxide | - HMOX1-positive astrocytes in MS spinal cord[124]<br>- Pro-oxidant and inflammatory stimuli can induce HMOX1 in CNS glia[62, 150]<br>- IFN-β ameliorates HMOX1 induction by TNFα and IL1β[124] |
| NT5E | 5' Nucleotidase (CD73) | - Plasma membrane protein<br>- Hydrolyzation of AMP into adenosine | - *CD73* expression is required for lymphocyte entry into the CNS[5, 127]<br>- *CD73-/-* mice were highly resistant to induction of EAE[127] |
| EGR1 | Early Growth Response 1 | - Transcriptional regulator | - Enhanced expression in MS lesions[130]<br>- Might play a role in regulation of gene expression in MS[109] |
| KCNN4 | Intermediate conductance $Ca^{2+}$-activated $K^{+}$-channel protein 4 | - Voltage-independent potassium channel activated by intracellular calcium | - Blocking reduced production of proinflammatory mediators after spinal cord injury[29]<br>- Blocking KCNN4/KCa3.1 alleviates symptoms of EAE[151] |
| SPHK1 | Sphingosine Kinase 1 | - Phosphorylation of sphingosine to form sphingosine 1-phosphate (S1P) | - Upregulated in astrocytes of MS patients[63]<br>- Elevated S1P levels in CSF of MS patients[100]<br>- S1P receptors are known drug targets in MS[135] |
| LIF | Leukemia Inhibitory Factor | - Pleiotropic cytokine of the CNTF family | - Neuroprotective[170]<br>- Limits autoimmune demyelination and oligodendroglial loss[39, 170]<br>- Promotes remyelination in vitro[81]<br>- Elevated LIF levels in the CSF of MS patients[115]<br>- Modulation of immune response[107, 170] |

DEGs upregulated after 8 h and 24 h in FGF1-treated human astrocytes with possible implications in MS. DEGs were identified by a transcriptome microarray analysis and changes in RNA expression were further validated by RT-qPCR (figure 13) and ELISA (LIF; figure 19).

It is self-evident that one can get only a limited insight in the actual FGF1-dependent astrocyte-mediated functions by examining FGF1-induced differential gene expression. The multitude of effects which FGF1 triggers in other cell types of the MS lesion environment adds an additional dimension to the considerations of FGF1-regulated processes in the context of MS pathology. Nevertheless, FGF1 led to a vast induction of genes with various functions in MS. Together with the previous finding of differential *FGF1* expression in MS lesions (Mohan et al., in preparation) this supports the assumption of FGF1 being an important regulator in MS lesion development.

### 5.2.3 Secretome analysis

Besides the transcriptome microarray analysis, a secretome analysis was performed to unravel FGF1-mediated effects in human astrocytes which might not have become apparent by screening the RNA level. In total, 72 proteins were found to be significantly altered in response to FGF1 of which 33 were up- and 39 were downregulated. These 72 proteins detected in the secretome analysis could be assigned to 12 specific groups using gene ontology classification (figure 15). The focus was set on proteins which were induced above average in response to FGF1 treatment (>|3|-fold). They were found to be disproportionately represented in the two gene ontology groups “collagen catabolic process” and “ECM disassembly”. Within these groups ECM degrading metalloproteinases (MMP1, MMP9) and metalloproteinase regulators (TIMP1) were strongly induced, whereas, constituents of the ECM (COL1A1, COL1A2, COL4A2, COL5A2) were diminished. Results of the secretome analysis were validated by RT-qPCR. Using an activity assay, MMP9 was found to be present in the cell culture supernatant of astrocytes as zymogen.

*Induction of MMP1 and MMP9.* In the present study it was found that MMP1 and MMP9 were strongly induced in astrocytes following FGF1 stimulation.

Matrix metalloproteinases (MMPs) are endopeptidases, best known for their ability to cleave components of the ECM. They are expressed during embryonic development and in pathological situations in which tissue remodeling occurs. MMPs are synthesized as inactive zymogens containing a pro-peptide domain and are activated in the extracellular lumen. This activation can be catalyzed by other MMPs, the plasmin-plasminogen cascade, and a range of proteinases and nonproteolytic agents[223] and is strictly regulated by chemokines and cytokines.

MMP9 is known to degrade collagen IV and collagen V[171], whereas collagen I can be degraded by MMP1[171]. MMP9 does play an important regulatory role in the penetration of lymphocytes into the CNS, which is under normal healthy conditions limited by the BBB[3].

The BBB is formed by capillary endothelial cell, which are surrounded by the basal lamina, pericytes and astrocyte foot processes[1]. The microvasculature of the CNS has a specialized double basement membrane structure. In the CNS, endothelial cells of post-capillary venules are ensheathed by an underlying endothelial basement membrane. This endothelial basement membrane covers the pericytes. A second parenchymal basement membrane, synthesized by astrocytes is ensheathing the endothelial basement membrane[60].

During inflammation, infiltrating leukocytes first cross the endothelial cells and the endothelial basement membrane before they accumulate as so called “perivascular cuffs” in the perivascular space between endothelial and parenchymal basement membranes. It has been shown that the mechanisms by which leukocytes cross the endothelial- and the parenchymal basement membranes, differ. In EAE, peripheral macrophages seem to be associated with penetration of the endothelial basement membrane[202], whereas, it was shown that MMP9 and MMP2 activity was essential for leukocytes to cross the parenchymal basement membrane[3]. Importantly, astrocytes were found to be anchored by dystroglycan to the parenchymal basement membrane, which can be cleaved by MMP9 and MMP2[3]. Thereby, the stability of the basement membrane could be compromised. The expression of MMP9 by astrocytes was found to be elevated in response to oxidative stress[192], thrombin[44], TNFα[12] or tissue plasminogen activator[104] stimulation.

Besides the role of MMPs in remodeling of the ECM during development and regeneration, also other aspects have been reported. MMPs are strictly regulated and can modulate the immune response. This can be achieved by cleavage of cytokines which inactivates[67, 82, 165] or modulates[206] their function or by the specific cleavage of ECM components[213] resulting in fragments with altered functions. MMP9, e.g., was shown to inactivate CXCL12[122] and to activate IL8[206], CXCL6 and CXCL5[207]. MMP1 on the other hand was shown to cleave monocyte chemoattractant proteins which can act as antagonists for their cognate CC chemokine receptors[123]. It has also been shown that MMPs can impact glial scar formation as well as the scar composition[54]. MMP9, in particular, was demonstrated to support the formation of glial scars in injured spinal cord and, furthermore, facilitated astrocyte migration *in vitro*[78].

Therefore, FGF1-induced upregulation of MMP9 could directly impact the integrity of the BBB and impact leukocyte infiltration into the CNS. Additionally, FGF1-mediated upregulation of MMP1 and MMP9 could release or modify ECM-anchored cytokines or impact glial scar formation.

Few studies report about the induction of MMPs in response to FGF1. However, FGF1-mediated upregulation of MMP1 in human lung fibroblast was described and

FGF1 was suggested to reduce lung fibrosis[25]. Comparable to results of the present study, FGF1 treatment was shown to increase MMP1 and to reduce collagen I. In contrast, no changes in TIMP1 expression were seen in fibroblasts[25]. Furthermore, FGF1-dependent induction of MMP9 was seen in breast cancer cells and was suggested to be involved in metastasis[113].

*Induction of TIMP1.* Besides MMP1 and MMP9, TIMP1 was found to be upregulated in response to FGF1.

Following activation, MMP activity can be modulated by TIMPs[32]. An imbalance of TIMP and MMPs is implicated in different CNS diseases, including Parkinson's disease[110], brain tumors[131] but also MS[96]. Because of its role in BBB maintenance, TIMP1 was shown to convey neuroprotection in the CNS. Amongst the family of TIMPs, TIMP1 is inducible and is known to be upregulated in reactive astrocytes by proinflammatory cytokines[38]. An increased expression has also been reported by astrocytes in EAE[134]. The increase of TIMP1 may serve to counterbalance the simultaneous rise in MMP9[131] which supports the role of TIMP1 as an endogenous factor expressed to modulate MMP-dependent ECM remodeling during neuroinflammation[9]. However, also MMP-independent functions have been described for TIMP1 as it was shown to induce proliferation of astrocytes and OPC differentiation[129]. Therefore, the FGF1-dependent upregulation of TIMP1 could, on the one hand, counterbalance the simultaneous upregulation of MMP1 and MMP9, on the other hand, it could impact proliferation and differentiation of glia cells.

*Reduction of collagens.* Whereas MMP1, MMP9 and TIMP1 were found to be induced by FGF1 in astrocytes, the protein level of different collagens was reduced. Those were: COL1A1 and COL1A2, which are major components of fibrillar type I collagen and the main component of the interstitial membrane. COL4A2 is part of type IV collagen, an important component of basement membranes[175]. Like collagen I, COL5A2 is a fibrillar collagen, however, with a low abundance and normally found in association with collagen I.

The ECM in the CNS has a unique composition. Fibrous proteins such as collagens, laminins and fibronectin are present in low amounts, whereas, glycosaminoglycans such hyaluronan, chondroitin sulfate and heparan sulfate are more frequent[133, 149, 210]. The ECM does have a structural role but does also provide physical support for CNS cells, is involved in the regulation of homeostasis and can act as a growth factor reservoir[149]. Several studies have shown an alteration in the composition of the ECM during the course of MS, including the increased immunoreactivity for collagen IV around blood vessels[209].

In a study performed by Mohan et al.[128], IHC was used to demonstrate that fibrillar collagens were strongly induced in MS lesions, whereas, minor levels of fibrillar collagens were detected in brain from healthy controls. In particular, collagen I, collagen III and collagen V formed a dense meshwork in the perivascular space of MS lesions[128]. Evidence was provided that perivascular fibrosis is a feature of chronic lesions as it was less pronounced in active compared to chronic active lesions[128]. Therefore, perivascular fibrosis might act as a physical barrier limiting the invasion of immune cells into the CNS.

Therefore, an FGF1-dependent decrease in protein levels of fibrillar collagens, such as COL1A1, COL1A2 and COL5A2 as well as non-fibrillar collagens such as COL4A2, an important component of basement membranes, could have a direct impact on the invasion of immune cells during the course of MS.

In summary, the upregulation of ECM degrading enzymes and the simultaneous downregulation of different components of fibrillar collagens and of collagen IV, strongly suggest that FGF1 signaling in astrocytes plays an important role in the remodeling of the ECM which is implicated in MS pathology. This could not only enable cell growth and migration but also might trigger the release of cytokines that are anchored in the ECM. Furthermore, cytokines could be processed and regulate the immune response. Additionally, due to the known role of MMP9 in the degradation of parenchymal basement membranes and the facilitation of leukocyte entry into the CNS, FGF1 signaling in astrocytes might directly enhance the permeability of the basement membrane. MMP9 and TIMP1 are both upregulated during the acute phase of injury or inflammatory processes in the CNS[134, 192] and the expression is induced by proinflammatory cytokines[12, 38]. This supports the findings of the transcriptome microarray analysis that FGF1 might act as mediator in acute inflammation triggering the complex detrimental or protective response of astrocytes to tissue damage, as it is known for proinflammatory stimuli such as TNFα and IL1β.

### 5.2.4 Comparison of secretome and transcriptome results

In the present study, two independent approaches were used to unravel FGF1-mediated effects in human astrocytes. In the transcriptome approach FGF1 was found to increase RNA levels of factors involved in modulation of myelination and inflammation, whereas, in the secretome analysis an effect of FGF1 on remodeling of the ECM was revealed.

FGF1-induced proteins, identified in the secretome approach (n=72) were directly compared with differentially expressed genes (272 DEGs at 8 h and 859 DEGs at 24 h) detected in the transcriptome microarray analysis. Of 72 proteins which were identified

to be altered in the secretome approach, 15 were also found to be regulated in the transcriptome approach. For 14/15 proteins, the protein and RNA levels were altered in equal directions (qualitative correlation). However, no correlation of the fold-changes of RNA and protein levels was found (no quantitative correlation). To exclude, that this was due to different incubation times used in the transcriptome (8 h, 24 h) and the secretome approach (48 h), the protein concentrations of LIF, IL11 and MMP9 were determined at 8 h and 24 h. No correlation of the fold-changes of RNA and protein levels could be detected at 8 h and 24 h.

The reason, why the majority of the proteins detected in the secretome approach (57 out of 72 proteins), was not detected in the transcriptome approach is unknown. However, this could result from the stringent threshold criteria applied in the transcriptome approach which might have excluded the corresponding RNAs of proteins which were detected in the secretome approach.

The detected difference between fold-changes in RNA and protein levels is in accordance with work of Schwanhäusser et al.[166]. In a parallel quantification of cellular RNA and protein levels in mouse fibroblasts, they found a correlation between RNA and protein expression but also described variations in quantities. This was ascribed to alterations in translation rates.

It should be mentioned that LIF has also been detected in the secretome approach (2.9-fold upregulated), but was slightly below the significance threshold (p=0.082) and, therefore, was not stated in the results. IL11, in contrast, is lacking glycosylation and therefore could not be detected in the secretome approach.

In summary, for the majority of detected proteins (14/15) RNA and protein levels were regulated in equal directions by the treatment of human astrocytes with FGF1. No correlation of fold-changes in RNA and protein levels could be detected. Therefore, it might be misleading to draw conclusions about protein levels on the basis of the corresponding RNA level. This is not surprising as protein expression is regulated on multiple levels, including translation rate and protein degradation.

Both methods, as applied in the present study, do have pros and cons (summarized in table 21). By merely applying one or the other method, FGF1-mediated aspects in human astrocytes would have been missed. This study clearly shows that the combination of a secretome- and transcriptome microarray analysis is superior to each analysis by itself.

Table 21: Advantages/disadvantages of the secretome and transcriptome approach

| | Advantages | Disadvantages |
|---|---|---|
| Secretome analysis | Direct detection of protein expression:<br>- No misinterpretation due to differences in RNA and protein induction | Detection is restricted to proteins matching the criteria:<br>- Secreted<br>- Glycosylated<br>- Proteins > 30 kDa |
| Transcriptome microarray analysis | Comprehensive approach:<br>- Detection of RNA coding for intra- and extracellular proteins<br>- Identification of stimulatory pathways | Changes on the RNA level:<br>- Increase in RNA levels does not correlate with increase on protein levels |

## 5.3 FGF1-POSITIVE CELLS IN MS LESIONS

FGF1 is known to exhibit widespread functions in the developing as well as in the adult brain. It is expressed by various cell types, in the CNS predominantly by neurons but also by glial cells[153]. In the secretome- and transcriptome microarray analysis, FGF1 was found to mediate the induction of a multitude of genes and proteins in human astrocytes. These pointed to functions of FGF1 in the regulation of remyelination, modulation of inflammation and remodeling of the ECM. To better understand FGF1-mediated effects in MS lesions, FGF1-positive cells in control brain as well as in different MS lesions were identified using IHC. It could be shown that subsets of oligodendroglia in white matter of control brain and NAWM in MS lesions were FGF1-positive. Additionally, subsets of neurons in gray matter of control brain were FGF1-positive. Hypertrophic astrocytes were found to be FGF1-positive in re- as well as in demyelinated lesions. In (chronic) active lesions, Iba-1/FGF1-double positive macrophages and microglia were observed. Furthermore, double staining with CD3 and CD20 revealed FGF1-positive T and B cells in perivascular cuffs of active lesions.

*FGF1 in neurons.* In the CNS, FGF1 was predominantly found to be synthesized by neurons[24, 57, 153, 183]. In the adult rat CNS, FGF1-positive neurons were found in spinal motor neurons and neurons related to the somatosensory system[57] as well as in dopaminergic neurons of the substantia nigra[24]. In a study of Stock et al.[183], differences in the cellular distribution of FGF1 between CNS compartments were determined. They compared the cerebral cortex, subcortical telencephalon, the thalamus, the hypothalamus, midbrain as well as brainstem and cerebellum[183]. Within the cerebral cortex only a subset of small to medium sized neurons was FGF1-positive which were predominantly localized in cortical layers IV and V. Furthermore, it was found that the staining pattern of FGF1 in neurons also depended on the neuronal population[183]. This is in accordance with the finding of FGF1-positive neuronal subsets in cortical sections of control brain (figure 20).

*FGF1 in oligodendrocytes.* Besides neurons, oligodendroglia in parts of the white matter in control brain as well as in NAWM surrounding MS lesions were detected to be FGF1-positive. Correspondingly, FGF1 staining of oligodendrocytes has been described for the white matter of spinal cord in adult mice[201] in which double staining with MBP identified FGF1 in a subset of oligodendrocytes. Comparably, in the present study FGF1 was not detected in all but in subsets of oligodendroglia which mostly appeared to be focally accumulated.

*FGF1 in astrocytes.* A prominent FGF1 staining was detected in hypertrophic astrocytes forming the glial scar in remyelinated and demyelinated MS lesions. Some astrocytes, with a rather mild hypertrophic phenotype localized in the NAWM were FGF1-negative.

Although, in various immunohistochemical studies, apart from neurons, no FGF1-positive cells could be detected[24, 183], others reported *in vitro* FGF1 production in astrocytes[83, 114]. Furthermore, FGF1-positive astrocytes were detected in rodent[187, 201] and human CNS[198]. Interestingly, FGF1 expression in astrocytes was often described in response to stress or brain damage[83, 114, 187]. This includes *in vitro* FGF1 induction in rat astrocytes by long-term culture[83] or by stimulation with corticosteroids[114]. Furthermore, FGF1 has been found to be upregulated in mouse brain at a post cryoinjury stage[187]. Here, FGF1 production was located to astrocytes in the peri-injury regions, especially in the foci of gliosis. Further support for the expression of FGF1 in reactive astrocytes comes from immunohistochemical studies describing FGF1 expression in post-mortem tissue of Alzheimer patients. In brain specimen of Alzheimer patients, reactive FGF1-positive astrocytes were particularly localized in the surroundings of senile plaques[94, 199]. However, in Alzheimer's disease not all GFAP-positive astrocytes did express FGF1. It was hypothesized that FGF1 could participate to neurite abnormalities and glial proliferation due to its neurotrophic and gliotrophic effects. These findings are similar to the observation of the present study that FGF1-positive astrocytes are localized in the glial scar of remyelinated and demyelinated lesions, whereas, FGF1-negative hypertrophic astrocytes can be found outside of the lesion in the NAWM. It is feasible that an autocrine FGF1-mediated mechanism participates in the proliferation of astrocytes and the formation of the glial scar. This would also match the detection of FGF1-mediated cell cycle regulation in astrocytes, as it was suggested from a pathway enrichment analysis performed with the data obtained in the transcriptome microarray analysis. Further support for this theory comes from studies identifying FGF1 as a potent mitogen for glial cells[59, 159, 163, 168]. FGF1 expression in astrocytes of remyelinated MS lesions may contribute to the elevated

FGF1 levels which were previously observed by RT-qPCR in remyelinated MS lesions (Mohan et al., in preparation).

*FGF1 in active lesions.* Analyzing FGF1 staining in (chronic) active lesion, subsets of microglia and macrophages as well as B and T lymphocytes were FGF1-positive. Previously, FGF1 was immunohistochemically identified in infiltrating macrophages in the pathology of various renal diseases[157] and in alveolar macrophages in normal lung of mice[76] and human[97]. In the CNS, previous studies reported about FGF1-positive macrophages and microglia invading an acute, chemically induced demyelinating lesion in the spinal cord of adult mice[200]. Comparable to our results, expression of FGF1 was limited to subsets of macrophages and microglia. Literature about FGF1 expression in lymphocytes is limited. However, there are reports about FGF1 expression in lymphocytes under different pathological conditions. FGF1-positive CD4 and CD8 T cells were found in human tissue of different inflammatory renal diseases[157]. FGF1-positive, B cell-derived Hodgkin and Reed/Sternberg cells were detected in different subtypes of Hodgkin's lymphoma[91]. Interestingly, *in vitro* evidence was found for FGF1 induction in glatiramer acetate-reactive Th1 and Th2 polarized cell lines[224]. Glatiramer acetate is a synthetic copolymer approved for the therapy of RR MS and was shown to have modulatory functions on the innate and adaptive immune response[4]. This argues for a FGF1 expression in lymphocytes in response to external stimuli or inflammatory processes which are not yet identified. FGF1-positive T cell, B cells and macrophages may contribute to the slightly elevated FGF1 expression which was observed by RT-qPCR in active MS lesions (Mohan et al., in preparation).

To further investigate FGF1 expression in T and B cells, human adenoids were analyzed by IHC. Furthermore, tonsillar T and B cells were purified and FGF1 levels were determined by RT-qPCR. A small proportion of T cells, particularly in the germinal centers, stained FGF1-positive. Purified T cells exhibited low RNA levels of FGF1 which also argues for a small subset of T cells expressing FGF1. B cells were not found to be FGF1-positive in adenoids and displayed only marginal FGF1 RNA levels.

Taken together, FGF1 expression in MS brain was localized to different cell types. FGF1-positive subsets of neurons, oligodendrocytes, astrocytes as well as microglia/macrophages and lymphocytes were detected in different MS lesions. Remarkably, the number of FGF1-positive lymphocytes in perivascular cuffs of MS lesions was relatively high compared to the number of lymphocytes identified in tonsils. Furthermore, macrophages were not detected to express FGF1 in lymphatic tissue, whereas they did in (chronic) active MS lesions. Further studies have to address the mechanisms of FGF1 induction in the different cell types as well as the functions which might be regulated by FGF1 in MS lesion environment.

## 5.4 CONCLUSIONS

FGF1 is an abundant factor in human brain and was found to be upregulated in remyelinated MS lesions (Mohan et al., in preparation).

In the present study, FGF1 protein was localized to the different cell types in MS lesions. FGF1-positive subsets of neurons in gray matter as well as oligodendrocytes in white matter of control brain and NAWM surrounding MS lesions were detected. FGF1-positive astrocytes were identified in remyelinated and demyelinated MS plaques. In active lesions, microglia, macrophages and lymphocytes, located in perivascular cuffs, were found to be FGF1-positive. Mechanisms, regulating FGF1 in the different cell types remain to be analyzed.

Using the *in vitro* myelinating culture system established in the present work, FGF1 was found to promote myelination in an independent study (Mohan et al., in preparation). However, the mechanisms of FGF1-promoted myelination are not yet clear.

This question was addressed in the present study. Functions of FGF1 on *FGFR*-expressing human astrocytes in cell culture were explored. A transcriptome approach revealed the induction of RNAs which might be implicated in modulation of remyelination (*LIF*, *IL8* and *PTX3*) and in the regulation of inflammation (*PTX3, IL8, KCNN4, SPHK1*, *HMOX1, PTHLH, and NT5E).*

The indirect FGF1-mediated upregulation of factors with pro-myelinating activity in astrocytes could contribute to the enhanced remyelination and to CNS recovery. Additionally, FGF1-dependent upregulation of factors involved in the inflammatory response, point to a modulatory role of FGF1 during acute inflammation.

Results, obtained from a recently developed secretome approach, pointed to a participation of FGF1 signaling in the remodeling of the ECM. By disintegration of the ECM, FGF1 could support cell growth, cell migration and the release of cytokines. Additionally, FGF1-dependent upregulation of MMP9 could be involved in the degradation of the parenchymal basement membrane and facilitate the extravasation of leukocytes.

Currently, the potential therapeutic application of various members of the FGF family is investigated because of their mitogenic, cytoprotective and angiogenic properties[26]. A more detailed understanding of FGF1-mediated effects in the CNS could provide a therapeutic basis for the promotion of repair mechanisms in MS.

# 6 REFERENCES


1 N. J. Abbott, L. Ronnback, and E. Hansson, 'Astrocyte-Endothelial Interactions at the Blood-Brain Barrier', *Nat Rev Neurosci,* 7 (2006), 41-53.

2 D. Agnello, L. Carvelli, V. Muzio, P. Villa, B. Bottazzi, N. Polentarutti, T. Mennini, A. Mantovani, and P. Ghezzi, 'Increased Peripheral Benzodiazepine Binding Sites and Pentraxin 3 Expression in the Spinal Cord During Eae: Relation to Inflammatory Cytokines and Modulation by Dexamethasone and Rolipram', *J Neuroimmunol,* 109 (2000), 105-11.

3 S. Agrawal, P. Anderson, M. Durbeej, N. van Rooijen, F. Ivars, G. Opdenakker, and L. M. Sorokin, 'Dystroglycan Is Selectively Cleaved at the Parenchymal Basement Membrane at Sites of Leukocyte Extravasation in Experimental Autoimmune Encephalomyelitis', *J Exp Med,* 203 (2006), 1007-19.

4 R. Aharoni, 'The Mechanism of Action of Glatiramer Acetate in Multiple Sclerosis and Beyond', *Autoimmun Rev,* 12 (2013), 543-53.

5 L. Airas, J. Niemelä, and S. Jalkanen, 'Cd73 Engagement Promotes Lymphocyte Binding to Endothelial Cells Via a Lymphocyte Function-Associated Antigen-1-Dependent Mechanism', *J Immunol,* 165 (2000), 5411-17.

6 P. J. Albrecht, J. C. Murtie, J. K. Ness, J. M. Redwine, J. R. Enterline, R. C. Armstrong, and S. W. Levison, 'Astrocytes Produce Cntf During the Remyelination Phase of Viral-Induced Spinal Cord Demyelination to Stimulate Fgf-2 Production', *Neurobiol Dis,* 13 (2003), 89-101.

7 F. Aloisi, G. Borsellino, P. Samoggia, U. Testa, C. Chelucci, G. Russo, C. Peschle, and G. Levi, 'Astrocyte Cultures from Human Embryonic Brain: Characterization and Modulation of Surface Molecules by Inflammatory Cytokines', *J Neurosci Res,* 32 (1992), 494-506.

8 F. Aloisi, A. Carè, G. Borsellino, P. Gallo, S. Rosa, A. Bassani, A. Cabibbo, U. Testa, G. Levi, and C. Peschle, 'Production of Hemolymphopoietic Cytokines (Il-6, Il-8, Colony-Stimulating Factors) by Normal Human Astrocytes in Response to Il-1 Beta and Tumor Necrosis Factor-Alpha', *J Immunol,* 149 (1992), 2358-66.

9 G. E. Althoff, D. P. Wolfer, N. Timmesfeld, B. Kanzler, H. Schrewe, and A. Pagenstecher, 'Long-Term Expression of Tissue-Inhibitor of Matrix Metalloproteinase-1 in the Murine Central Nervous System Does Not Alter the Morphological and Behavioral Phenotype but Alleviates the Course of Experimental Allergic Encephalomyelitis', *Am J Pathol,* 177 (2010), 840-53.

10 A. Altmeyer, L. Klampfer, A. R. Goodman, and J. Vilcek, 'Promoter Structure and Transcriptional Activation of the Murine Tsg-14 Gene Encoding a Tumor Necrosis Factor/Interleukin-1-Inducible Pentraxin Protein', *J Biol Chem,* 270 (1995), 25584-90.

11 V. Anelli, R. Bassi, G. Tettamanti, P. Viani, and L. Riboni, 'Extracellular Release of Newly Synthesized Sphingosine-1-Phosphate by Cerebellar Granule Cells and Astrocytes', *J Neurochem,* 92 (2005), 1204-15.

12 K. Arai, S.-R. Lee, and E. H. Lo, 'Essential Role for Erk Mitogen-Activated Protein Kinase in Matrix Metalloproteinase-9 Regulation in Rat Cortical Astrocytes', *Glia,* 43 (2003), 254-64.

13 T. Asai, A. Wanaka, H. Kato, Y. Masana, M. Seo, and M. Tohyama, 'Differential Expression of Two Members of Fgf Receptor Gene Family, Fgfr-1 and Fgfr-2 Mrna, in the Adult Rat Central Nervous System', *Mol Brain Res,* 17 (1993), 174-78.

14 L. Balaci, M. Presta, M. G. Ennas, P. Dell'Era, V. Sogos, G. Lauro, and F. Gremo, 'Differential Expression of Fibroblast Growth Factor Receptors by Human Neurones, Astrocytes and Microglia', *Neuroreport,* 6 (1994), 197-200.

15 J. Ballabriga, E. Pozas, A. M. Planas, and I. Ferrer, 'Bfgf and Fgfr-3 Immunoreactivity in the Rat Brain Following Systemic Kainic Acid Administration at Convulsant Doses: Localization of Bfgf and Fgfr-3 in Reactive Astrocytes, and Fgfr-3 in Reactive Microglia', *Brain Res,* 752 (1997), 315-18.

16 L. R. Banner, P. H. Patterson, A. Allchorne, S. Poole, and C. J. Woolf, 'Leukemia Inhibitory Factor Is an Anti-Inflammatory and Analgesic Cytokine', *J Neurosci,* 18 (1998), 5456-62.

17 P. Bannerman, A. Hahn, A. Soulika, V. Gallo, and D. Pleasure, 'Astrogliosis in Eae Spinal Cord: Derivation from Radial Glia, and Relationships to Oligodendroglia', *Glia,* 55 (2007), 57-64.
18 R. Bansal, M. Kumar, K. Murray, R. S. Morrison, and S. E. Pfeiffer, 'Regulation of Fgf Receptors in the Oligodendrocyte Lineage', *Mol Cell Neurosci,* 7 (1996), 263-75.
19 R. Bansal, H. Miyake, I. Nakamura, H. Eto, A. Gotoh, M. Fujisawa, H. Okada, S. R. Arakawa, S. Kamidono, and I. Hara, 'Fibroblast Growth Factors and Their Receptors in Oligodendrocyte Development: Implications for Demyelination and Remyelination', *Dev Neurosci,* 24 (2002), 35-46.
20 F. Barkhof, P. Scheltens, S. T. Frequin, J. J. Nauta, M. W. Tas, J. Valk, and O. R. Hommes, 'Relapsing-Remitting Multiple Sclerosis: Sequential Enhanced Mr Imaging Vs Clinical Findings in Determining Disease Activity', *Am J Roentgenol,* 159 (1992), 1041-47.
21 B. A. Barres, R. Schmid, M. Sendnter, and M. C. Raff, 'Multiple Extracellular Signals Are Required for Long-Term Oligodendrocyte Survival', *Development,* 118 (1993), 283-95.
22 A. Basile, A. Sica, E. d'Aniello, F. Breviario, G. Garrido, M. Castellano, A. Mantovani, and M. Introna, 'Characterization of the Promoter for the Human Long Pentraxin Ptx3: Role of Nf-Kb in Tumor Necrosis Factor-A and Interleukin-1β Regulation', *J Biol Chem,* 272 (1997), 8172-78.
23 J. F. Bazan, K. B. Bacon, G. Hardiman, W. Wang, K. Soo, D. Rossi, D. R. Greaves, A. Zlotnik, and T. J. Schall, 'A New Class of Membrane-Bound Chemokine with a Cx3c Motif', *Nature,* 385 (1997), 640-44.
24 A. J. Bean, R. Elde, Y. H. Cao, C. Oellig, C. Tamminga, M. Goldstein, R. F. Pettersson, and T. Hökfelt, 'Expression of Acidic and Basic Fibroblast Growth Factors in the Substantia Nigra of Rat, Monkey, and Human', *Proc Natl Acad Sci,* 88 (1991), 10237-41.
25 C. Becerril, A. Pardo, M. Montaño, C. Ramos, R. Ramírez, and M. Selman, 'Acidic Fibroblast Growth Factor Induces an Antifibrogenic Phenotype in Human Lung Fibroblasts', *Am J Respir Cell Mol Biol,* 20 (1999), 1020-27.
26 A. Beenken, and M. Mohammadi, 'The Fgf Family: Biology, Pathophysiology and Therapy', *Nat Rev Drug Discov,* 8 (2009), 235-53.
27 N. Belluardo, G. Wu, G. Mudo, A. C. Hansson, R. Pettersson, and K. Fuxe, 'Comparative Localization of Fibroblast Growth Factor Receptor-1, -2, and -3 Mrnas in the Rat Brain: In Situ Hybridization Analysis', *J Comp Neurol,* 379 (1997), 226-46.
28 C. Bjartmar, R. P. Kinkel, G. Kidd, R. A. Rudick, and B. D. Trapp, 'Axonal Loss in Normal-Appearing White Matter in a Patient with Acute Ms', *Neurology,* 57 (2001), 1248-52.
29 D. Bouhy, N. Ghasemlou, S. Lively, A. Redensek, K. I. Rathore, L. C. Schlichter, and S. David, 'Inhibition of the Ca(2)(+)-Dependent K(+) Channel, Kcnn4/Kca3.1, Improves Tissue Protection and Locomotor Recovery after Spinal Cord Injury', *J Neurosci,* 31 (2011), 16298-308.
30 M. J. Bours, E. L. Swennen, F. Di Virgilio, B. N. Cronstein, and P. C. Dagnelie, 'Adenosine 5'-Triphosphate and Adenosine as Endogenous Signaling Molecules in Immunity and Inflammation', *Pharmacol Ther,* 112 (2006), 358-404.
31 E. I. Boyle, S. Weng, J. Gollub, H. Jin, D. Botstein, J. M. Cherry, and G. Sherlock, 'Go::Termfinder--Open Source Software for Accessing Gene Ontology Information and Finding Significantly Enriched Gene Ontology Terms Associated with a List of Genes', *Bioinformatics,* 20 (2004), 3710-5.
32 K. Brew, D. Dinakarpandian, and H. Nagase, 'Tissue Inhibitors of Metalloproteinases: Evolution, Structure and Function', *BBA-Protein Struct M,* 1477 (2000), 267-83.
33 V. Brinkmann, 'Fty720 (Fingolimod) in Multiple Sclerosis: Therapeutic Effects in the Immune and the Central Nervous System', *Br J Pharmacol,* 158 (2009), 1173-82.
34 V. Brinkmann, 'Sphingosine 1-Phosphate Receptors in Health and Disease: Mechanistic Insights from Gene Deletion Studies and Reverse Pharmacology', *Pharmacol Ther,* 115 (2007), 84-105.
35 D. Brisevac, I. Bjelobaba, A. Bajic, T. Clarner, M. Stojiljkovic, C. Beyer, P. Andjus, M. Kipp, and N. Nedeljkovic, 'Regulation of Ecto-5′-Nucleotidase (Cd73) in Cultured Cortical Astrocytes by Different Inflammatory Factors', *Neurochem Int,* 61 (2012), 681-88.
36 C. F. Brosnan, and C. S. Raine, 'The Astrocyte in Multiple Sclerosis Revisited', *Glia,* 61 (2013), 453-65.

37 A. Buffo, C. Rolando, and S. Ceruti, 'Astrocytes in the Damaged Brain: Molecular and Cellular Insights into Their Reactive Response and Healing Potential', *Biochem Pharmacol,* 79 (2010), 77-89.
38 M. Bugno, B. Witek, J. Bereta, M. Bereta, D. R. Edwards, and T. Kordula, 'Reprogramming of Timp-1 and Timp-3 Expression Profiles in Brain Microvascular Endothelial Cells and Astrocytes in Response to Proinflammatory Cytokines', *FEBS Lett,* 448 (1999), 9-14.
39 H. Butzkueven, J.-G. Zhang, M. Soilu-Hanninen, H. Hochrein, F. Chionh, K. A. Shipham, B. Emery, A. M. Turnley, S. Petratos, M. Ernst, P. F. Bartlett, and T. J. Kilpatrick, 'Lif Receptor Signaling Limits Immune-Mediated Demyelination by Enhancing Oligodendrocyte Survival', *Nat Med,* 8 (2002), 613-19.
40 T. M. Calderon, E. A. Eugenin, L. Lopez, S. S. Kumar, J. Hesselgesser, C. S. Raine, and J. W. Berman, 'A Role for Cxcl12 (Sdf-1alpha) in the Pathogenesis of Multiple Sclerosis: Regulation of Cxcl12 Expression in Astrocytes by Soluble Myelin Basic Protein', *J Neuroimmunol,* 177 (2006), 27-39.
41 P. Cassina, M. Pehar, M. R. Vargas, R. Castellanos, A. G. Barbeito, A. G. Estevez, J. A. Thompson, J. S. Beckman, and L. Barbeito, 'Astrocyte Activation by Fibroblast Growth Factor-1 and Motor Neuron Apoptosis: Implications for Amyotrophic Lateral Sclerosis', *J Neurochem,* 93 (2005), 38-46.
42 T. Chadashvili, and D. A. Peterson, 'Cytoarchitecture of Fibroblast Growth Factor Receptor 2 (Fgfr-2) Immunoreactivity in Astrocytes of Neurogenic and Non-Neurogenic Regions of the Young Adult and Aged Rat Brain', *J Comp Neurol,* 498 (2006), 1-15.
43 K. Chen, K. Gunter, and M. D. Maines, 'Neurons Overexpressing Heme Oxygenase-1 Resist Oxidative Stress-Mediated Cell Death', *J Neurochem,* 75 (2000), 304-13.
44 M. S. Choi, Y. E. Kim, W. J. Lee, J. W. Choi, G. H. Park, S. D. Kim, S. J. Jeon, H. S. Go, S. M. Shin, W. K. Kim, C. Y. Shin, and K. H. Ko, 'Activation of Protease-Activated Receptor1 Mediates Induction of Matrix Metalloproteinase-9 by Thrombin in Rat Primary Astrocytes', *Brain Res Bull,* 76 (2008), 368-75.
45 O. Coste, C. Brenneis, B. Linke, S. Pierre, C. Maeurer, W. Becker, H. Schmidt, W. Gao, G. Geisslinger, and K. Scholich, 'Sphingosine 1-Phosphate Modulates Spinal Nociceptive Processing', *J Biol Chem,* 283 (2008), 32442-51.
46 F. Cotton, H. L. Weiner, F. A. Jolesz, and C. R. G. Guttmann, 'Mri Contrast Uptake in New Lesions in Relapsing-Remitting Ms Followed at Weekly Intervals', *Neurology,* 60 (2003), 640-46.
47 P. Cuevas, F. Carceller, I. Muñoz-Willery, and G. Giménez-Gallego, 'Intravenous Fibroblast Growth Factor Penetrates the Blood-Brain Barrier and Protects Hippocampal Neurons against Ischemia-Reperfusion Injury', *Surg Neurol,* 49 (1998), 77-84.
48 P. Cuevas, F. Carceller, S. Ortega, M. Zazo, I. Nieto, and G. Gimenez-Gallego, 'Hypotensive Activity of Fibroblast Growth Factor', *Science,* 254 (1991), 1208-10.
49 P. Cuevas, C. Revilla, O. Herreras, C. Largo, and G. Gimenez-Gallego, 'Neuroprotective Effect of Acidic Fibroblast Growth Factor on Seizure-Associated Brain Damage', *Neurol Res,* 16 (1994), 365.
50 L. Dailey, D. Ambrosetti, A. Mansukhani, and C. Basilico, 'Mechanisms Underlying Differential Responses to Fgf Signaling', *Cytokine Growth Factor Rev,* 16 (2005), 233-47.
51 C. J. De Groot, S. R. Ruuls, J. W. Theeuwes, C. D. Dijkstra, and P. Van Der Valk, 'Immunocytochemical Characterization of the Expression of Inducible and Constitutive Isoforms of Nitric Oxide Synthase in Demyelinating Multiple Sclerosis Lesions', *J Neuropathol Exp Neurol,* 56 (1997), 10-20.
52 G. C. DeLuca, K. Williams, N. Evangelou, G. C. Ebers, and M. M. Esiri, 'The Contribution of Demyelination to Axonal Loss in Multiple Sclerosis', *Brain,* 129 (2006), 1507-16.
53 B. Dubois, S. Masure, U. Hurtenbach, L. Paemen, H. Heremans, J. van den Oord, R. Sciot, T. Meinhardt, G. Hämmerling, G. Opdenakker, and B. Arnold, 'Resistance of Young Gelatinase B-Deficient Mice to Experimental Autoimmune Encephalomyelitis and Necrotizing Tail Lesions', *J Clin Invest,* 104 (1999), 1507-15.
54 Y. Duchossoy, J.-C. Horvat, and O. Stettler, 'Mmp-Related Gelatinase Activity Is Strongly Induced in Scar Tissue of Injured Adult Spinal Cord and Forms Pathways for Ingrowing Neurites', *Mol Cell Neurosci,* 17 (2001), 945-56.
55 R. Dutta, and B. D. Trapp, 'Gene Expression Profiling in Multiple Sclerosis Brain', *Neurobiol Dis,* 45 (2012), 108-14.

56 F. Eckenstein, G. Shipley, and R. Nishi, 'Acidic and Basic Fibroblast Growth Factors in the Nervous System: Distribution and Differential Alteration of Levels after Injury of Central Versus Peripheral Nerve', *J Neurosci,* 11 (1991), 412-19.
57 R. Elde, Y. Cao, A. Cintra, T. C. Brelje, M. Pelto-Huikko, T. Junttila, K. Fuxe, R. F. Pettersson, and T. Hökfelt, 'Prominent Expression of Acidic Fibroblast Growth Factor in Motor and Sensory Neurons', *Neuron,* 7 (1991), 349-64.
58 C. Elliott, M. Lindner, A. Arthur, K. Brennan, S. Jarius, J. Hussey, A. Chan, A. Stroet, T. Olsson, H. Willison, S. C. Barnett, E. Meinl, and C. Linington, 'Functional Identification of Pathogenic Autoantibody Responses in Patients with Multiple Sclerosis', *Brain,* 135 (2012), 1819-33.
59 J. Engele, and M. C. Bohn, 'Effects of Acidic and Basic Fibroblast Growth Factors (Afgf, Bfgf) on Glial Precursor Cell Proliferation: Age Dependency and Brain Region Specificity', *Dev Biol,* 152 (1992), 363-72.
60 B. Engelhardt, and L. Sorokin, 'The Blood-Brain and the Blood-Cerebrospinal Fluid Barriers: Function and Dysfunction', *Semin Immunopathol,* 31 (2009), 497-511.
61 J.-L. Escary, J. Perreau, D. Dumenil, S. Ezine, and P. Brulet, 'Leukaemia Inhibitory Factor Is Necessary for Maintenance of Haematopoietic Stem Cells and Thymocyte Stimulation', *Nature,* 363 (1993), 361-64.
62 B. Fauconneau, V. Petegnief, C. Sanfeliu, A. Piriou, and A. M. Planas, 'Induction of Heat Shock Proteins (Hsps) by Sodium Arsenite in Cultured Astrocytes and Reduction of Hydrogen Peroxide-Induced Cell Death', *J Neurochem,* 83 (2002), 1338-48.
63 I. Fischer, C. Alliod, N. Martinier, J. Newcombe, C. Brana, and S. Pouly, 'Sphingosine Kinase 1 and Sphingosine 1-Phosphate Receptor 3 Are Functionally Upregulated on Astrocytes under Pro-Inflammatory Conditions', *PLoS ONE,* 6 (2011), e23905.
64 R. Fischer, H. Wajant, R. Kontermann, K. Pfizenmaier, and O. Maier, 'Astrocyte-Specific Activation of Tnfr2 Promotes Oligodendrocyte Maturation by Secretion of Leukemia Inhibitory Factor', *Glia* (2013).
65 J. A. Frank, N. Richert, B. Lewis, C. Bash, T. Howard, R. Civil, R. Stone, J. Eaton, H. McFarland, and T. Leist, 'A Pilot Study of Recombinant Insulin-Like Growth Factor-1 in Seven Multiple Sclerosis Patients', *Mult Scler,* 8 (2002), 24-29.
66 R. Friesel, and T. Maciag, 'Fibroblast Growth Factor Prototype Release and Fibroblast Growth Factor Receptor Signaling', *Thromb Haemost,* 82 (1999), 748-54.
67 A. J. H. Gearing, P. Beckett, M. Christodoulou, M. Churchill, J. Clements, A. H. Davidson, A. H. Drummond, W. A. Galloway, R. Gilbert, J. L. Gordon, T. M. Leber, M. Mangan, K. Miller, P. Nayee, K. Owen, S. Patel, W. Thomas, G. Wells, L. M. Wood, and K. Woolley, 'Processing of Tumour Necrosis Factor-[Alpha] Precursor by Metalloproteinases', *Nature,* 370 (1994), 555-57.
68 R. E. Gerszten, E. A. Garcia-Zepeda, Y.-C. Lim, M. Yoshida, H. A. Ding, M. A. Gimbrone, A. D. Luster, F. W. Luscinskas, and A. Rosenzweig, 'Mcp-1 and Il-8 Trigger Firm Adhesion of Monocytes to Vascular Endothelium under Flow Conditions', *Nature,* 398 (1999), 718-23.
69 D. M. S. Gesellschaft, 'Www.Dmsg.De', (cited 11.11.2013).
70 S. Ghanshani, H. Wulff, M. J. Miller, H. Rohm, A. Neben, G. A. Gutman, M. D. Cahalan, and K. G. Chandy, 'Up-Regulation of the Ikca1 Potassium Channel During T-Cell Activation: Molecular Mechanism and Functional Consequences', *J Biol Chem,* 275 (2000), 37137-49.
71 M. A. Gimenez, J. E. Sim, and J. H. Russell, 'Tnfr1-Dependent Vcam-1 Expression by Astrocytes Exposes the Cns to Destructive Inflammation', *J Neuroimmunol,* 151 (2004), 116-25.
72 D. Gospodarowicz, and J. Cheng, 'Heparin Protects Basic and Acidic Fgf from Inactivation', *J Cell Physiol,* 128 (1986), 475-84.
73 J. Goverman, 'Autoimmune T Cell Responses in the Central Nervous System', *Nat Rev Immunol,* 9 (2009), 393-407.
74 R. Grose, and C. Dickson, 'Fibroblast Growth Factor Signaling in Tumorigenesis', *Cytokine Growth Factor Rev,* 16 (2005), 179-86.
75 D. C. Hargreaves, P. L. Hyman, T. T. Lu, V. N. Ngo, A. Bidgol, G. Suzuki, Y.-R. Zou, D. R. Littman, and J. G. Cyster, 'A Coordinated Change in Chemokine Responsiveness Guides Plasma Cell Movements', *J Exp Med,* 194 (2001), 45-56.
76 H. Hiruma, S. Hikawa, and T. Kawakami, 'Immunocytochemical Colocalization of Fibroblast Growth Factor-1 with Neurotrophin-3 in Mouse Alveolar Macrophages', *Acta Histochem Cytochem,* 45 (2012), 131-7.

77 J. Hsieh, J. B. Aimone, B. K. Kaspar, T. Kuwabara, K. Nakashima, and F. H. Gage, 'Igf-I Instructs Multipotent Adult Neural Progenitor Cells to Become Oligodendrocytes', *J Cell Biol,* 164 (2004), 111-22.
78 J. Y. Hsu, L. Y. Bourguignon, C. M. Adams, K. Peyrollier, H. Zhang, T. Fandel, C. L. Cun, Z. Werb, and L. J. Noble-Haeusslein, 'Matrix Metalloproteinase-9 Facilitates Glial Scar Formation in the Injured Spinal Cord', *J Neurosci,* 28 (2008), 13467-77.
79 J. D. Huber, R. D. Egleton, and T. P. Davis, 'Molecular Physiology and Pathophysiology of Tight Junctions in the Blood–Brain Barrier', *Trends Neurosci,* 24 (2001), 719-25.
80 L. Hutley, W. Shurety, F. Newell, R. McGeary, N. Pelton, J. Grant, A. Herington, D. Cameron, J. Whitehead, and J. Prins, 'Fibroblast Growth Factor 1: A Key Regulator of Human Adipogenesis', *Diabetes,* 53 (2004), 3097-106.
81 T. Ishibashi, K. A. Dakin, B. Stevens, P. R. Lee, S. V. Kozlov, C. L. Stewart, and R. D. Fields, 'Astrocytes Promote Myelination in Response to Electrical Impulses', *Neuron,* 49 (2006), 823-32.
82 A. Ito, A. Mukaiyama, Y. Itoh, H. Nagase, I. B. Thøgersen, J. J. Enghild, Y. Sasaguri, and Y. Mori, 'Degradation of Interleukin 1β by Matrix Metalloproteinases', *J Biol Chem,* 271 (1996), 14657-60.
83 J. Ito, Y. Nagayasu, R. Lu, A. Kheirollah, M. Hayashi, and S. Yokoyama, 'Astrocytes Produce and Secrete Fgf-1, Which Promotes the Production of Apoe-Hdl in a Manner of Autocrine Action', *J Lipid Res,* 46 (2005), 679-86.
84 N. Itoh, and D. M. Ornitz, 'Evolution of the Fgf and Fgfr Gene Families', *Trends Genet,* 20 (2004), 563-9.
85 S. Jang, S. H. Suh, H. S. Yoo, Y. M. Lee, and S. Oh, 'Changes in Inos, Gfap and Nr1 Expression in Various Brain Regions and Elevation of Sphingosine-1-Phosphate in Serum after Immobilized Stress', *Neurochem Res,* 33 (2008), 842-51.
86 G. R. John, S. L. Shankar, B. Shafit-Zagardo, A. Massimi, S. C. Lee, C. S. Raine, and C. F. Brosnan, 'Multiple Sclerosis: Re-Expression of a Developmental Pathway That Restricts Oligodendrocyte Maturation', *Nat Med,* 8 (2002), 1115-21.
87 W. J. Joiner, L.-Y. Wang, M. D. Tang, and L. K. Kaczmarek, 'Hsk4, a Member of a Novel Subfamily of Calcium-Activated Potassium Channels', *Proc Natl Acad Sci,* 94 (1997), 11013-18.
88 V. Kaushal, P. D. Koeberle, Y. Wang, and L. C. Schlichter, 'The Ca2+-Activated K+ Channel Kcnn4/Kca3.1 Contributes to Microglia Activation and Nitric Oxide-Dependent Neurodegeneration', *J Neurosci,* 27 (2007), 234-44.
89 B. J. Kerr, and P. H. Patterson, 'Leukemia Inhibitory Factor Promotes Oligodendrocyte Survival after Spinal Cord Injury', *Glia,* 51 (2005), 73-9.
90 R. Khanna, M. C. Chang, W. J. Joiner, L. K. Kaczmarek, and L. C. Schlichter, 'Hsk4/Hik1, a Calmodulin-Binding Kca Channel in Human T Lymphocytes: Roles in Proliferation and Volume Regulation', *J Biol Chem,* 274 (1999), 14838-49.
91 D. Khnykin, G. Troen, J. M. Berner, and J. Delabie, 'The Expression of Fibroblast Growth Factors and Their Receptors in Hodgkin's Lymphoma', *J Pathol,* 208 (2006), 431-8.
92 A. Kimura, T. Ohmori, Y. Kashiwakura, R. Ohkawa, S. Madoiwa, J. Mimuro, K. Shimazaki, Y. Hoshino, Y. Yatomi, and Y. Sakata, 'Antagonism of Sphingosine 1-Phosphate Receptor-2 Enhances Migration of Neural Progenitor Cells toward an Area of Brain', *Stroke,* 39 (2008), 3411-7.
93 A. Kimura, T. Ohmori, R. Ohkawa, S. Madoiwa, J. Mimuro, T. Murakami, E. Kobayashi, Y. Hoshino, Y. Yatomi, and Y. Sakata, 'Essential Roles of Sphingosine 1-Phosphate/S1p1 Receptor Axis in the Migration of Neural Stem Cells toward a Site of Spinal Cord Injury', *Stem Cells,* 25 (2007), 115-24.
94 H. Kimura, I. Tooyama, and P. L. McGeer, 'Acidic Fgf Expression in the Surroundings of Senile Plaques', *Tohoku J. Exp. Med.,* 174 (1994), 279-93.
95 P. Koszalka, B. Ozuyaman, Y. Huo, A. Zernecke, U. Flogel, N. Braun, A. Buchheiser, U. K. Decking, M. L. Smith, J. Sevigny, A. Gear, A. A. Weber, A. Molojavyi, Z. Ding, C. Weber, K. Ley, H. Zimmermann, A. Godecke, and J. Schrader, 'Targeted Disruption of Cd73/Ecto-5'-Nucleotidase Alters Thromboregulation and Augments Vascular Inflammatory Response', *Circ Res,* 95 (2004), 814-21.
96 M. Kouwenhoven, V. Özenci, A. Gomes, D. Yarilin, V. Giedraitis, R. Press, and H. Link, 'Multiple Sclerosis: Elevated Expression of Matrix Metalloproteinases in Blood Monocytes', *J Autoimmun,* 16 (2001), 463-70.
97 A. R. Kranenburg, A. Willems-Widyastuti, W. J. Mooi, P. R. Saxena, P. J. Sterk, W. I. de Boer, and H. S. Sharma, 'Chronic Obstructive Pulmonary Disease Is Associated with

Enhanced Bronchial Expression of Fgf-1, Fgf-2, and Fgfr-1', *J Pathol,* 206 (2005), 28-38.

98 M. Krumbholz, D. Theil, T. Derfuss, A. Rosenwald, F. Schrader, C. M. Monoranu, S. L. Kalled, D. M. Hess, B. Serafini, F. Aloisi, H. Wekerle, R. Hohlfeld, and E. Meinl, 'Baff Is Produced by Astrocytes and up-Regulated in Multiple Sclerosis Lesions and Primary Central Nervous System Lymphoma', *J Exp Med,* 201 (2005), 195-200.

99 P. H. Kuhn, K. Koroniak, S. Hogl, A. Colombo, U. Zeitschel, M. Willem, C. Volbracht, U. Schepers, A. Imhof, A. Hoffmeister, C. Haass, S. Rossner, S. Brase, and S. F. Lichtenthaler, 'Secretome Protein Enrichment Identifies Physiological Bace1 Protease Substrates in Neurons', *EMBO J,* 31 (2012), 3157-68.

100 A. Kulakowska, M. Zendzian-Piotrowska, M. Baranowski, T. Kononczuk, W. Drozdowski, J. Gorski, and R. Bucki, 'Intrathecal Increase of Sphingosine 1-Phosphate at Early Stage Multiple Sclerosis', *Neurosci Lett,* 477 (2010), 149-52.

101 H. Lassmann, 'Review: The Architecture of Inflammatory Demyelinating Lesions: Implications for Studies on Pathogenesis', *Neuropathol Appl Neurobiol,* 37 (2011), 698-710.

102 H. Lassmann, W. Bruck, and C. F. Lucchinetti, 'The Immunopathology of Multiple Sclerosis: An Overview', *Brain Pathol,* 17 (2007), 210-8.

103 M. Lee, Y. Kang, K. Suk, C. Schwab, S. Yu, and P. L. McGeer, 'Acidic Fibroblast Growth Factor (Fgf) Potentiates Glial-Mediated Neurotoxicity by Activating Fgfr2 Iiib Protein', *J Biol Chem,* 286 (2011), 41230-45.

104 S. R. Lee, S. Z. Guo, R. H. Scannevin, B. C. Magliaro, K. J. Rhodes, X. Wang, and E. H. Lo, 'Induction of Matrix Metalloproteinase, Cytokines and Chemokines in Rat Cortical Astrocytes Exposed to Plasminogen Activators', *Neurosci Lett,* 417 (2007), 1-5.

105 S. M. Levine, and A. Chakrabarty, 'The Role of Iron in the Pathogenesis of Experimental Allergic Encephalomyelitis and Multiple Sclerosis', *Ann N Y Acad Sci,* 1012 (2004), 252-66.

106 A. Li, S. Dubey, M. L. Varney, B. J. Dave, and R. K. Singh, 'Il-8 Directly Enhanced Endothelial Cell Survival, Proliferation, and Matrix Metalloproteinases Production and Regulated Angiogenesis', *J Immunol,* 170 (2003), 3369-76.

107 R. A. Linker, N. Kruse, S. Israel, T. Wei, S. Seubert, A. Hombach, B. Holtmann, F. Luhder, R. M. Ransohoff, M. Sendtner, and R. Gold, 'Leukemia Inhibitory Factor Deficiency Modulates the Immune Response and Limits Autoimmune Demyelination: A New Role for Neurotrophic Cytokines in Neuroinflammation', *J Immunol,* 180 (2008), 2204-13.

108 C. Linnington, M. Webb, and P. L. Woodhams, 'A Novel Myelin-Associated Glycoprotein Defined by a Mouse Monoclonal Antibody', *J Neuroimmunol,* 6 (1984), 387-96.

109 M. Liu, X. Hou, P. Zhang, Y. Hao, Y. Yang, X. Wu, D. Zhu, and Y. Guan, 'Microarray Gene Expression Profiling Analysis Combined with Bioinformatics in Multiple Sclerosis', *Mol Biol Rep,* 40 (2013), 3731-37.

110 S. Lorenzl, D. S. Albers, S. Narr, J. Chirichigno, and M. F. Beal, 'Expression of Mmp-2, Mmp-9, and Mmp-1 and Their Endogenous Counterregulators Timp-1 and Timp-2 in Postmortem Brain Tissue of Parkinson's Disease', *Exp Neurol,* 178 (2002), 13-20.

111 C. Lucchinetti, J. Parisi, B. Scheithauer, and M. Rodriguez, 'Heterogeneity of Multiple Sclerosis Lesions: Implications for the Pathogenesis of Demyelination', *Ann Neurol,* 47 (2000), 707-17.

112 B. T. Lund, N. Ashikian, H. Q. Ta, Y. Chakryan, K. Manoukian, S. Groshen, W. Gilmore, G. S. Cheema, W. Stohl, M. E. Burnett, D. Ko, N. J. Kachuck, and L. P. Weiner, 'Increased Cxcl8 (Il-8) Expression in Multiple Sclerosis', *J Neuroimmunol,* 155 (2004), 161-71.

113 G. Lungu, L. Covaleda, O. Mendes, H. Martini-Stoica, and G. Stoica, 'Fgf-1-Induced Matrix Metalloproteinase-9 Expression in Breast Cancer Cells Is Mediated by Increased Activities of Nf-Kappab and Activating Protein-1', *Mol Carcinog,* 47 (2008), 424-35.

114 V. Magnaghi, M. A. Riva, I. Cavarretta, L. Martini, and R. C. Melcangi, 'Corticosteroids Regulate the Gene Expression of Fgf-1 and Fgf-2 in Cultured Rat Astrocytes', *J Mol Neurosci,* 15 (2000), 11-18.

115 F. Mashayekhi, and Z. Salehi, 'Expression of Leukemia Inhibitory Factor in the Cerebrospinal Fluid of Patients with Multiple Sclerosis', *J Clin Neurosci,* 18 (2011), 951-4.

116 J. L. Mason, K. Suzuki, D. D. Chaplin, and G. K. Matsushima, 'Interleukin-1β Promotes Repair of the Cns', *J Neurosci,* 21 (2001), 7046-52.

117 E. K. Mathey, T. Derfuss, M. K. Storch, K. R. Williams, K. Hales, D. R. Woolley, A. Al-Hayani, S. N. Davies, M. N. Rasband, T. Olsson, A. Moldenhauer, S. Velhin, R. Hohlfeld, E. Meinl, and C. Linington, 'Neurofascin as a Novel Target for Autoantibody-Mediated Axonal Injury', *J Exp Med,* 204 (2007), 2363-72.

118 M. Mayer, K. Bhakoo, and M. Noble, 'Ciliary Neurotrophic Factor and Leukemia Inhibitory Factor Promote the Generation, Maturation and Survival of Oligodendrocytes in Vitro', *Development,* 120 (1994), 143-53.

119 L. Mayo, F. J. Quintana, and H. L. Weiner, 'The Innate Immune System in Demyelinating Disease', *Immunol Rev,* 248 (2012), 170-87.

120 R. D. McKinnon, G. Piras, J. A. Ida, and M. Dubois-Dalcq, 'A Role for Tgf-Beta in Oligodendrocyte Differentiation', *J Cell Biol,* 121 (1993), 1397-407.

121 C. McManus, J. W. Berman, F. M. Brett, H. Staunton, M. Farrell, and C. F. Brosnan, 'Mcp-1, Mcp-2 and Mcp-3 Expression in Multiple Sclerosis Lesions: An Immunohistochemical and in Situ Hybridization Study', *J Neuroimmunol,* 86 (1998), 20-29.

122 G. A. McQuibban, G. S. Butler, J.-H. Gong, L. Bendall, C. Power, I. Clark-Lewis, and C. M. Overall, 'Matrix Metalloproteinase Activity Inactivates the Cxc Chemokine Stromal Cell-Derived Factor-1', *J Biol Chem,* 276 (2001), 43503-08.

123 G. A. McQuibban, J.-H. Gong, J. P. Wong, J. L. Wallace, I. Clark-Lewis, and C. M. Overall, 'Matrix Metalloproteinase Processing of Monocyte Chemoattractant Proteins Generates Cc Chemokine Receptor Antagonists with Anti-Inflammatory Properties in Vivo', *Blood,* 100 (2002), 1160-67.

124 K. Mehindate, D. J. Sahlas, D. Frankel, Y. Mawal, A. Liberman, J. Corcos, S. Dion, and H. M. Schipper, 'Proinflammatory Cytokines Promote Glial Heme Oxygenase-1 Expression and Mitochondrial Iron Deposition: Implications for Multiple Sclerosis', *J Neurochem,* 77 (2001), 1386-95.

125 D. J. Messersmith, J. C. Murtie, T. Q. Le, E. E. Frost, and R. C. Armstrong, 'Fibroblast Growth Factor 2 (Fgf2) and Fgf Receptor Expression in an Experimental Demyelinating Disease with Extensive Remyelination', *J Neurosci Res,* 62 (2000), 241-56.

126 P. Mignatti, T. Morimoto, and D. B. Rifkin, 'Basic Fibroblast Growth Factor, a Protein Devoid of Secretory Signal Sequence, Is Released by Cells Via a Pathway Independent of the Endoplasmic Reticulum-Golgi Complex', *J Cell Physiol,* 151 (1992), 81-93.

127 J. H. Mills, L. F. Thompson, C. Mueller, A. T. Waickman, S. Jalkanen, J. Niemela, L. Airas, and M. S. Bynoe, 'Cd73 Is Required for Efficient Entry of Lymphocytes into the Central Nervous System During Experimental Autoimmune Encephalomyelitis', *Proc Natl Acad Sci U S A,* 105 (2008), 9325-30.

128 H. Mohan, M. Krumbholz, R. Sharma, S. Eisele, A. Junker, M. Sixt, J. Newcombe, H. Wekerle, R. Hohlfeld, H. Lassmann, and E. Meinl, 'Extracellular Matrix in Multiple Sclerosis Lesions: Fibrillar Collagens, Biglycan and Decorin Are Upregulated and Associated with Infiltrating Immune Cells', *Brain Pathol,* 20 (2010), 966-75.

129 C. S. Moore, R. Milner, A. Nishiyama, R. F. Frausto, D. R. Serwanski, R. R. Pagarigan, J. L. Whitton, R. H. Miller, and S. J. Crocker, 'Astrocytic Tissue Inhibitor of Metalloproteinase-1 (Timp-1) Promotes Oligodendrocyte Differentiation and Enhances Cns Myelination', *J Neurosci,* 31 (2011), 6247-54.

130 M. P. Mycko, R. Papoian, U. Boschert, C. S. Raine, and K. W. Selmaj, 'Cdna Microarray Analysis in Multiple Sclerosis Lesions: Detection of Genes Associated with Disease Activity', *Brain,* 126 (2003), 1048-57.

131 T. Nakagawa, T. Kubota, M. Kabuto, K. Sato, H. Kawano, T. Hayakawa, and Y. Okada, 'Production of Matrix Metalloproteinases and Tissue Inhibitor of Metalloproteinases-1 by Human Brain Tumors', *J Neurosurg,* 81 (1994), 69-77.

132 D. Nguyen, and M. Stangel, 'Expression of the Chemokine Receptors Cxcr1 and Cxcr2 in Rat Oligodendroglial Cells', *Dev Brain Res,* 128 (2001), 77-81.

133 U. Novak, and A. H. Kaye, 'Extracellular Matrix and the Brain: Components and Function', *J Clin Neurosci,* 7 (2000), 280-90.

134 P. T. Nygårdas, and A. E. Hinkkanen, 'Up-Regulation of Mmp-8 and Mmp-9 Activity in the Balb/C Mouse Spinal Cord Correlates with the Severity of Experimental Autoimmune Encephalomyelitis', *Clin Exp Immunol,* 128 (2002), 245-54.

135 C. O'Sullivan, and K. K. Dev, 'The Structure and Function of the S1p1 Receptor', *Trends Pharmacol Sci,* 34 (2013), 401-12.

136 K. M. Omari, G. R. John, S. C. Sealfon, and C. S. Raine, 'Cxc Chemokine Receptors on Human Oligodendrocytes: Implications for Multiple Sclerosis', *Brain,* 128 (2005), 1003-15.

137 P. Patrikios, C. Stadelmann, A. Kutzelnigg, H. Rauschka, M. Schmidbauer, H. Laursen, P. S. Sorensen, W. Bruck, C. Lucchinetti, and H. Lassmann, 'Remyelination Is Extensive in a Subset of Multiple Sclerosis Patients', *Brain,* 129 (2006), 3165-72.
138 S. J. Piddlesden, H. Lassmann, F. Zimprich, B. P. Morgan, and C. Linington, 'The Demyelinating Potential of Antibodies to Myelin Oligodendrocyte Glycoprotein Is Related to Their Ability to Fix Complement', *Am J Pathol* (1993).
139 D. Pitt, P. Werner, and C. S. Raine, 'Glutamate Excitotoxicity in a Model of Multiple Sclerosis', *Nat Med,* 6 (2000), 67-70.
140 M. Podbielska, H. Krotkiewski, and E. L. Hogan, 'Signaling and Regulatory Functions of Bioactive Sphingolipids as Therapeutic Targets in Multiple Sclerosis', *Neurochem Res,* 37 (2012), 1154-69.
141 N. Polentarutti, B. Bottazzi, E. Di Santo, E. Blasi, D. Agnello, P. Ghezzi, M. Introna, T. Bartfai, G. Richards, and A. Mantovani, 'Inducible Expression of the Long Pentraxin Ptx3 in the Central Nervous System', *J Neuroimmunol,* 106 (2000), 87-94.
142 C. H. Polman, P. W. O'Connor, E. Havrdova, M. Hutchinson, L. Kappos, D. H. Miller, J. T. Phillips, F. D. Lublin, G. Giovannoni, A. Wajgt, M. Toal, F. Lynn, M. A. Panzara, and A. W. Sandrock, 'A Randomized, Placebo-Controlled Trial of Natalizumab for Relapsing Multiple Sclerosis', *N Engl J Med,* 354 (2006), 899-910.
143 J. W. Prineas, and F. Connell, 'Remyelination in Multiple Sclerosis', *Ann Neurol,* 5 (1979), 22-31.
144 J. W. Prineas, E. E. Kwon, E.-S. Cho, L. R. Sharer, M. H. Barnett, E. L. Oleszak, B. Hoffman, and B. P. Morgan, 'Immunopathology of Secondary-Progressive Multiple Sclerosis', *Ann Neurol,* 50 (2001), 646-57.
145 J. W. Prineas, E. E. Kwon, P. Z. Goldenberg, A. A. Ilyas, R. H. Quarles, J. A. Benjamins, and T. J. Sprinkle, 'Multiple Sclerosis. Oligodendrocyte Proliferation and Differentiation in Fresh Lesions', *Lab Invest,* 61 (1989), 489-503.
146 H. Radzun, M. Hansmann, H. Heidebrecht, S. Bödewadt-Radzun, H. Wacker, H. Kreipe, H. Lumbeck, C. Hernandez, C. Kuhn, and M. Parwaresch, 'Detection of a Monocyte/Macrophage Differentiation Antigen in Routinely Processed Paraffin-Embedded Tissues by Monoclonal Antibody Ki-M1p', *Lab Invest,* 65 (1991), 306.
147 R. M. Ransohoff, T. A. Hamilton, M. Tani, M. H. Stoler, H. E. Shick, J. A. Major, M. L. Estes, D. M. Thomas, and V. K. Tuohy, 'Astrocyte Expression of Mrna Encoding Cytokines Ip-10 and Je/Mcp-1 in Experimental Autoimmune Encephalomyelitis', *FASEB J,* 7 (1993), 592-600.
148 R. M. Ransohoff, C. L. Howe, and M. Rodriguez, 'Growth Factor Treatment of Demyelinating Disease: At Last, a Leap into the Light', *Trends Immunol,* 23 (2002), 512-16.
149 U. Rauch, 'Extracellular Matrix Components Associated with Remodeling Processes in Brain', *Cellular and Molecular Life Sciences CMLS,* 61 (2004), 2031-45.
150 R. F. Regan, Y. Guo, and N. Kumar, 'Heme Oxygenase-1 Induction Protects Murine Cortical Astrocytes from Hemoglobin Toxicity', *Neurosci Lett,* 282 (2000), 1-4.
151 E.-P. Reich, L. Cui, L. Yang, C. Pugliese-Sivo, A. Golovko, M. Petro, G. Vassileva, I. Chu, A. A. Nomeir, L.-K. Zhang, X. Liang, J. A. Kozlowski, S. K. Narula, P. J. Zavodny, and C.-C. Chou, 'Blocking Ion Channel Kcnn4 Alleviates the Symptoms of Experimental Autoimmune Encephalomyelitis in Mice', *Eur J Immunol,* 35 (2005), 1027-36.
152 J. F. Reilly, and V. G. Kumari, 'Alterations in Fibroblast Growth Factor Receptor Expression Following Brain Injury', *Exp Neurol,* 140 (1996), 139-50.
153 B. Reuss, and O. von Bohlen und Halbach, 'Fibroblast Growth Factors and Their Receptors in the Central Nervous System', *Cell Tissue Res,* 313 (2003), 139-57.
154 B. A. Reynolds, and S. Weiss, 'Clonal and Population Analyses Demonstrate That an Egf-Responsive Mammalian Embryonic Cns Precursor Is a Stem Cell', *Dev Biol,* 175 (1996), 1-13.
155 B. A. Reynolds, and S. Weiss, 'Generation of Neurons and Astrocytes from Isolated Cells of the Adult Mammalian Central Nervous System', *Science,* 255 (1992), 1707-10.
156 J. A. Ribeiro, A. M. Sebastiao, and A. de Mendonca, 'Participation of Adenosine Receptors in Neuroprotection', *Drug News Perspect,* 16 (2003), 80-6.
157 M. Rossini, B. Cheunsuchon, E. Donnert, L.-j. Ma, J. W. Thomas, E. G. Neilson, and A. B. Fogo, 'Immunolocalization of Fibroblast Growth Factor-1 (Fgf-1), Its Receptor (Fgfr-1), and Fibroblast-Specific Protein-1 (Fsp-1) in Inflammatory Renal Disease', *Kidney Int,* 68 (2005), 2621-28.

158 M. Rusnati, M. Camozzi, E. Moroni, B. Bottazzi, G. Peri, S. Indraccolo, A. Amadori, A. Mantovani, and M. Presta, 'Selective Recognition of Fibroblast Growth Factor-2 by the Long Pentraxin Ptx3 Inhibits Angiogenesis', *Blood,* 104 (2004), 92-99.
159 T. C. Ryken, V. C. Traynelis, and R. Lim, 'Interaction of Acidic Fibroblast Growth Factor and Transforming Growth Factor-B in Normal and Transformed Glia in Vitro', *J Neurosurg,* 76 (1992), 850-55.
160 R. Sanges, F. Cordero, and R. A. Calogero, 'Onechannelgui: A Graphical Interface to Bioconductor Tools, Designed for Life Scientists Who Are Not Familiar with R Language', *Bioinformatics,* 23 (2007), 3406-8.
161 K. Sasaki, Y. Oomura, A. Figurov, and H. Yagi, 'Acidic Fibroblast Growth Factor Facilitates Generation of Long-Term Potentiation in Rat Hippocampal Slices', *Brain Res Bull,* 33 (1994), 505-11.
162 K. Sasaki, Y. Oomura, K. Suzuki, K. Hanai, and H. Yagi, 'Acidic Fibroblast Growth Factor Prevents Death of Hippocampal Ca1 Pyramidal Cells Following Ischemia', *Neurochem Int,* 21 (1992), 397-402.
163 J. Scherer, and J. Schnitzer, 'Growth Factor Effects on the Proliferation of Different Retinal Glial Cells in Vitro', *Dev Brain Res,* 80 (1994), 209-21.
164 H. M. Schipper, W. Song, H. Zukor, J. R. Hascalovici, and D. Zeligman, 'Heme Oxygenase-1 and Neurodegeneration: Expanding Frontiers of Engagement', *J Neurochem,* 110 (2009), 469-85.
165 U. Schönbeck, F. Mach, and P. Libby, 'Generation of Biologically Active Il-1β by Matrix Metalloproteinases: A Novel Caspase-1-Independent Pathway of Il-1β Processing', *J Immunol,* 161 (1998), 3340-46.
166 B. Schwanhausser, D. Busse, N. Li, G. Dittmar, J. Schuchhardt, J. Wolf, W. Chen, and M. Selbach, 'Global Quantification of Mammalian Gene Expression Control', *Nature,* 473 (2011), 337-42.
167 B. D. Semple, T. Kossmann, and M. C. Morganti-Kossmann, 'Role of Chemokines in Cns Health and Pathology: A Focus on the Ccl2/Ccr2 and Cxcl8/Cxcr2 Networks', *J Cereb Blood Flow Metab,* 30 (2010), 459-73.
168 N. Shao, H. Wang, T. Zhou, Y. Xue, and C. Liu, 'Heparin Potentiation of the Effect of Acidic Fibroblast Growth Factor on Astrocytes and Neurons', *Life Sci,* 54 (1994), 785-89.
169 A. Shevchenko, H. Tomas, J. Havlis, J. V. Olsen, and M. Mann, 'In-Gel Digestion for Mass Spectrometric Characterization of Proteins and Proteomes', *Nat Protoc,* 1 (2006), 2856-60.
170 H. Slaets, J. J. Hendriks, P. Stinissen, T. J. Kilpatrick, and N. Hellings, 'Therapeutic Potential of Lif in Multiple Sclerosis', *Trends Mol Med,* 16 (2010), 493-500.
171 J. P. Sluijter, D. P. de Kleijn, and G. Pasterkamp, 'Vascular Remodeling and Protease Inhibition--Bench to Bedside', *Cardiovasc Res,* 69 (2006), 595-603.
172 G. K. Smyth, 'Linear Models and Empirical Bayes Methods for Assessing Differential Expression in Microarray Experiments', *Stat Appl Genet Mol Biol,* 3 (2004), Article3.
173 M. V. Sofroniew, and H. V. Vinters, 'Astrocytes: Biology and Pathology', *Acta Neuropathol,* 119 (2010), 7-35.
174 A. Sorensen, K. Moffat, C. Thomson, and S. C. Barnett, 'Astrocytes, but Not Olfactory Ensheathing Cells or Schwann Cells, Promote Myelination of Cns Axons in Vitro', *Glia,* 56 (2008), 750-63.
175 L. Sorokin, 'The Impact of the Extracellular Matrix on Inflammation', *Nat Rev Immunol,* 10 (2010), 712-23.
176 M. Sospedra, and R. Martin, 'Immunology of Multiple Sclerosis', *Annu Rev Immunol,* 23 (2005), 683-747.
177 S. Spiegel, and S. Milstien, 'Sphingosine 1-Phosphate, a Key Cell Signaling Molecule', *J Biol Chem,* 277 (2002), 25851-54.
178 T. Spivak-Kroizman, M. A. Lemmon, I. Dikic, J. E. Ladbury, D. Pinchasi, J. Huang, M. Jaye, G. Crumley, J. Schlessinger, and I. Lax, 'Heparin-Induced Oligomerization of Fgf Molecules Is Responsible for Fgf Receptor Dimerization, Activation, and Cell Proliferation', *Cell,* 79 (1994), 1015-24.
179 M. K. Stachowiak, P. A. Maher, A. Joy, E. Mordechai, and E. K. Stachowiak, 'Nuclear Localization of Functional Fgf Receptor 1 in Human Astrocytes Suggests a Novel Mechanism for Growth Factor Action', *Mol Brain Res,* 38 (1996), 161-65.
180 T. Stahnke, C. Richter-Landsberg, C. Stadelmann, A. Netzler, and W. Brück, 'Differential Upregulation of Heme Oxygenase-1 (Hsp32) in Glial Cells after Oxidative Stress and in Demyelinating Disorders', *J Mol Neurosci,* 32 (2007), 25-37.

181 B. Stankoff, M.-S. Aigrot, F. Noël, A. Wattilliaux, B. Zalc, and C. Lubetzki, 'Ciliary Neurotrophic Factor (Cntf) Enhances Myelin Formation: A Novel Role for Cntf and Cntf-Related Molecules', *J Neurosci,* 22 (2002), 9221-27.
182 B. Stevens, S. Porta, L. L. Haak, V. Gallo, and R. D. Fields, 'Adenosine: A Neuron-Glial Transmitter Promoting Myelination in the Cns in Response to Action Potentials', *Neuron,* 36 (2002), 855-68.
183 A. Stock, K. Kuzis, W. Woodward, R. Nishi, and F. Eckenstein, 'Localization of Acidic Fibroblast Growth Factor in Specific Subcortical Neuronal Populations', *J Neurosci,* 12 (1992), 4688-700.
184 G. R. Strohmeier, W. I. Lencer, T. W. Patapoff, L. F. Thompson, S. L. Carlson, S. J. Moe, D. K. Carnes, R. J. Mrsny, and J. L. Madara, 'Surface Expression, Polarization, and Functional Significance of Cd73 in Human Intestinal Epithelia', *J Clin Invest,* 99 (1997), 2588-601.
185 S. Sugiura, R. Lahav, J. Han, S.-Y. Kou, L. R. Banner, F. De Pablo, and P. H. Patterson, 'Leukaemia Inhibitory Factor Is Required for Normal Inflammatory Responses to Injury in the Peripheral and Central Nervous Systems in Vivo and Is Chemotactic for Macrophages in Vitro', *Eur J Neurosci,* 12 (2000), 457-66.
186 D. Sunnemark, S. Eltayeb, M. Nilsson, E. Wallstrom, H. Lassmann, T. Olsson, A. L. Berg, and A. Ericsson-Dahlstrand, 'Cx3cl1 (Fractalkine) and Cx3cr1 Expression in Myelin Oligodendrocyte Glycoprotein-Induced Experimental Autoimmune Encephalomyelitis: Kinetics and Cellular Origin', *J Neuroinflammation,* 2 (2005), 17.
187 T. Tada, J. Ito, M. Asai, and S. Yokoyama, 'Fibroblast Growth Factor 1 Is Produced Prior to Apolipoprotein E in the Astrocytes after Cryo-Injury of Mouse Brain', *Neurochem Int,* 45 (2004), 23-30.
188 K. Takami, Y. Kiyota, M. Iwane, M. Miyamoto, R. Tsukuda, K. Igarashi, A. Shino, A. Wanaka, S. Shiosaka, and M. Tohyama, 'Upregulation of Fibroblast Growth Factor-Receptor Messenger Rna Expression in Rat Brain Following Transient Forebrain Ischemia', *Exp Brain Res,* 97 (1993), 185-94.
189 K. Takami, A. Matsuo, K. Terai, D. G. Walker, E. G. McGeer, and P. L. McGeer, 'Fibroblast Growth Factor Receptor-1 Expression in the Cortex and Hippocampus in Alzheimer's Disease', *Brain Res,* 802 (1998), 89-97.
190 N. Takasugi, T. Sasaki, K. Suzuki, S. Osawa, H. Isshiki, Y. Hori, N. Shimada, T. Higo, S. Yokoshima, T. Fukuyama, V. M. Lee, J. Q. Trojanowski, T. Tomita, and T. Iwatsubo, 'Bace1 Activity Is Modulated by Cell-Associated Sphingosine-1-Phosphate', *J Neurosci,* 31 (2011), 6850-7.
191 A. Takeda, G. Perry, N. G. Abraham, B. E. Dwyer, R. K. Kutty, J. T. Laitinen, R. B. Petersen, and M. A. Smith, 'Overexpression of Heme Oxygenase in Neuronal Cells, the Possible Interaction with Tau', *J Biol Chem,* 275 (2000), 5395-99.
192 E. Tejima, B. Q. Zhao, K. Tsuji, A. Rosell, K. van Leyen, R. G. Gonzalez, J. Montaner, X. Wang, and E. H. Lo, 'Astrocytic Induction of Matrix Metalloproteinase-9 and Edema in Brain Hemorrhage', *J Cereb Blood Flow Metab,* 27 (2007), 460-8.
193 A. F. Terwisscha van Scheltinga, S. C. Bakker, and R. S. Kahn, 'Fibroblast Growth Factors in Schizophrenia', *Schizophr Bull,* 36 (2010), 1157-66.
194 K. A. Thomas, M. Rios-Candelore, and S. Fitzpatrick, 'Purification and Characterization of Acidic Fibroblast Growth Factor from Bovine Brain', *Proc Natl Acad Sci,* 81 (1984), 357-61.
195 C. E. Thomson, A. M. Hunter, I. R. Griffiths, J. M. Edgar, and M. C. McCulloch, 'Murine Spinal Cord Explants: A Model for Evaluating Axonal Growth and Myelination in Vitro', *J Neurosci Res,* 84 (2006), 1703-15.
196 C. E. Thomson, M. McCulloch, A. Sorenson, S. C. Barnett, B. V. Seed, I. R. Griffiths, and M. McLaughlin, 'Myelinated, Synapsing Cultures of Murine Spinal Cord-Validation as an in Vitro Model of the Central Nervous System', *Eur J Neurosci,* 28 (2008), 1518-35.
197 G. K. Tofaris, P. H. Patterson, K. R. Jessen, and R. Mirsky, 'Denervated Schwann Cells Attract Macrophages by Secretion of Leukemia Inhibitory Factor (Lif) and Monocyte Chemoattractant Protein-1 in a Process Regulated by Interleukin-6 and Lif', *J Neurosci,* 22 (2002), 6696-703.
198 I. Tooyama, H. Akiyama, P. L. McGeer, Y. Hara, O. Yasuhara, and H. Kimura, 'Acidic Fibroblast Growth Factor-Like Immunoreactivity in Brain of Alzheimer Patients', *Neurosci Lett,* 121 (1991), 155-58.
199 I. Tooyama, Y. Hara, O. Yasuhara, Y. Oomura, K. Sasaki, T. Muto, K. Suzuki, K. Hanai, and H. Kimura, 'Production of Antisera to Acidic Fibroblast Growth Factor and Their

Application to Immunohistochemical Study in Rat Brain', *Neuroscience,* 40 (1991), 769-79.

200 A. Tourbah, A. Baron-van Evercooren, L. Oliver, D. Raulais, J. C. Jeanny, and M. Gumpel, 'Endogenous Afgf Expression and Cellular Changes after a Demyelinating Lesion in the Spinal Cord of Adult Normal Mice: Immunohistochemical Study', *J Neurosci Res,* 33 (1992), 47-59.

201 A. Tourbah, L. Oliver, J. C. Jeanny, and M. Gumpel, 'Acidic Fibroblast Growth Factor (Afgf) Is Expressed in the Neuronal and Glial Spinal Cord Cells of Adult Mice', *J Neurosci Res,* 29 (1991), 560-68.

202 E. H. Tran, K. Hoekstra, N. van Rooijen, C. D. Dijkstra, and T. Owens, 'Immune Invasion of the Central Nervous System Parenchyma and Experimental Allergic Encephalomyelitis, but Not Leukocyte Extravasation from Blood, Are Prevented in Macrophage-Depleted Mice', *J Immunol,* 161 (1998), 3767-75.

203 B. D. Trapp, and K. A. Nave, 'Multiple Sclerosis: An Immune or Neurodegenerative Disorder?', *Annu Rev Neurosci,* 31 (2008), 247-69.

204 B. D. Trapp, J. Peterson, R. M. Ransohoff, R. Rudick, S. Mörk, and L. Bö, 'Axonal Transection in the Lesions of Multiple Sclerosis', *N Engl J Med,* 338 (1998), 278-85.

205 K. Tureyen, N. Brooks, K. Bowen, J. Svaren, and R. Vemuganti, 'Transcription Factor Early Growth Response-1 Induction Mediates Inflammatory Gene Expression and Brain Damage Following Transient Focal Ischemia', *J Neurochem,* 105 (2008), 1313-24.

206 P. E. Van den Steen, P. Proost, A. Wuyts, J. Van Damme, and G. Opdenakker, 'Neutrophil Gelatinase B Potentiates Interleukin-8 Tenfold by Aminoterminal Processing, Whereas It Degrades Ctap-Iii, Pf-4, and Gro-A and Leaves Rantes and Mcp-2 Intact', *Blood,* 96 (2000), 2673-81.

207 P. E. Van den Steen, A. Wuyts, S. J. Husson, P. Proost, J. Van Damme, and G. Opdenakker, 'Gelatinase B/Mmp-9 and Neutrophil Collagenase/Mmp-8 Process the Chemokines Human Gcp-2/Cxcl6, Ena-78/Cxcl5 and Mouse Gcp-2/Lix and Modulate Their Physiological Activities', *Eur J Biochem,* 270 (2003), 3739-49.

208 R. Van Doorn, J. Van Horssen, D. Verzijl, M. Witte, E. Ronken, B. Van Het Hof, K. Lakeman, C. D. Dijkstra, P. Van Der Valk, A. Reijerkerk, A. E. Alewijnse, S. L. Peters, and H. E. De Vries, 'Sphingosine 1-Phosphate Receptor 1 and 3 Are Upregulated in Multiple Sclerosis Lesions', *Glia,* 58 (2010), 1465-76.

209 J. van Horssen, L. Bö, C. M. P. Vos, I. Virtanen, and H. E. de Vries, 'Basement Membrane Proteins in Multiple Sclerosis-Associated Inflammatory Cuffs: Potential Role in Influx and Transport of Leukocytes', *J Neuropathol Exp Neurol,* 64 (2005), 722-29.

210 J. van Horssen, C. D. Dijkstra, and H. E. de Vries, 'The Extracellular Matrix in Multiple Sclerosis Pathology', *J Neurochem,* 103 (2007), 1293-301.

211 M. R. Vargas, M. Pehar, P. Cassina, L. Martinez-Palma, J. A. Thompson, J. S. Beckman, and L. Barbeito, 'Fibroblast Growth Factor-1 Induces Heme Oxygenase-1 Via Nuclear Factor Erythroid 2-Related Factor 2 (Nrf2) in Spinal Cord Astrocytes: Consequences for Motor Neuron Survival', *J Biol Chem,* 280 (2005), 25571-9.

212 H. Wang, K. Wang, C. Wang, X. Zhong, W. Qiu, and X. Hu, 'Increased Plasma Levels of Pentraxin 3 in Patients with Multiple Sclerosis and Neuromyelitis Optica', *Mult Scler,* 19 (2013), 926-31.

213 N. M. Weathington, A. H. van Houwelingen, B. D. Noerager, P. L. Jackson, A. D. Kraneveld, F. S. Galin, G. Folkerts, F. P. Nijkamp, and J. E. Blalock, 'A Novel Peptide Cxcr Ligand Derived from Extracellular Matrix Degradation During Airway Inflammation', *Nat Med,* 12 (2006), 317-23.

214 A. Więdłocha, and V. Sørensen, 'Signaling, Internalization, and Intracellular Activity of Fibroblast Growth Factor', in *(Signalling from Internalized Growth Factor Receptors*, ed. by I. H. Madshus Springer Berlin Heidelberg, 2004), pp. 45-79.

215 A. Williams, G. Piaton, M. S. Aigrot, A. Belhadi, M. Theaudin, F. Petermann, J. L. Thomas, B. Zalc, and C. Lubetzki, 'Semaphorin 3a and 3f: Key Players in Myelin Repair in Multiple Sclerosis?', *Brain,* 130 (2007), 2554-65.

216 A. Williams, G. Piaton, and C. Lubetzki, 'Astrocytes--Friends or Foes in Multiple Sclerosis?', *Glia,* 55 (2007), 1300-12.

217 Y. Yamashita, S. W. Hooker, H. Jiang, A. B. Laurent, R. Resta, K. Khare, A. Coe, P. W. Kincade, and L. F. Thompson, 'Cd73 Expression and Fyn-Dependent Signaling on Murine Lymphocytes', *Eur J Immunol,* 28 (1998), 2981-90.

218 S.-F. Yan, T. Fujita, J. Lu, K. Okada, Y. Shan Zou, N. Mackman, D. J. Pinsky, and D. M. Stern, 'Egr-1, a Master Switch Coordinating Upregulation of Divergent Gene Families Underlying Ischemic Stress', *Nat Med,* 6 (2000), 1355-61.

219 Y. Yang, E. Y. Estrada, J. F. Thompson, W. Liu, and G. A. Rosenberg, 'Matrix Metalloproteinase-Mediated Disruption of Tight Junction Proteins in Cerebral Vessels Is Reversed by Synthetic Matrix Metalloproteinase Inhibitor in Focal Ischemia in Rat', *J Cereb Blood Flow Metab,* 27 (2007), 697-709.

220 A. Yayon, M. Klagsbrun, J. D. Esko, P. Leder, and D. M. Ornitz, 'Cell Surface, Heparin-Like Molecules Are Required for Binding of Basic Fibroblast Growth Factor to Its High Affinity Receptor', *Cell,* 64 (1991), 841-48.

221 N. Yazaki, Y. Hosoi, K. Kawabata, A. Miyake, M. Minami, M. Satoh, M. Ohta, T. Kawasaki, and N. Itoh, 'Differential Expression Patterns of Mrnas for Members of the Fibroblast Growth Factor Receptor Family, Fgfr-1–Fgfr-4, in Rat Brain', *J Neurosci Res,* 37 (1994), 445-52.

222 J. H. Yi, S. W. Park, R. Kapadia, and R. Vemuganti, 'Role of Transcription Factors in Mediating Post-Ischemic Cerebral Inflammation and Brain Damage', *Neurochem Int,* 50 (2007), 1014-27.

223 H. Zhang, H. Adwanikar, Z. Werb, and L. J. Noble-Haeusslein, 'Matrix Metalloproteinases and Neurotrauma: Evolving Roles in Injury and Reparative Processes', *Neuroscientist,* 16 (2010), 156-70.

224 Y. Zhang, F. Jalili, N. Ouamara, A. Zameer, G. Cosentino, M. Mayne, L. Hayardeny, J. P. Antel, A. Bar-Or, and G. R. John, 'Glatiramer Acetate-Reactive T Lymphocytes Regulate Oligodendrocyte Progenitor Cell Number in Vitro: Role of Igf-2', *J Neuroimmunol,* 227 (2010), 71-9.

225 Y. Zhang, C. Taveggia, C. Melendez-Vasquez, S. Einheber, C. S. Raine, J. L. Salzer, C. F. Brosnan, and G. R. John, 'Interleukin-11 Potentiates Oligodendrocyte Survival and Maturation, and Myelin Formation', *J Neurosci,* 26 (2006), 12174-85.

226 M. Zhu, K. Oishi, S. Chul Lee, and P. H. Patterson, 'Studies Using Leukemia Inhibitory Factor (Lif) Knockout Mice and a Lif Adenoviral Vector Demonstrate a Key Anti-Inflammatory Role for This Cytokine in Cutaneous Inflammation', *J Immunol,* 166 (2001), 2049-54.

227 H. Zimmermann, 'Biochemistry, Localization and Functional Roles of Ecto-Nucleotidases in the Nervous System', *Prog Neurobiol,* 49 (1996), 589-618.

228 E. Zindler, and F. Zipp, 'Neuronal Injury in Chronic Cns Inflammation', *Best Pract Res Clin Anaesthesiol,* 24 (2010), 551-62.

# 7 ABBREVIATIONS

| | |
|---|---|
| ATP | Adenosine triphosphate |
| AUC | Area under the curve |
| BSA | Bovine serum albumin |
| c | Concentration |
| CD | Cluster of differentiation |
| cDNA | Complementary DNA |
| CNS | Central nervous system |
| CNTF | Ciliary neurotrophic factor |
| COL | Collagen |
| CSF | Cerebrospinal fluid |
| CX3CL1 | Chemokine (C-X3-C motif) ligand 1 |
| CXCL | Chemokine (C-X-C motif) ligand |
| Da | Dalton |
| DAB | 3.3'-Diaminobenzidine |
| DAPI | 4'.6-diamidino-2-phenylindol dihydrochlorid |
| DEG | Differentially expressed genes |
| DIV | Days *in vitro* |
| DM | Differentiation medium |
| DM/I | Differentiation medium with insulin |
| DMEM | Dulbecco's modified eagle medium |
| EAE | Experimental autoimmune encephalomyelitis |
| EDSS | Expanded disability status scale |
| EDTA | Ethylenediaminetetraacetic acid |
| EGF | Epidermal growth factor |
| EGR1 | Early growth response 1 |
| ELISA | Enzyme-linked immunosorbent assay |
| FFPE | Formalin fixed paraffin embedded |
| FGF1 | Fibroblast growth factor 1 |
| FGFR | Fibroblast growth factor receptor |
| FRS2 | FGFR substrate 2 |
| GAPDH | Glycerinaldehyd-3-phosphat-Dehydrogenase |
| GFAP | Glial fibrillary acidic protein |
| HBSS | Hank's balanced salt solution |
| HE | Haematoxylin and eosin |
| HEPES | 4-(2-Hydroxyethyl)piperazine-1-ethanesulfonic acid |
| HIER | Heat induced epitope retrieval |
| HMOX1 | Heme oxygenase (decycling) 1 |
| Iba-1 | Ionized calcium-binding adapter molecule-1 |

| | |
|---|---|
| Ig | Immunoglobulin |
| IGF1 | Insulin-like growth factor 1 |
| IHC | Immunohistochemistry |
| IL | Interleukin |
| iNOS | Inducible nitric oxide synthases |
| KCNN4 | Potassium intermediate/small conductance calcium-activated channel, subfamily N, member 4 |
| LFA-1 | Lymphocyte function-associated antigen-1 |
| LFB | Luxol fast blue |
| LIF | Leukemia inhibitory factor |
| LIMMA | Linear models for microarray data |
| LTα | Lymphotoxin α |
| ManNAz | Tetraacetyl-N-azidoacetyl-mannosamine |
| MCP1 | Monocyte chemoattractant protein 1 |
| MHC | Major histocompatibility complex |
| MMP | Matrix metalloproteinases |
| MOG | Myelin oligodendrocyte glycoprotein |
| MS | Multiple sclerosis |
| $NaHCO_3$ | Sodium bicarbonate |
| NMO | Neuromyelitis optica |
| ns | Not significant |
| NT5E | 5'-nucleotidase, ecto (CD73) |
| OPCs | Oligodendrocyte precursor cells |
| PBS | Phosphate buffered saline |
| PDGF | Platelet-derived growth factor |
| PerCP | Peridinin chlorophyll protein |
| PI3K | Phosphoinositide-3-kinase |
| PLC | Phospholipase C |
| PM | Plating medium |
| PP | Primary progressive |
| PPIA | Peptidylprolyl isomerase A (human cyclophilin A) |
| PTX3 | Pentraxin 3, long |
| qPCR | Quantitative polymerase chain reaction |
| Ras MAPK | Ras mitogen activated protein kinase |
| RPE | R-Phycoerythrin |
| RR | Relapsing remitting |
| RT | Reverse transcription |
| RT-qPCR | Reverse transcription quantitative PCR |
| S1P | Sphingosine 1-phosphate |
| S1P1 | S1P receptor 1 |
| SD | Standard deviation |

| | |
|---|---|
| SDS | Sodium dodecyl sulfate |
| SEM | Standard error of the mean |
| SEMA | Semaphorin |
| SP | Secondary progressive |
| SPECS | Secretome protein enrichment with click sugars |
| SPHK1 | Sphingosine kinase 1 |
| TCEP | Tris-(2-carboxyethyl)-phosphine-hydrochloride |
| TGFβ | Transforming growth factor β |
| TIMP | Tissue inhibitor of metalloproteinases |
| TMB | 3,3',5,5'-tetramethylbenzidine |
| TNFα | Tumor necrosis factor α |
| Tris | Tris(hydroxymethyl)aminomethane |
| TSA | Tyramide signal amplification |
| VCAM1 | Vascular cell adhesion protein 1 |
| VLA-4 | Very late antigen-4 |

# 8 RESOURCES

*Primary human astrocytes.* Primary human astrocytes were kindly provided by Prof. Dr. Francesca Aloisi (ISS, Rome, Italy).

*Human tonsils.* Tissue from human tonsils was obtained from PD Dr. Klaus Stelter (Klinik und Poliklinik für Hals-Nasen-Ohrenheilkunde, Klinikum LMU, Germany).

*Transcriptome microarray analysis.* Analysis of the raw data (Affymetrix GeneChip® Human Gene 1.0 ST arrays) was performed in the laboratory of Prof. Dr. Cinthia Farina (San Raffaele Scientific Institute, Milan, Italy).

*Secretome analysis.* Sample processing, subsequent to FGF1 stimulation, and mass spectrometry analysis was performed by Dr. Peer-Hendrik Kuhn (DZNE, Munich, Germany).

*LFB/HE and KiM1P staining.* The LFB/HE and the KiM1P staining of the chronic active lesion shown in figure 22 were performed in the laboratory of Prof. Dr. Tanja Kuhlmann (WWU Münster, Germany).

# 9 APPENDIX

## 9.1 APPENDIX 1: MICROARRAY SCREENING

The RNA concentration of the samples used for the microarray screening varied between 85 ng/µl and 201 ng/µl and was sufficient for microarray analysis (table 22, column 2). The A260/280 ratios of all samples were found to be > 2.0, indicating no contamination with proteins (table 22, column 3). The purity ratio of A260/A230 was sufficient for nine out of the 12 samples and < 1.0 only for the following samples: “Control 8h 2”, “FGF1 24 h 1” and “FGF1 24 h 3” (table 22, column 4). Due to the good overall quality of these samples regarding the other parameters, they were used for further analysis. All RNA integrity numbers were similar and ≥ 8.9 indicating an excellent RNA quality and ensured a good comparability of the samples in the microarray analysis (table 22, column 5).

The achieved cRNA yield ranged from 29 µg to 81 µg, which was above the recommended threshold of 20 µg proposed by Affymetrix (table 22, column 6). The second cycle cDNA yield ranged from 7 µg to 9 µg which exceeded the recommended threshold of 6 µg proposed by Affymetrix (table 22, column 7). The quality of cRNA, second cycle cDNA and fragmented sense strand cDNA was controlled using the 2100 Bioanalyzer. Results indicated successful cRNA and cDNA synthesis as well as fragmentation of all samples (not shown). Therefore, all samples could be applied in the hybridization reaction.

Table 22: RNA concentration and quality, cRNA yield, cDNA yield

| Sample ID | RNA [ng/µl] | RNA A260/280 | RNA A260/230 | RNA integrity number (RIN) | cRNA yield [µg] | cDNA yield [µg] |
|---|---|---|---|---|---|---|
| Control 8 h 1 | 149 | 2.08 | 1.30 | 8.90 | 75 | 8 |
| Control 8 h 2 | 139 | 2.11 | 0.38 | 9.80 | 65 | 7 |
| Control 8 h 3 | 166 | 2.09 | 1.08 | 10.00 | 53 | 8 |
| FGF1 8 h 1 | 179 | 2.07 | 1.50 | 10.00 | 81 | 9 |
| FGF1 8 h 2 | 134 | 2.09 | 2.13 | 9.60 | 76 | 8 |
| FGF1 8 h 3 | 147 | 2.08 | 1.42 | 9.90 | 73 | 8 |
| Control 24 h 1 | 85 | 2.07 | 2.20 | 9.80 | 45 | 8 |
| Control 24 h 2 | 91 | 2.06 | 1.55 | 10.00 | 50 | 8 |
| Control 24 h 3 | 103 | 2.04 | 2.06 | 9.80 | 47 | 8 |
| FGF1 24 h 1 | 180 | 2.07 | 0.94 | 9.70 | 51 | 8 |
| FGF1 24 h 2 | 182 | 2.07 | 1.65 | 9.80 | 51 | 8 |
| FGF1 24 h 3 | 201 | 2.10 | 0.90 | 9.80 | 29 | 7 |

The overall good performance was checked by calculating the area under the curve (AUC) of positive controls against negative controls, in which 0.5 represented a random match and 1.0 a perfect match. All arrays had AUC values > 0.8 and, therefore, specificity of signals could be demonstrated (table 23, column 2). The labeling process was monitored by examination of hybridization intensities of poly-A spike-in controls (*B. subtilis* genes: *lys*, *phe*, *thr*, and *dap*). Signal intensities should appear in the following order: *dap* > *thr* > *phe* > *lys*. Typical behavior as well as high sensitivity and accuracy of target preparation could be verified for all samples (figure 26, A). The high accuracy and sensitivity of the hybridization reaction as well as the staining and washing procedures were checked by comparing the signal intensities of 3'- and 5'-hybridization control probe sets. The signal intensities for both probe sets should be placed in the following order: *cre* > *bioD* > *bioC* > *bioB*, which could be demonstrated for all the samples (figure 26, B).

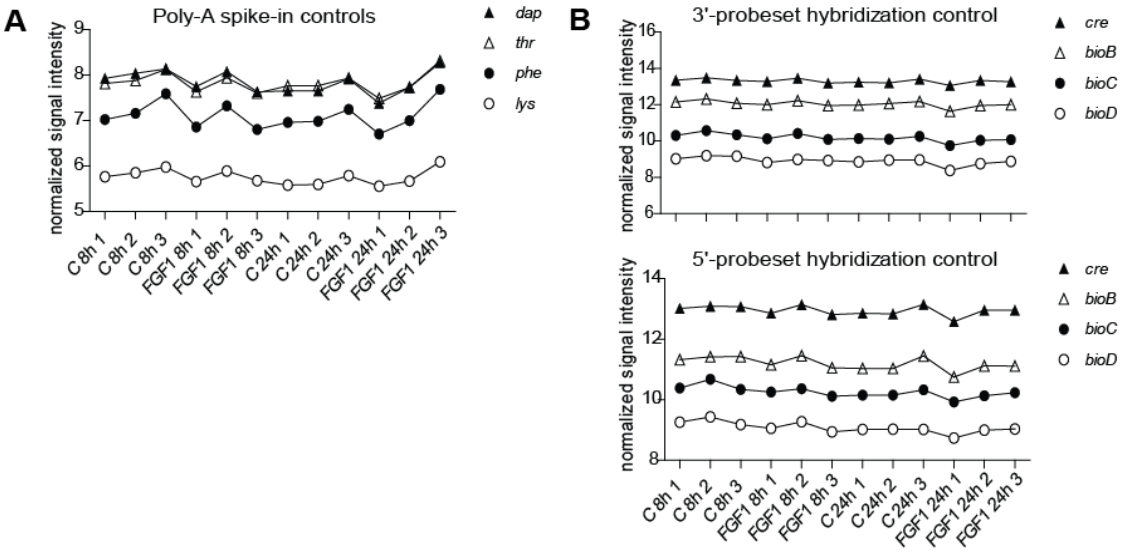


Figure 26: Quality control of transcriptome microarray analysis

C: control (medium treated); FGF1: 10 ng/ml FGF1 and 5 U/ml heparin
**(A)** Signal intensities for poly-A spike-in controls. **(B)** Signal intensities of 3'- and 5'-hybridization control probesets.

The unbiased performance of the array was checked by calculating the ratio of the signal intensities of the 3'- and the 5'-probesets. All the ratios were < 3, demonstrating an unbiased performance (table 23, column 3 to 6).

Taken together, the total RNA samples were found to have overall excellent RNA quality. They were successfully analyzed on Affymetrix GeneChip® Human Gene 1.0 ST arrays and the quality criteria were fulfilled for all analyzed samples.

Table 23: AUC and ratio of signal intensities of 3'- and 5'-hybridization controls

| | | Ratio 3'- / 5'-probesets of hybridization controls | | | |
|---|---|---|---|---|---|
| Sample ID | AUC | *cre* | *bioB* | *bioC* | *bioD* |
| Control 8 h 1 | 0.9058 | 0.9739 | 0.9917 | 1.0719 | 1.025 |
| Control 8 h 2 | 0.9041 | 0.9743 | 0.9892 | 1.0787 | 1.0294 |
| Control 8 h 3 | 0.9088 | 0.9989 | 0.9995 | 1.0569 | 1.0193 |
| FGF1 8 h 1 | 0.902 | 0.9735 | 0.9871 | 1.076 | 1.032 |
| FGF1 8 h 2 | 0.9085 | 0.9693 | 1.0045 | 1.067 | 1.0236 |
| FGF1 8 h 3 | 0.9015 | 0.9978 | 0.997 | 1.0816 | 1.029 |
| Control 24 h 1 | 0.9034 | 0.9812 | 0.998 | 1.0855 | 1.0296 |
| Control 24 h 2 | 0.8991 | 0.9906 | 0.9938 | 1.0929 | 1.0285 |
| Control 24 h 3 | 0.907 | 0.9937 | 0.9936 | 1.0633 | 1.019 |
| FGF1 24 h 1 | 0.898 | 0.9592 | 0.9819 | 1.0827 | 1.0377 |
| FGF1 24 h 2 | 0.9055 | 0.9726 | 0.9912 | 1.0749 | 1.0286 |
| FGF1 24 h 3 | 0.9036 | 0.9831 | 0.9849 | 1.0796 | 1.0231 |

## 9.2 APPENDIX 2: TRANSCRIPTOME APPROACH

RNA levels of genes upregulated after 8 h and 24 h FGF1 treatment

| Gene name | RefSeq-no. | Probe ID | Gene description | 8 h FC | 24 h FC |
|---|---|---|---|---|---|
| MMP1 | NM_002421 | 7951271 | Matrix metallopeptidase 1 (interstitial collagenase) | 2.2302 | 8.7368 |
| SLC16A6 | NM_001174166 | 8017843 | Solute carrier family 16, member 6 (monocarboxylic acid transporter 7) | 3.1361 | 6.3291 |
| MPP4 | NM_033066 | 8058273 | Membrane protein, palmitoylated 4 (MAGUK p55 subfamily member 4) | 1.6453 | 6.1999 |
| STC1 | NM_003155 | 8149825 | Stanniocalcin 1 | 2.7252 | 4.7958 |
| ANGPTL4 | NM_139314 | 8025402 | Angiopoietin-like 4 | 4.7091 | 4.3668 |
| GFPT2 | NM_005110 | 8116418 | Glutamine-fructose-6-phosphate transaminase 2 | 3.0658 | 4.2560 |
| RGS4 | NM_001102445 | 7906919 | Regulator of G-protein signaling 4 | 3.3535 | 4.1901 |
| SEMA7A | NM_003612 | 7990345 | Semaphorin 7A, GPI membrane anchor (John Milton Hagen blood group) | 3.1396 | 4.1673 |
| EMP1 | NM_001423 | 7954090 | Epithelial membrane protein 1 | 3.0680 | 3.7633 |
| RPSAP52 | NR_026825 | 7964733 | Ribosomal protein SA pseudogene 52 | 2.9191 | 3.6028 |
| DUSP6 | NM_001946 | 7965335 | Dual specificity phosphatase 6 | 3.4226 | 3.4630 |
| PTX3 | NM_002852 | 8083594 | Pentraxin 3, long | 3.0199 | 3.4033 |
| RGS2 | NM_002923 | 7908409 | Regulator of G-protein signaling 2, 24kDa | 2.6080 | 3.3080 |
| SCG5 | NM_001144757 | 7982366 | Secretogranin V (7B2 protein) | 1.8474 | 3.2399 |
| SLAMF8 | NM_020125 | 7906486 | SLAM family member 8 | 1.9222 | 3.2188 |
| PLAT | NM_000930 | 8150509 | Plasminogen activator, tissue | 1.9372 | 3.2087 |
| IL8 | NM_000584 | 8095680 | Interleukin 8 | 2.3215 | 3.2043 |
| HMGA2 | NM_003483 | 7956867 | High mobility group AT-hook 2 | 2.4129 | 3.1053 |
| ITGA2 | NM_002203 | 8105267 | Integrin, alpha 2 (CD49B, alpha 2 subunit of VLA-2 receptor) | 2.1076 | 3.0553 |
| C13orf33 | NM_032849 | 7968351 | Chromosome 13 open reading frame 33 | 1.5389 | 2.9861 |
| SLC20A1 | NM_005415 | 8044499 | Solute carrier family 20 (phosphate transporter), member 1 | 2.5578 | 2.9758 |

| | | | | | |
|---|---|---|---|---|---|
| EDNRA | NM_001957 | 8097692 | Endothelin receptor type A | 1.9355 | 2.9373 |
| PLAUR | NM_002659 | 8037374 | Plasminogen activator, urokinase receptor | 1.9707 | 2.8845 |
| KRTAP2-4 | NM_033184 | 8015210 | Keratin associated protein 2-4 | 1.7975 | 2.8564 |
| KRT34 | NM_021013 | 8015268 | Keratin 34 | 2.1095 | 2.8413 |
| HMOX1 | NM_002133 | 8072678 | Heme oxygenase (decycling) 1 | 2.2461 | 2.7947 |
| KRTAP2-1 | NM_001123387 | 8015208 | Keratin associated protein 2-1 | 1.8109 | 2.6783 |
| SERPINA9 | NM_175739 | 7981084 | Serpin peptidase inhibitor, clade A (alpha-1 antiproteinase, antitrypsin), member 9 | 1.4185 | 2.6445 |
| ARHGAP22 | NM_021226 | 7933469 | Rho GTPase activating protein 22 | 2.0990 | 2.5753 |
| MGLL | NM_007283 | 8090433 | Monoglyceride lipase | 1.7052 | 2.5587 |
| MIR221 | NR_029635 | 8172266 | MicroRNA 221 | 2.6787 | 2.5530 |
| MLPH | NM_024101 | 8049487 | Melanophilin | 1.9122 | 2.5485 |
| SHC3 | NM_016848 | 8162216 | SHC (Src homology 2 domain containing) transforming protein 3 | 1.6137 | 2.5167 |
| PODXL | NM_001018111 | 8142981 | Podocalyxin-like | 1.5496 | 2.4964 |
| ADAMTS14 | NM_139155 | 7928147 | ADAM metallopeptidase with thrombospondin type 1 motif, 14 | 1.5304 | 2.3702 |
| TFPI2 | NM_006528 | 8141016 | Tissue factor pathway inhibitor 2 | 2.3622 | 2.3686 |
| TNFAIP6 | NM_007115 | 8045688 | Tumor necrosis factor, alpha-induced protein 6 | 1.9252 | 2.3609 |
| HAS2 | NM_005328 | 8152617 | Hyaluronan synthase 2 | 2.9637 | 2.3394 |
| PNP | NM_000270 | 7973067 | Purine nucleoside phosphorylase | 1.6645 | 2.3287 |
| RGMB | NM_001012761 | 8107100 | RGM domain family, member B | 2.1325 | 2.3276 |
| CD9 | NM_001769 | 7953291 | CD9 molecule | 1.4575 | 2.2806 |
| CNIH3 | NM_152495 | 7910022 | Cornichon homolog 3 (Drosophila) | 2.0185 | 2.2621 |
| ARHGAP18 | NM_033515 | 8129458 | Rho GTPase activating protein 18 | 1.5691 | 2.2199 |
| DUSP5 | NM_004419 | 7930413 | Dual specificity phosphatase 5 | 2.2691 | 2.2177 |
| SMAGP | NM_001033873 | 7963280 | Small cell adhesion glycoprotein | 1.6696 | 2.2152 |
| CORO2B | NM_006091 | 7984475 | Coronin, actin binding protein, 2B | 1.5794 | 2.2100 |
| E2F7 | NM_203394 | 7965094 | E2F transcription factor 7 | 1.8905 | 2.2006 |
| PLAU | NM_002658 | 7928429 | Plasminogen activator, urokinase | 1.5921 | 2.1556 |
| SPRY4 | NM_030964 | 8114797 | Sprouty homolog 4 (Drosophila) | 2.0936 | 2.1527 |
| SPOCD1 | NM_144569 | 7914467 | SPOC domain containing 1 | 1.5975 | 2.1472 |
| ERRFI1 | NM_018948 | 7912157 | ERBB receptor feedback inhibitor 1 | 2.2777 | 2.1298 |
| TM4SF1 | NM_014220 | 8091411 | Transmembrane 4 L six family member 1 | 1.5164 | 2.1072 |
| WNK4 | NM_032387 | 8007363 | WNK lysine deficient protein kinase 4 | 1.9211 | 2.0977 |
| CDK17 | NM_002595 | 7965652 | Cyclin-dependent kinase 17 | 1.6159 | 2.0876 |
| EREG | NM_001432 | 8095728 | Epiregulin | 2.4678 | 2.0858 |
| SPRY2 | NM_005842 | 7972217 | Sprouty homolog 2 (Drosophila) | 2.1107 | 2.0839 |
| MT1L | NR_001447 | 7995793 | Metallothionein 1L (gene/pseudogene) | 1.4700 | 2.0359 |
| ASAM | NM_024769 | 7952341 | Adipocyte-specific adhesion molecule | 1.4059 | 1.9858 |
| MT1X | NM_005952 | 7995838 | Metallothionein 1X | 1.5018 | 1.9663 |
| NT5E | NM_002526 | 8120967 | 5'-nucleotidase, ecto (CD73) | 1.4099 | 1.9545 |
| EGR1 | NM_001964 | 8108370 | Early growth response 1 | 3.6266 | 1.9492 |
| TBX3 | NM_016569 | 7966690 | T-box 3 | 1.9109 | 1.9490 |
| DNMBP | NM_015221 | 7935660 | Dynamin binding protein | 1.5534 | 1.9308 |
| NETO1 | NM_138966 | 8023828 | Neuropilin (NRP) and tolloid (TLL)-like 1 | 1.7473 | 1.9044 |
| TMEM200A | NM_052913 | 8122038 | Transmembrane protein 200A | 1.7218 | 1.9004 |

| | | | | | |
|---|---|---|---|---|---|
| ITPRIP | NM_033397 | 7936242 | Inositol 1,4,5-triphosphate receptor interacting protein | 1.6575 | 1.8926 |
| AKAP12 | NM_005100 | 8122807 | A kinase (PRKA) anchor protein 12 | 1.5919 | 1.8719 |
| KRT19 | NM_002276 | 8015349 | Keratin 19 | 1.5295 | 1.8383 |
| FZD8 | NM_031866 | 7933075 | Frizzled homolog 8 (Drosophila) | 1.5577 | 1.8369 |
| KCNG1 | NM_002237 | 8067029 | Potassium voltage-gated channel, subfamily G, member 1 | 1.7128 | 1.8181 |
| VCAM1 | NM_001078 | 7903358 | Vascular cell adhesion molecule 1 | 1.7414 | 1.8136 |
| SLCO4A1 | NM_016354 | 8063923 | Solute carrier organic anion transporter family, member 4A1 | 1.6585 | 1.7991 |
| TMCC3 | NM_020698 | 7965510 | Transmembrane and coiled-coil domain family 3 | 1.5637 | 1.7974 |
| HBEGF | NM_001945 | 8114572 | Heparin-binding EGF-like growth factor | 2.4184 | 1.7852 |
| MT1E | NM_175617 | 7995797 | Metallothionein 1E | 1.4396 | 1.7723 |
| FGF16 | NM_003868 | 8168463 | Fibroblast growth factor 16 | 1.8014 | 1.7715 |
| KCNN4 | NM_002250 | 8037408 | Potassium intermediate/small conductance calcium-activated channel, subfamily N, member 4 | 1.7143 | 1.7656 |
| HOXB2 | NM_002145 | 8016438 | Homeobox B2 | 1.4062 | 1.7505 |
| VEGFC | NM_005429 | 8103822 | Vascular endothelial growth factor C | 1.4453 | 1.7430 |
| SH2B3 | NM_005475 | 7958749 | SH2B adaptor protein 3 | 1.6869 | 1.7424 |
| FGF5 | NM_004464 | 8096050 | Fibroblast growth factor 5 | 1.4500 | 1.7379 |
| CHST11 | NM_018413 | 7958202 | Carbohydrate (chondroitin 4) sulfotransferase 11 | 1.4214 | 1.7260 |
| RALA | NM_005402 | 8132406 | V-ral simian leukemia viral oncogene homolog A (ras related) | 1.4628 | 1.7176 |
| TMEM51 | NM_001136218 | 7898115 | Transmembrane protein 51 | 1.4686 | 1.7154 |
| SPHK1 | NM_182965 | 8010061 | Sphingosine kinase 1 | 1.4716 | 1.6998 |
| RAGE | NM_014226 | 7981346 | Renal tumor antigen | 1.7203 | 1.6983 |
| BCL2A1 | NM_001114735 | 7990818 | BCL2-related protein A1 | 1.7736 | 1.6896 |
| RASA1 | NM_002890 | 8106784 | RAS p21 protein activator (GTPase activating protein) 1 | 1.5217 | 1.6786 |
| RASSF8 | NM_007211 | 7954469 | Ras association (RalGDS/AF-6) domain family (N-terminal) member 8 | 1.6241 | 1.6770 |
| LIF | NM_002309 | 8075310 | Leukemia inhibitory factor (cholinergic differentiation factor) | 1.9161 | 1.6604 |
| STX1A | NM_004603 | 8140113 | Syntaxin 1A (brain) | 1.4711 | 1.6542 |
| SMTN | NM_134269 | 8072413 | Smoothelin | 1.5489 | 1.6484 |
| PHLDA1 | NM_007350 | 7965040 | Pleckstrin homology-like domain, family A, member 1 | 1.7026 | 1.6437 |
| FOSL1 | NM_005438 | 7949532 | FOS-like antigen 1 | 1.4513 | 1.6326 |
| JUN | NM_002228 | 7916609 | Jun proto-oncogene | 1.7369 | 1.6177 |
| HK2 | NM_000189 | 8042942 | Hexokinase 2 | 1.7026 | 1.6042 |
| BNC1 | NM_001717 | 7991080 | Basonuclin 1 | 1.4799 | 1.5939 |
| MFSD2A | NM_001136493 | 7900365 | Major facilitator superfamily domain containing 2A | 1.5920 | 1.5643 |
| BCL10 | NM_003921 | 7917338 | B-cell CLL/lymphoma 10 | 1.6987 | 1.5608 |
| HS3ST3B1 | NM_006041 | 8005097 | Heparan sulfate (glucosamine) 3-O-sulfotransferase 3B1 | 1.5557 | 1.5584 |
| WNT5A | NM_003392 | 8088180 | Wingless-type MMTV integration site family, member 5A | 1.5298 | 1.5427 |
| IER2 | NM_004907 | 8026163 | Immediate early response 2 | 1.6113 | 1.5420 |

| | | | | | |
|---|---|---|---|---|---|
| HPCAL1 | NM_134421 | 8040238 | Hippocalcin-like 1 | 1.4894 | 1.5397 |
| CCIN | NM_005893 | 8155200 | Calicin | 1.5670 | 1.5289 |
| KCNG1 | NM_002237 | 8067033 | Potassium voltage-gated channel, subfamily G, member 1 | 1.4543 | 1.5201 |
| ASB1 | NM_001040445 | 8049657 | Ankyrin repeat and SOCS box-containing 1 | 1.4155 | 1.5137 |
| AGPAT9 | NM_032717 | 8096116 | 1-acylglycerol-3-phosphate O-acyltransferase 9 | 1.5180 | 1.5018 |
| SLC4A7 | NM_003615 | 8085914 | Solute carrier family 4, sodium bicarbonate cotransporter, member 7 | 1.4949 | 1.5006 |
| IRX3 | NM_024336 | 8001449 | Iroquois homeobox 3 | 1.4011 | 1.4958 |
| PTHLH | NM_198965 | 7962000 | Parathyroid hormone-like hormone | 1.9606 | 1.4920 |
| SLC25A37 | NM_016612 | 8145281 | Solute carrier family 25, member 37 | 1.4638 | 1.4517 |
| DPF3 | NM_012074 | 7979963 | D4, zinc and double PHD fingers, family 3 | 1.5239 | 1.4451 |
| GPR68 | NM_003485 | 7980765 | G protein-coupled receptor 68 | 1.4904 | 1.4360 |
| SPSB1 | NM_025106 | 7897449 | SplA/ryanodine receptor domain and SOCS box containing 1 | 1.4113 | 1.4159 |
| AREG | NM_001657 | 8095736 | Amphiregulin | 1.6490 | 1.4019 |

FC: fold-change
Double underlined genes are known from literature to be implicated in MS and their induction was verified using RT-qPCR.

## 9.3 APPENDIX 3: SECRETOME APPROACH

Secreted and glycosylated proteins induced by FGF1 treatment

| Protein name | ACCN (UniProt KB) | Gene name | FC Sec 48 h | FC Trans 8 h | FC Trans 24 h |
|---|---|---|---|---|---|
| CD44 antigen | P16070 | CD44 | 26.99 | - | 1.53 |
| Matrix metalloproteinase-9 (67 kDa; 82 kDa) | P14780 | MMP9 | 24.12 | - | - |
| Semaphorin 7A | O75326 | SEMA7A | 10.98 | 3.13 | 4.17 |
| Interstitial collagenase | P03956 | MMP1 | 10.84 | 2.23 | 8.74 |
| Polyubiquitin-C; Ubiquitin | P0CG48 | UBC;UBB | 8.51 | - | - |
| CUB domain-containing protein 1 | Q9H5V8 | CDCP1 | 6.90 | - | 2.00 |
| Angiopoietin-related protein 4 | Q9BY76 | ANGPTL4 | 5.94 | 4.71 | 4.37 |
| Integrin alpha-3 (heavy and light chain) | P26006 | ITGA3 | 5.55 | - | - |
| Metalloproteinase inhibitor 1 | P01033 | TIMP1 | 5.30 | - | 1.51 |
| Chondroitin sulfate proteoglycan 4 | Q6UVK1 | CSPG4 | 4.33 | - | - |
| C-type mannose receptor 2 | Q9UBG0 | MRC2 | 3.97 | - | - |
| Low-density lipoprotein receptor | H0YMD1 | LDLR | 2.48 | - | - |
| Cathepsin B (heavy and light chain) | P07858 | CTSB | 2.45 | - | - |
| Integrin beta-1 | P05556 | ITGB1 | 2.41 | - | - |
| Tyrosine-protein kinase receptor UFO | P30530 | AXL | 2.40 | - | - |
| CD166 antigen | Q13740 | ALCAM | 2.29 | - | - |
| Neogenin | Q92859 | NEO1 | 2.25 | - | - |
| Neuropilin-1 | O14786 | NRP1 | 2.18 | - | 1.64 |
| Inactive tyrosine-protein kinase 7 | Q13308 | PTK7 | 2.13 | - | -1.41 |
| Plasminogen activator inhibitor 1 | P05121 | SERPINE1 | 2.11 | - | - |
| Transmembrane protein 132A | Q24JP5 | TMEM132A | 2.06 | - | - |
| 4F2 cell-surface antigen heavy chain | P08195 | SLC3A2 | 2.03 | - | - |

| | | | | | |
|---|---|---|---|---|---|
| Low-density lipoprotein receptor-related protein 1 (85 kDa; 515 kDa; intracellular domain) | Q07954 | LRP1 | 2.02 | - | - |
| Cadherin-13 | P55290 | CDH13 | 2.00 | - | - |
| Endothelin-converting enzyme 1 | P42892 | ECE1 | 1.91 | - | - |
| Glypican-1; Secreted glypican-1 | P35052 | GPC1 | 1.81 | - | - |
| CD109 antigen | Q6YHK3 | CD109 | 1.79 | - | - |
| Nidogen-1 | P14543 | NID1 | 1.75 | - | - |
| Elongation factor 2 | Q6PK56 | EEF2 | 1.71 | - | - |
| Attractin | O75882 | ATRN | 1.61 | - | - |
| Hepatocyte growth factor receptor | P08581 | MET | 1.57 | - | - |
| Prostaglandin F2 receptor negative regulator | Q9P2B2 | PTGFRN | 1.17 | - | - |
| Collagen alpha-1(VI) chain | P12109 | COL6A1 | 1.16 | - | - |
| Adipocyte enhancer-binding protein 1 | Q8IUX7 | AEBP1 | -1.07 | - | - |
| Heat shock protein HSP 90-beta | Q6PK50 | HSP90AB1 | -1.13 | - | - |
| Proteasome activator complex subunit 2 | Q9UL46 | PSME2 | -1.23 | - | - |
| Carbohydrate sulfotransferase 3 | Q7LGC8 | CHST3 | -1.27 | - | - |
| Tenascin | P24821 | TNC | -1.29 | - | - |
| Carbohydrate sulfotransferase 14 | Q8NCH0 | CHST14 | -1.39 | - | - |
| Beta-galactosidase | P16278 | GLB1 | -1.46 | - | - |
| Macrophage colony-stimulating factor 1 | P09603 | CSF1 | -1.47 | - | - |
| Follistatin-related protein 3 | O95633 | FSTL3 | -1.51 | - | -1.40 |
| Myosin-9 | P35579 | MYH9 | -1.52 | - | - |
| Granulins (-1; -2; -3; -4; -5; -6; -7; Acrogranulin; Paragranulin) | P28799 | GRN | -1.53 | - | - |
| Thrombospondin-1 | P07996 | THBS1 | -1.56 | - | - |
| Complement C1s subcomponent (heavy and light chain) | P09871 | C1S | -1.61 | - | - |
| ADP-sugar pyrophosphatase | Q9UKK9 | NUDT5 | -1.62 | - | - |
| Platelet-derived growth factor C (latent form; receptor-binding form) | Q9NRA1 | PDGFC | -1.63 | - | - |
| Calsyntenin-2 | Q9H4D0 | CLSTN2 | -1.69 | - | -1.50 |
| Plectin | Q15149 | PLEC | -1.71 | - | - |
| Multiple epidermal growth factor-like domains protein 6 | O75095 | MEGF6 | -1.74 | - | - |
| Mammalian ependymin-related protein 1 | A4D1W8 | UCC1;EPDR1 | -1.77 | - | - |
| Serine protease 23 | O95084 | PRSS23 | -1.80 | - | -1.56 |
| Alpha-actinin-4 | O43707 | ACTN4 | -1.81 | - | - |
| Heparan sulfate N-deacetylase/N-sulfotransferase 1 | P52848 | NDST1 | -1.87 | - | -1.41 |
| Periostin | B1ALD8 | POSTN | -2.00 | - | - |
| Fructose-bisphosphate aldolase A | P04075 | ALDOA | -2.02 | - | - |
| Brother of CDO | Q9BWV1 | BOC | -2.08 | - | - |
| Protein-lysine 6-oxidase | P28300 | LOX | -2.09 | - | - |
| Microfibrillar-associated protein 2 | P55001 | MFAP2 | -2.15 | - | - |
| Connective tissue growth factor | P29279 | CTGF | -2.22 | - | - |
| Soluble scavenger receptor cysteine-rich domain-containing protein SSC5D | A1L4H1 | SSC5D | -2.26 | - | - |
| Actin-related protein 2/3 complex subunit 2 | O15144 | ARPC2 | -2.30 | - | - |
| Stanniocalcin-2 | O76061 | STC2 | -2.82 | - | -1.81 |

| | | | | | |
|---|---|---|---|---|---|
| Insulin-like growth factor-binding protein 3 | P17936 | IGFBP3 | -3.12 | - | -1.98 |
| Collagen alpha-2(V) chain | P05997 | COL5A2 | -3.32 | - | - |
| Collagen alpha-2(IV) chain; Canstatin | P08572 | COL4A2 | -3.33 | - | - |
| Decorin | P07585 | DCN | -3.36 | - | - |
| Protein KIAA1199 | Q8WUJ3 | KIAA1199 | -3.69 | -1.45 | -4.01 |
| Collagen alpha-1(I) chain | P02452 | COL1A1 | -3.72 | - | - |
| Collagen alpha-2(I) chain | P08123 | COL1A2 | -4.07 | - | - |
| Transforming growth factor beta-2 | P61812 | TGFB2 | -5.19 | - | -1.93 |

ACCN: Accession number; FC: fold-change; Sec: Secretome; Trans: Transcriptome
Double underlined proteins were detected in the transcriptome and the secretome approach. These proteins are also summarized in table 19.

# 10 ACKNOWLEDGEMENTS

First, I want to thank Prof. Dr. Reinhard Hohlfeld and Prof. Dr. Hartmut Wekerle for the opportunity to perform my PhD at their departments at the Max Planck Institute of Neuroimmunology and at the Institute of Clinical Neuroimmunology of the LMU. I am deeply thankful also to my direct supervisor Prof. Dr. Edgar Meinl for accepting me in his group, for his constant support and advice, for fruitful discussions and for the possibility to develop and realize my own ideas and to become an independent scientist.

I am grateful to Prof. Dr. Elisabeth Weiß for kindly accepting the position as my principal supervisor at the Faculty of Biology of the LMU and also want to thank her and the other members of my examination committee, in particular Prof. Dr. Edgar Meinl and Prof. Dr. Michael Schleicher for their time to examine my thesis.

I want to acknowledge the members of my thesis advisory committee Prof. Dr. Klaus Dornmair and Prof. Dr. Leda Dimou for the discussion on my project, for their suggestions and their advice.

I want to express my appreciation for all the practical and theoretical aid I obtained from our co-operation partners. Thanks to Prof. Dr. Francesca Aloisi and PD Dr. Klaus Stelter for providing primary human astrocytes and tonsil tissue, respectively. Thanks to Prof. Dr. Cinthia Farina for the analysis of the transcriptome data, for helpful suggestions and discussions. I am fortunate to have benefitted from the expertise of Prof. Dr. Tanja Kuhlmann. Thank you, for teaching me the basics of neuropathology and for your valuable advice. Special thanks also to Peer from the Lichtenthaler-lab for the help with the mass spec analysis, lively discussions and brilliant ideas.

Many thanks not only to my direct lab members Cathrin, Cora, Franziska, Heike, Markus, Melania, Sarah and Sissi but also to all the members of the Dornmair-, the Guru- and the Naoto-lab. Thank you all for a friendly and relaxed working atmosphere and for being great colleagues and friends. I also want to thank my former colleague Dr. Hema Mohan for getting my experiments started in the beginning.

I am grateful for all the support I received from my friends in and outside the lab. Simone, Kerstin, Jenny and Viktor, I am glad that I got to know you in Munich. Evi, Iris, Alex and Jule, thank you for always being around, although, living miles away.

My love and deepest gratitude goes to my parents. Thank you, for your endless support, guidance, understanding, and for helping me to become the person I am.

Johannes, thanks a lot for always being there, for your advice, for your patience, for encouraging me and making me smile.